



National Library
of Canada

Acquisitions and
Bibliographic Services Branch

395 Wellington Street
Ottawa, Ontario
K1A 0N4

Bibliothèque nationale
du Canada

Direction des acquisitions et
des services bibliographiques

395, rue Wellington
Ottawa (Ontario)
K1A 0N4

Your file - Votre référence :

Our file - Notre référence :

NOTICE

The quality of this microform is heavily dependent upon the quality of the original thesis submitted for microfilming. Every effort has been made to ensure the highest quality of reproduction possible.

If pages are missing, contact the university which granted the degree.

Some pages may have indistinct print especially if the original pages were typed with a poor typewriter ribbon or if the university sent us an inferior photocopy.

Reproduction in full or in part of this microform is governed by the Canadian Copyright Act, R.S.C. 1970, c. C-30, and subsequent amendments.

AVIS

La qualité de cette microforme dépend grandement de la qualité de la thèse soumise au microfilmage. Nous avons tout fait pour assurer une qualité supérieure de reproduction.

S'il manque des pages, veuillez communiquer avec l'université qui a conféré le grade.

La qualité d'impression de certaines pages peut laisser à désirer, surtout si les pages originales ont été dactylographiées à l'aide d'un ruban usé ou si l'université nous a fait parvenir une photocopie de qualité inférieure.

La reproduction, même partielle, de cette microforme est soumise à la Loi canadienne sur le droit d'auteur, SRC 1970, c. C-30, et ses amendements subséquents.

UNIVERSITY OF ALBERTA

**CAPILLARY ZONE ELECTROPHORESIS WITH LASER-INDUCED
FLUORESCENCE AND CHEMILUMINESCENCE DETECTION FOR
BIOMOLECULE ANALYSIS**

BY

JIAN YING ZHAO



**A thesis submitted to the faculty of graduate studies and research in partial
fulfillment of the requirements for the degree of DOCTOR OF PHILOSOPHY**

DEPARTMENT OF CHEMISTRY

Edmonton, Alberta

SPRING 1994



National Library
of Canada

Acquisitions and
Bibliographic Services Branch

395 Wellington Street
Ottawa, Ontario
K1A 0N4

Bibliothèque nationale
du Canada

Direction des acquisitions et
des services bibliographiques

395, rue Wellington
Ottawa (Ontario)
K1A 0N4

Your file - Votre référence

Our file - Notre référence

The author has granted an irrevocable non-exclusive licence allowing the National Library of Canada to reproduce, loan, distribute or sell copies of his/her thesis by any means and in any form or format, making this thesis available to interested persons.

L'auteur a accordé une licence irrévocable et non exclusive permettant à la Bibliothèque nationale du Canada de reproduire, prêter, distribuer ou vendre des copies de sa thèse de quelque manière et sous quelque forme que ce soit pour mettre des exemplaires de cette thèse à la disposition des personnes intéressées.

The author retains ownership of the copyright in his/her thesis. Neither the thesis nor substantial extracts from it may be printed or otherwise reproduced without his/her permission.

L'auteur conserve la propriété du droit d'auteur qui protège sa thèse. Ni la thèse ni des extraits substantiels de celle-ci ne doivent être imprimés ou autrement reproduits sans son autorisation.

ISBN 0-612-11425-2

Canada

**Commit to the Lord whatever you do, and
your plans will succeed.**

- Proverbs 16: 3

UNIVERSITY OF ALBERTA

RELEASE FORM

NAME OF AUTHOR: **Jian Ying Zhao**


TITLE OF THESIS: **Capillary Zone Electrophoresis With Laser-Induced
Fluorescence And Chemiluminescence Detection
For Biomolecule Analysis**

DEGREE: **Doctor Of Philosophy**

YEAR THIS DEGREE GRANTED: **1994**

Permission is here by granted to the university of alberta library to reproduce single copies of this thesis and to lend or sell such copies for private, scholarly or scientific research purposes only.

The author reserves all other publication and other rights in association with the copyright in the thesis, and expect as herein before provided neither the thesis nor any substantial portion thereof may be printed or otherwise reproduced in any material form whatever without the author's prior written permission.



509RH, Michener Park
Edmonton, Alberta T6H 4M5

February/8, 1994

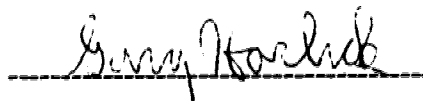
UNIVERSITY OF ALBERTA

FACULTY OF GRADUATE STUDIES AND RESEARCH

The undersigned certify that they have read, and recommend to the Faculty of Graduate Studies and Research for acceptance, a thesis entitled **CAPILLARY ZONE ELECTROPHORESIS WITH LASER-INDUCED FLUORESCENCE AND CHEMILUMINESCENCE DETECTION FOR BIOMOLECULE ANALYSIS** submitted by **JIAN YING ZHAO** in partial fulfillments of the requirements for the degree of **DOCTOR OF PHILOSOPHY**



Dr. Norman J. Dovichi



Dr. Gary Horlick



Dr. Ole Hindsgaul



Dr. Liang Li



Dr. Tim Mosmann



Dr. Nicholas H. Low

February 4, 1994

TO MY PARENTS

Acknowledgments

I would like to extend my sincere gratitude to my supervisor, Dr. Norman J. Dovichi, for providing excellent scientific guidance and endless encouragement doing my research. His understanding and sense of humor have made my five years of Ph. D. life full of meaning and fun.

I would like to thank everyone in Northern Lights Laser Lab for everything. Whenever I needed a help, it was always there.

I would like to express my heartfelt appreciation to my Ph. D. final exam committee members. Special thanks go to Dr. Ole Hindsgaul, Dr. Monica M. Palcic, Paul Diedrich, and Sylvie Gosselin for their help in the carbohydrate project (Chapter 4 and 5).

I would like to thank the Alberta Heritage Foundation for Medical Research for granting me a full-time scholarship for two years (1992/93 and 1993/94) and the Department of Chemistry at the University of Alberta for a one-year TA scholarship (1991/92).

I would like to say my thanks to the members of the Machine Shop and the Electronics Shop for their help in constructing all sorts of instrumentation .

Finally, I am deeply indebted to my parents, Sufen and Fuchen Zhao, for their encouragement and support of my graduate study in Canada. From the bottom of my heart, I want to acknowledge my dear husband, Binghai, and our lovely son, Sida. Their love, care, understanding, and moral support are the foundation of my whole life.

Abstract

Capillary electrophoresis (CE) offers excellent separation efficiency for the analysis of complex mixtures. Also, the small dimensions of capillary tubes offer opportunities for the analysis of extremely small amount of samples, especially those of biological interest. In this thesis, capillary zone electrophoresis (CZE) and micellar electrokinetic capillary chromatography (MECC) are used to separate fluorescently labeled amino acids (chapter 2), peptides (chapter 3), saccharides (chapter 4 and 5), and chemiluminescently labeled amino acids (chapter 6).

Post-column laser-induced fluorescence (LIF) detection in a sheath flow cuvette is the most sensitive technique for capillary electrophoresis. In this thesis, a low-cost and low-power helium-neon laser, operating in the green at 543.5 nm, is used to excite fluorescently labeled biomolecules. The relative long excitation wavelength, the low light scatter of the sheath flow cuvette, and the low excitation power results in a very low background signal, which, in combination with high efficiency collection optics, produces detection limits as low as 100 molecules. Two pre-column fluorescent dyes, tetramethylrhodamine isothiocyanate (TRITC) and 5-carboxy-tetramethylrhodamine succinimidyl ester (TRSE), are used to label 20 common amino acids, six monosaccharide standards for oligosaccharide sequencing, and synthetic oligosaccharide substrates for glycosyltransferase assays.

Incomplete pre-column fluorescent labeling of ϵ -amino groups on lysine residues of a peptide results in multiple reaction products. A single label, fluorescein isothiocyanate (FITC), is attached to the peptide by first taking the

peptide through one cycle of the Edman degradation reaction. All ϵ -amino groups are converted to the phenyl thiocarbamyl and the cleavage step exposes one α -amino group at the N-terminus of the peptide; the fluorescent label is attached to the N-terminus and excited with the 488 nm line of an argon ion laser.

A post-column chemiluminescence detector using a sheath flow cuvette is designed for capillary electrophoresis separation of isoluminol thiocarbamyl derivatives of 20 amino acids. This system is optimized and linear calibration curves are constructed. The dynamic range of the instrument is at least three orders of magnitude. Detection limits for isoluminol and isoluminol thiocarbamyl derivative of valine are 40 and 500 attomole, respectively.

Table of Contents

CHAPTER 1 INTRODUCTION TO CAPILLARY ELECTROPHORESIS WITH LASER-INDUCED FLUORESCENCE AND CHEMILUMINESCENCE DETECTION	1
1.1 CAPILLARY ELECTROPHORESIS.....	2
1.1.1 General Introduction	2
1.1.2 Typical Capillary Electrophoresis System Setup.....	4
1.1.3 Sample Introduction into Capillary	4
1.1.4 Electrophoresis and Electroosmosis	8
1.1.5 Separation Efficiency	11
1.1.6 Resolution.....	12
1.1.7 Capillary Electrophoresis Separation Modes	13
1.1.8 Micellar Electrokinetic Capillary Chromatography (MECC)	16
1.1.8A The Formation of Micelles	16
1.1.8B Separation Principle	17
1.1.8C Important Parameters in MECC.....	17
1.1.8D Selectivity Manipulation in MECC.....	19
1.1.8E Sodium Dodecyl Sulfate (SDS)	20
1.1.9 Detection Methods	22
1.1.10 Detection Limits	23
1.2 POST-COLUMN LASER-INDUCED FLUORESCENCE (LIF) DETECTION	25
1.2.1 General Introduction	25
1.2.2 Instrumentation	27
1.2.2A Sheath Flow Cuvette.....	27

1.2.2B Lasers	29
1.2.2C Focusing Optics	30
1.2.2D Fluorescence Collection	31
1.2.2E Spectral Filters	32
1.2.2F Photo Detectors	32
1.2.3 Fluorescent Derivatization of Analytes	33
1.2.3A Criteria for Choosing Fluorescent Dyes.....	34
1.2.3B Fluorescent Dyes	38
1.3 CHEMILUMINESCENCE (CL) DETECTION FOR CE.....	39
1.3.1 General Introduction	39
1.3.2 Chemiluminescence Reactions	40
REFERENCES	43

CHAPTER 2 LOW-COST LASER-INDUCED FLUORESCENCE

DETECTION FOR MICELLAR CAPILLARY ELECTROPHORESIS:

ZEPTOMOLE DETECTION OF TETRAMETHYLRHODAMINE

THIOCARBAMYL AMINO ACID DERIVATIVES

2.1 INTRODUCTION	49
2.2 EXPERIMENTAL	52
2.2.1 Capillary Electrophoresis Setup.....	52
2.2.2 Laser-Induced Fluorescence Detector	55
2.2.3 Stock Solutions.....	62
2.2.3A Preparation of Borate Buffers	62
2.2.3B Preparation of Borate / SDS Buffer	63
2.2.3C Amino Acid Stock Solutions	63
2.2.3D TRITC Stock Solutions	63

2.2.4 Labeling Reactions	63
2.2.5 Capillary Electrophoresis Conditions	66
2.3. RESULTS AND DISCUSSION	66
2.3.1 Spectral Properties of Tetramethylrhodamine Isothiocyanate	66
2.3.2 Labeling Reaction: Time Effect.....	68
2.3.3 Detection Limits	73
2.3.4 Separation of 20 Tetramethylrhodamine Isothiocyanate	74
2.4 CONCLUSIONS	76
REFERENCES	78

CHAPTER 3 ATTACHMENT OF A SINGLE FLUORESCENT LABEL TO PEPTIDES FOR DETERMINATION BY CAPILLARY ZONE

ELECTROPHORESIS.....	80
3.1 INTRODUCTION	81
3.2 EXPERIMENTAL	83
3.2.1 Labeling Peptide Directly	83
3.2.2 Manual Edmon Degradation Procedure.....	83
3.2.3 Labeling Truncated Peptide	84
3.2.4 Instrument Setup.....	85
3.2.5 Capillary Electrophoresis Conditions	85
3.3 RESULTS AND DISCUSSION	86
3.4 CONCLUSIONS	89
REFERENCES	91

CHAPTER 4 SEPARATION OF AMINATED MONOSACCHARIDES FOR OLIGOSSACHARIDE SEQUENCING BY MICELLAR CAPILLARY ELECTROPHORESIS WITH LASER-INDUCED FLUORESCENCE DETECTION	92
4.1 INTRODUCTION	93
4.2 EXPERIMENTAL	97
4.2.1 Synthesis of Six Standards of Aminated Monosaccharides (by P. Diedrich in Dr. O. Hindsgaul's group)	97
4.2.2 Labeling Reactions	103
4.2.3 Standard for Detection Limit and Calibration Curve	104
4.2.4 Instrument Setup	105
4.2.5 Electrophoresis Conditions	105
4.2.6 Separation Buffers	106
4.3 RESULTS AND DISCUSSION	106
4.3.1 The Fluorescent Dye: TRSE	106
4.3.2 Calibration Curve and Detection Limit	112
4.3.3 The Labeling Reactions	115
4.3.4 Plate Counts	115
4.3.5 Separation Buffer Effects	118
4.4 CONCLUSIONS	119
REFERENCES	122
 CHAPTER 5 DETECTION OF 100 MOLECULES OF ENZYME PRODUCT BY CAPILLARY ELECTROPHORESIS WITH LASER- INDUCED FLUORESCENCE DETECTION	 124
5.1 INTRODUCTION	125

5.2 EXPERIMENTAL	129
5.2.1 Synthesis of a Disaccharide	129
5.2.2 Labeling the Synthetic Disaccharide with TRSE.....	131
5.2.3 Synthesis of the Substrate for Specific Glycosyltransferase Assays	132
5.2.4 Enzymatic Reactions	132
5.2.5 Instrument Setup	134
5.2.6 Capillary Electrophoresis Conditions	135
5.3 RESULTS AND DISCUSSION	136
5.3.1 Labeling Reaction Between Disaccharide and TRSE	136
5.3.2 Enzyme Reactions	136
5.4 CONCLUSIONS	141
REFERENCES	143

CHAPTER 6 THE USE OF A SHEATH FLOW CUVETTE FOR CHEMILUMINESCENCE DETECTION OF ISOLUMINOL THIOCARBAMYL-AMINO ACIDS SEORATED BY MICELLAR CAPILLARY ELECTROPHORESIS	145
---	------------

6.1 INTRODUCTION	146
6.2 EXPERIMENTAL	150
6.2.1 Interface of a Chemiluminescence Detector with CE	150
6.3.2 Reagents.....	157
6.2.3 Labeling Reactions	159
6.2.4 Capillary Electrophoresis Conditions	159
6.3 RESULTS AND DISCUSSION	160
6.3.1 Catalyst: Microperoxidase	160

6.3.2 Optimization of the Chemiluminescence Detection System	160
6.3.2A As a Function of Hydrogen Peroxide Concentration	161
6.3.2B As a Function of Microperoxidase Concentration	164
6.3.2C As a Function of the Residence Time	164
6.3.2D As a Function of the Distance from the Exit of Capillary to the Center of the Cylindrical PMTs	167
6.3.2E As a Function of the Concentration of Sodium Dodecyl Sulfate	170
6.3.3 Background Signal Evaluation	173
6.3.4 Calibration Curve and Detection Limit of Isoluminol	176
6.3.5 Electropherograms of Isoluminol Isothiocyanate and ILITC Labeled Amino Acids	176
6.3.6 Calibration Curve , Theoretical Plate Counts and Detection Limit of ILITC Labeled Valine.....	183
6.3.7 Separation of Isoluminol Thiocarbamyl Derivatives of 20 Amino Acids	186
6.3.8 Possibility of Application in Protein Sequencing	188
6.4 CONCLUSIONS	188
REFERENCES	190

List of Figures

Figure 1.1 Schematic diagram of a typical capillary electrophoresis system.	5
Figure 1.2 Electrophoresis.....	8
Figure 1.3 Electroosmosis.....	9
Figure 1.4 Micellar electrokinetic capillary chromatography using sodium dodecyl sulfate (SDS).....	21
Figure 1.5 Sheath flow cuvette as a post-column laser-induced fluorescence detector for capillary electrophoresis	28
Figure 1.6 Luminol chemiluminescence reaction with hydrogen peroxide	42
Figure 2.1 Structures of two fluorescent isothiocyanates	51
Figure 2.2 TRITC and amino acid labeling reaction.....	53
Figure 2.3 Schematic diagram of the capillary electrophoresis system with post-column detection in a sheath flow cuvette.	54
Figure 2.4 Schematic diagram of the system setup for capillary electrophoresis with post-column laser-induced fluorescence detection in a sheath flow cuvette.	56
Figure 2.5 Spectrum of the interference filter 590DF40	60
Figure 2.6 Absorbance spectrum of TRITC	67
Figure 2.7 Fluorescence emission spectrum of TRITC.....	69
Figure 2.8 Electropherogram of TRITC labeled glycine	71
Figure 2.9 Fluorescence peak height vs. reaction time	72
Figure 2.10 Electropherogram of 20 TRITClabeled amino acids.....	75
Figure 3.1 Multiple labeling: electropherogram of direct fluorescein isothiocyanate labeled peptide 8656.....	87
Figure 3.2 Single labeling: electropherogram of truncated peptide 8656	88

Figure 4.1 Structure of 5-carboxytetramethylrhodamine succinimidyl ester	97
Figure 4.2 Structures of six aminated monosaccharides	98
Figure 4.3 Reductive amination of D-glucose	100
Figure 4.4 Reductive amination of D-glucosamine and D-galactosamine	102
Figure 4.5 Structure of TRSE labeled synthetic monosaccharide β -GlcNAc-O-(CH ₂) ₈ -CO-NH-CH ₂ -CH ₂ -NH ₂	104
Figure 4.6 Absorbance spectra of TRSE (2.4×10^{-6} M) in (a) methanol and (b) in 10 mM borate buffer	107
Figure 4.7 Absorbance spectrum of TRSE labeled synthetic sugar β -GlcNAc-O-(CH ₂) ₈ -CO-NH-CH ₂ -CH ₂ -NH ₂ (2.4×10^{-6} M in methanol)	108
Figure 4.8 Fluorescence emission spectrum of TRSE labeled synthetic sugar β -GlcNAc-O-(CH ₂) ₈ -CO-NH-CH ₂ -CH ₂ -NH ₂ (2.4×10^{-6} M in methanol).....	110
Figure 4.9 Electropherogram of TRSE (immediately after dilution from its stock solution by 10 mM borate buffer with 10 mM SDS)	111
Figure 4.10 Electropherogram of TRSE (22 hours at room temperature after dilution from its stock solution by 10 mM borate buffer with 10 mM SDS)	111
Figure 4.11 Log-log calibration curve for TRSE labeled synthetic sugar β -GlcNAc-O-(CH ₂) ₈ -CO-NH-CH ₂ -CH ₂ -NH ₂	113
Figure 4.12 Electropherogram of 260 molecules of TRSE labeled synthetic sugar β -GlcNAc-O-(CH ₂) ₈ -CO-NH-CH ₂ -CH ₂ -NH ₂	114
Figure 4.13 Electropherogram of TRSE labeled alanine	116
Figure 4.14 Electropherogram of TRSE labeled Mannose-NH ₂	117
Figure 4.15 Separation electropherogram of TRSE labeled six monosaccharide standards.	120
Figure 5.1 Biosynthesis of oligosaccharide catalyzed by glycosyltransferase	126

Figure 5.2 Synthesis of a disaccharide containing a primary amine	130
Figure 5.3 Structure of the synthetic disaccharide-TRSE	131
Figure 5.4 Fucosylation of disaccharide-TRSE to trisaccharide-TRSE by fucosyltransferase and de-fucosylation of trisaccharide-TRSE to disaccharide-TRSE by α -fucosidase	133
Figure 5.5 Schematic diagram of the electrical circuit for processing the PMT current output	135
Figure 5.6 Electropherograms of labeling reaction blank and labeling mixture of disaccharide with TRSE	137
Figure 5.7 Separation electropherograms of TRSE labeled disaccharide (peak 1) and trisaccharide (peak 2)	138
Figure 5.8 Separation electropherogram of a mixture of disaccharide-TRSE and trisaccharide-TRSE at concentration close to detection limits	140
Figure 6.1 Structures of isoluminol and isoluminol isothiocyanate	149
Figure 6.2 Schematic diagram of the capillary electrophoresis system with a post-column chemiluminescence detector	151
Figure 6.3 Single photon counting results of a R1635-02 PMT (serial number WA4509) by the manufacturer(Hamamatsu)	153
Figure 6.4 Single photon counting results of a R1635-02 PMT (serial number WA4566) by the manufacturer(Hamamatsu)	154
Figure 6.5 Cuvette and photomultiplier tube assembly in an aluminum box painted black	156
Figure 6.6 Structure of microperoxidase	158
Figure 6.7 Chemiluminescence signal as a function of hydrogen peroxide concentration introduced into the sheath flow cuvette	163
Figure 6.8 Chemiluminescence signal as a function of microperoxidase concentration in the separation buffer	166

Figure 6.9 Chemiluminescence signal as a function of residence time of analyte within the field-of-view of the PMTs	169
Figure 6.10 Chemiluminescence signal as a function of distance downstream from the exit of the capillary to the center of the PMTs	172
Figure 6.11 Chemiluminescence signal as a function of sodium dodecyl sulfate concentration in the separation buffer (according to Table 6.6b).....	175
Figure 6.12 Electropherogram of isoluminol (1.5×10^{-5} M).....	177
Figure 6.13 Log-log calibration curve for isoluminol.....	178
Figure 6.14 Electropherograms of ILITC (7.0×10^{-5} M).....	179
Figure 6.15 Electropherogram of ILITC blank (4.0×10^{-5} M)	181
Figure 6.16 Electropherograms of ILITC labeled valine and proline	182
Figure 6.17 Log-log calibration curve for ILITC labeled valine	184
Figure 6.18 Electropherogram of ILITC labeled thiocarbamyl derivatives of nine amino acids	187

List of Tables

Table 1.1 Multiplier constants for limit of detection of Knoll's method.....	24
Table 1.2 Collection efficiency of microscope objectives (n = 1.0).....	31
Table 1.3 Parameters of three fluorescent dyes	38
Table 2.1 Properties of the green helium-neon laser	58
Table 2.2 Structures of 20 common amino acids.....	64
Table 2.3 The 20 amino acid stock solutions	65
Table 2.4 Experimental data of reaction times and peak heights.....	70
Table 4.1 ¹³ C NMR (shift in ppm) and mass spectrum data	103
Table 4.2 Calibration curve data	112
Table 4.3 Plate counts for labeled sugars and labeling reagent TRSE	118
Table 6.1 Some parameters of the two R1635-02 PMTs	152
Table 6.2 Experimental data of the effect of H ₂ O ₂ concentration on CL signal	162
Table 6.3 Experimental data of the effect of microperoxidase concentration on chemiluminescence signal	165
Table 6.4 Experimental data of the effect of residence time of analyte within the field-of-view of the PMTs	168
Table 6.5 Experimental data of the effect of the distance down stream (d ₀ + X) on the chemiluminescence signal	171
Table 6.6 Experimental data of the effect of the SDS concentration on the chemiluminescence signal	174
Table 6.7 Experimental data for constructing a calibration curve for isoluminol	178
Table 6.8 Experimental data of a calibration curve for ILITC labeled valine	184

List of Abbreviations

CE	capillary electrophoresis
CZE	capillary zone electrophoresis
MECC	micellar electrokinetic capillary chromatography
CGE	capillary gel electrophoresis
CL	chemiluminescence
HPLC	high performance liquid chromatography
LC	liquid chromatography
UV	ultraviolet
LIF	laser-induced fluorescence
SDS	sodium dodecyl sulfate
PITC	phenylisothiocyanate
FITC	fluorescein isothiocyanate
TRITC	tetramethylrhodamine isothiocyanate
TRSE	tetramethylrhodamine succinimidyl ester
ILITC	isoluminol isothiocyanate
DNA	deoxyribonucleic acid
DMF	dimethylformamide
DMSO	dimethylsulfoxide
PMT	photomultiplier tube
He-Ne	helium-neon
GreNe	green helium-neon
I.D.	inner diameter
O.D.	outer diameter
LOD	limit of detection

CHAPTER 1

INTRODUCTION TO CAPILLARY ELECTROPHORESIS WITH LASER-INDUCED FLUORESCENCE AND CHEMILUMINESCENCE DETECTION

1.1 CAPILLARY ELECTROPHORESIS

1.1.1 General Introduction

Capillary electrophoresis (CE) has developed rapidly during the last decade as a powerful technique for separation of minute quantities of analytes, ranging from small inorganic ions to large molecules of biological importance. It has attracted great attention from both academia and industry.

Capillary scale zone electrophoresis has a surprisingly long history. Zone electrophoresis is performed in a buffer filled tube; separation is based on differences in the charge-to-size ratio of analyte. In 1957, Turner pointed out that the excellent heat transport properties of thin liquid films allowed use of high potentials in zone electrophoresis; unfortunately, applications were limited by difficulties associated not only with solvent evaporation but also with sample loading and detection [1, 2]. Hjerten performed open tubular electrophoresis in 1967 [3] by rotating the tube to minimize convection due to Joule heating. In 1979, Mikkers, Everaerts, and Verheggen described zone electrophoresis in Teflon capillaries [4, 5]; they reported both UV absorbance and conductivity detection. Jorgenson *et al.* published several seminal papers in the early 1980's that described capillary zone electrophoresis separation in fused silica capillaries for separation of protein digests [6-8]. Their research results demonstrated the potential of capillary electrophoresis. Since then more and more research papers have been published on various aspects and applications of capillary electrophoresis. In 1988, the first commercial CE instrument was introduced by Microphoretic Systems (Sunnyvale, CA, USA) at the conference of the Federation of the Societies for Experimental Biology (FASEB) [9].

Joule heating is the limiting factor in the use of high potentials in electrophoresis. Joule heat is produced when an electric current is flowing through a solution. The subsequent temperature gradients cause density gradients and convection, which in turn induces zone broadening. Because of the small dimension of a capillary tube and its large surface-to-volume ratio, heat dissipation is efficient allowing use of high separation potentials in capillary electrophoresis. The separation efficiency scales linearly with applied potential. In a well designed system, convection is minimized and mass diffusion limits the separation efficiency to a few million theoretical plates for low molecular weight analytes.

Capillary electrophoresis offers some advantages over high performance liquid chromatography (HPLC). First, capillary electrophoresis is ideally suited to aqueous solutions, especially those of biological significance, which is unlike most forms of HPLC, which require the use of non-aqueous solvents. Second, the amount of sample solution required by capillary electrophoresis is on the order of nanoliters or less while microliters are the typical volumes required by HPLC. Also capillary electrophoresis requires very small amount of buffer solution, which could lower significantly the costs of solvents and waste management compared to HPLC. Third, separation in capillary electrophoresis is much faster than in HPLC due to very high potentials that can be applied to capillary electrophoresis. Other advantages of capillary electrophoresis include ease of automation and the ability to achieve ultra-sensitive detection.

There are also some problems associated with capillary electrophoresis. Capillary electrophoresis will never be able to compete with HPLC in terms of preparative capability, even though many researchers are trying in different

ways to recover separated samples. Concentration detection limits in commercial instruments are much poorer than HPLC.

1.1.2 Typical Capillary Electrophoresis System Setup

Figure 1.1 shows a typical capillary electrophoresis system. Capillaries are normally made of fused silica often coated on the outside with a thin layer of polyimide to strengthen the tubes. The inner diameters range from 10 μ m to 200 μ m. The capillary is filled with buffer (typically 10 to 100 mM ionic strength) and the two ends are dipped in two separated buffer-containing reservoirs. The liquid levels in the two reservoirs are always kept the same to avoid unwanted hydrodynamic flow within the capillary. A platinum (Pt) electrode is put into the buffer vial containing the injection end of the capillary. The buffer reservoir containing the other end of the capillary is grounded. High voltage, up to 30 kV (either positive or negative), is applied across the capillary. To avoid electrical hazard, the high voltage end of the capillary must be enclosed within a non-conducting Plexiglas box equipped with a safety interlock. Detection takes place near the eluting end of the capillary.

1.1.3 Sample Introduction into Capillary

Overloading the capillary with samples will degrade the separation efficiency. The amount of sample solution required in capillary electrophoresis is on the order of a nanoliter or less. All of the conventional injection techniques, e.g. measuring samples with a syringe or use of an injection valve, are not suitable for introducing samples onto a capillary. Two injection schemes have

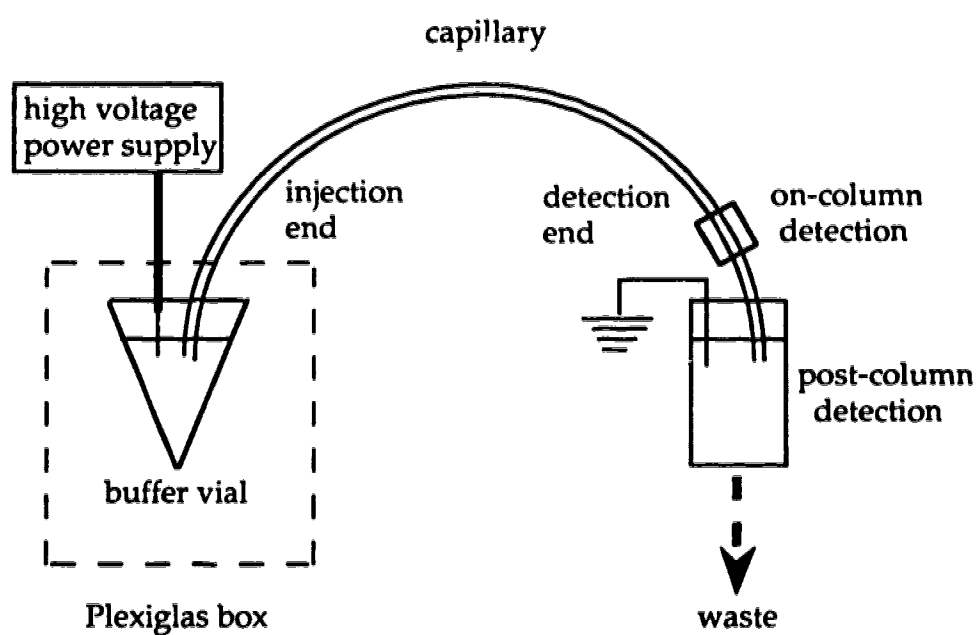


Figure 1.1 Schematic diagram of a typical capillary electrophoresis (CE) system

been employed in capillary electrophoresis: electrokinetic injection and hydrodynamic injection.

Electrokinetic injection

Electrokinetic injection is the most widely used injection form in capillary electrophoresis, also known as electromigration injection. The sample in a buffer solution is introduced by applying a low potential across the capillary for a short period of time. The voltage and time for injection can be easily controlled by a computer program.

When a voltage is applied, components with different charges (e.g. cations, neutrals, anions) and sizes will migrate at their specific velocities into the capillary. Analytes with higher electrophoretic mobilities travel faster and thus are injected to a greater extent than slower moving analytes. The corrected injection volume of individual component can be calculated by the following equation [10]:

$$V_{inj} = V_c \left(\frac{t_i}{t_r} \right) \left(\frac{V_i}{V_{ep}} \right) \quad (1.0)$$

where V_{inj} is the corrected injection volume of a specific component in the sample solution, V_c is the volume of the capillary in use, t_r is the migration time of the component, t_i is the electrokinetic injection time, V_i is the electrokinetic injection voltage, and V_{ep} is the high voltage employed for capillary electrophoresis.

Hydrodynamic injection

This can be easily done by lifting the sample vial with the injection end of the capillary for a finite time to a certain height above the buffer level at the detection end of the capillary. This method is also known as hydrostatic or siphoning injection. A small amount of sample solution flows into the injection end of the capillary as a narrow zone due to gravity. The siphoning injection can be performed manually or automatically. Manual siphoning injection gives very poor reproducibility. Precision of a few percent or less can be achieved by automated hydrodynamic injections [11, 12].

The hydrodynamically injected volume of the sample solution can be calculated by the following equation [13]:

$$V_{inj} = \pi r^2 L$$

$$V_{inj} = \frac{\pi r^4 \rho g \Delta h t_i}{8 \eta L_c} \quad (1.1)$$

where r is the radius of the capillary, L is the length of the sample injected into the capillary, ρ is the density of the liquid inside the capillary, g is the gravitational constant, Δh is the height difference between the two ends of the capillary, t_i is the injection time, η is the viscosity of the sample solution, and L_c is the length of the entire capillary. The injected volume is the same for all components in the bulk sample solution, no discrimination against components with different electrophoretic mobilities.

Other injection techniques are the rotary type injector [14], microinjectors [15, 16], and electric sampler splitter [17].

1.1.4 Electrophoresis and Electroosmosis

Electrophoresis

This is the fundamental separation process in capillary electrophoresis. When a voltage is applied across the capillary, the ionic components (cations or anions) will migrate toward the cathode or anode according to their charge. Based on differences in charge-to-mass ratio, ionic species can be separated into discrete zones through electrophoretic migration, **Figure 1.2**.

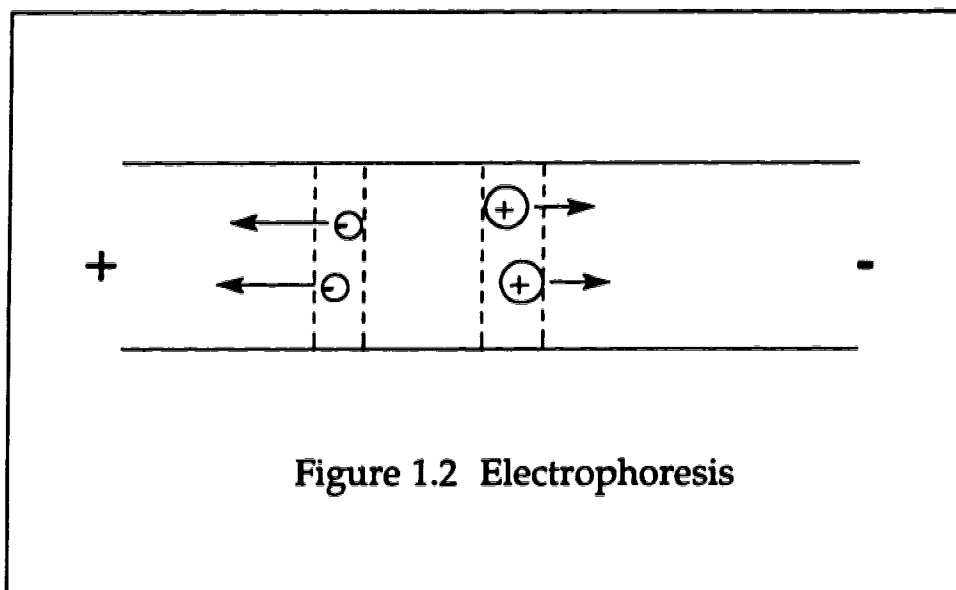


Figure 1.2 Electrophoresis

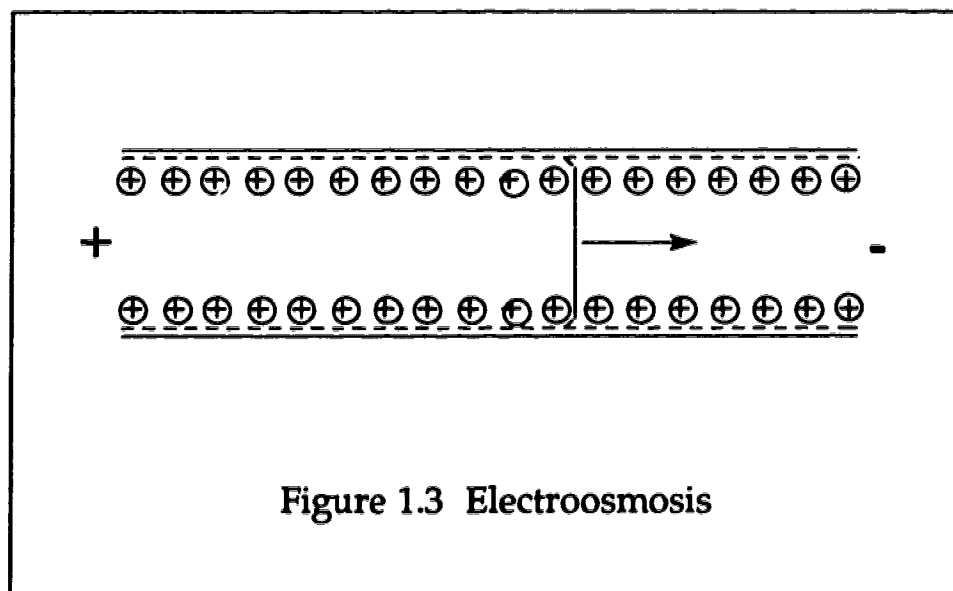
The electrophoretic mobility, μ_{ep} (cm²/sV) of an ion is defined as:

$$\mu_{ep} = \frac{v_{ep}}{E} = \frac{L_d/t_r}{V/L_c} \quad (1.2)$$

where v_{ep} is the electrophoretic velocity (cm/s), E is the electric field strength (V/cm), L_c is the length of the entire capillary, L_d is the length of the capillary from the injection end to the detection window, t_r is the migration time, and V is the voltage applied across the capillary.

Electroosmosis

Figure 1.3 shows another fundamental process in capillary zone electrophoresis: electroosmosis.



Due to their UV transparency, fused silica capillaries are typically used for separation in capillary electrophoresis. There are ionizable silanol groups on the inner surface of the capillary wall. The isoelectric point (pI) of the silanol group is 1.5 [18]. The degree of ionization depends mainly on the pH of the buffer within the capillary. When a capillary is filled with alkaline buffer, the silanol groups deprotonate, which results in a highly negatively charged surface. The negatively

charged capillary wall attracts positively charged ions from the bulk buffer solution, creating an electric double layer.

When a voltage is applied across the capillary, electroosmosis occurs: the solvated cations in the diffuse layer migrate toward the cathode (the detection end of the capillary). Electroosmosis moves the bulk buffer solution as a plug in the capillary toward the detection end.

The pH effect on electroosmotic mobility in fused silica capillaries has been demonstrated experimentally [19]. At low pH, the deprotonization of the inside capillary surface silanol groups is suppressed and the electroosmotic flow approaches zero. Under alkaline conditions, the silanol groups are fully charged and the electroosmotic flow reaches a plateau value. Therefore, the buffer pH is an important parameter used to optimize separations in capillary electrophoresis.

The electroosmotic mobility, μ_{eo} , is defined by [18]

$$\mu_{eo} = \frac{v_{eo}}{E} = \frac{\epsilon \zeta}{4 \pi \eta} \quad (1.3)$$

where v_{eo} is the electroosmotic flow velocity (cm/s), E is the electric field strength (V/cm), ϵ is the dielectric constant of the solution, η is the viscosity, and ζ is the zeta potential at the plane of shear close to the liquid-solid interface.

Because the electroosmotic flow is sufficiently stronger than the electrophoretic migration at neutral to alkaline pH, all sample components (anions, neutrals, and cations) are swept out of the capillary at the cathode end. The order of migration is cations, neutrals, and anions. The overall migration velocity is the sum of the electrophoretic velocity and the electroosmotic velocity:

$$v_{overall} = v_{ep} + v_{eo} \quad (1.4)$$

The time that it takes a solute to migrate the length of the capillary from the injection end to the detection window is defined as the migration time (t_r) of the analyte, which can be given by the following equation:

$$t_r = \frac{L_d}{u_{ep} + u_{eo}} \quad (1.5)$$

1.1.5 Separation Efficiency

In capillary electrophoresis, the separation efficiency can be described in terms of theoretical plate count (N). Since electroosmosis flow is the driving force in capillary zone electrophoresis, there is no pressure drop and the flow velocity is uniform across the entire tubing diameter except very close to the capillary wall where the velocity approaches zero. Longitudinal diffusion contributes the most to band broadening:

$$\begin{aligned} \sigma^2 &= 2 D t_r = 2 D \frac{L_d}{u_{ep} + u_{eo}} \\ \sigma^2 &= 2 D \frac{L_d}{(\mu_{ep} + \mu_{eo}) V} \end{aligned} \quad (1.6)$$

where σ^2 is the spatial variance of a zone after a time of t_r , D is the diffusion coefficient of the solute (cm^2/s), L_d is the capillary length (cm) from the injection end to the detection window, and V is the voltage applied across the capillary.

The number of theoretical plates due to diffusion can be calculated by the following equation:

$$N = \frac{L_c^2}{\sigma^2} = \frac{(\mu_{ep} + \mu_{eo}) V}{2 D} \quad (1.7)$$

The above equation shows that the theoretical plate count is independent of the capillary length and that there is a linear relationship between plate count and applied voltage. The practical limit for using high electric fields is Joule heating.

The plate count can be estimated experimentally by the following equation:

$$N = 5.54 \left(\frac{t_r}{w_{1/2}} \right)^2 \quad (1.8)$$

where t_r is the migration time of a component in the sample solution and $w_{1/2}$ is the full peak-width at one-half peak height (in units of time).

1.1.6 Resolution

Resolution (R) is a measure of the separation between two peaks. The resolution in capillary electrophoresis is given by

$$R = \frac{1}{4} N^{\frac{1}{2}} \frac{\Delta v}{\bar{v}} \quad (1.9)$$

where N is the average theoretical plate count, Δv is the difference in the migration velocities of the two components, and \bar{v} is the average zone migration velocity.

Resolution can be estimated experimentally by the same equation used in chromatography:

$$R = \frac{t_{r,1} - t_{r,2}}{\frac{1}{2} (w_1 + w_2)} \quad (1.10)$$

where $t_{r,1}$ and $t_{r,2}$ are the migration times of component 1 and component 2, respectively, w_1 and w_2 are the full peak-widths at base line (in unit of time) of peak 1 and peak 2.

1.1.7 Capillary Electrophoresis Separation Modes

Based on different separation and operation characteristics, capillary electrophoresis can be classified into the following modes: 1) capillary zone electrophoresis (CZE); 2) micellar electrokinetic capillary chromatography (MECC); 3) capillary gel electrophoresis (CGE); 4) capillary isoelectric focusing (CIEF); 5) capillary isotachopheresis (CITP).

Capillary Zone Electrophoresis (CZE)

As the simplest separation mode of capillary electrophoresis, CZE is also known as free solution capillary electrophoresis. The capillary is filled with an aqueous buffer solution. The separation of ionic species is based on electrophoretic mobility differences. Because all electrically neutral analytes have zero electrophoretic velocity ($v_{ep} = 0$ cm/s), they migrate out of the capillary at the electroosmotic flow rate (v_{eo}) with no separation. CZE is primarily restricted to separation of anionic and cationic analytes, with virtually no limitation in molecular size.

Micellar Electrokinetic Capillary Electrophoresis (MECC)

This very important capillary electrophoresis mode not only extends the separation power of capillary electrophoresis to neutral analytes, but also improves separation of ionic analytes. Ionic surfactants are normally added to

the aqueous separation buffer to form micelles with hydrophobic interior and hydrophilic spherical surface. MECC separation is mainly based on partition of analytes between micelles (pseudo-stationary phase) and the aqueous buffer solution in addition to electrophoretic migration of charged analytes. A detailed discussion about MECC is presented in section 1.1.8.

Capillary Gel Electrophoresis (CGE)

In 1953, Edstrom reported capillary-dimension gel electrophoresis on very fine cellulose fibers (5 μm diameter) for the separation of nucleic acids from single cells at an electric field of 125 V/cm [20, 21]. In 1965, Mاتيoli and Niewisch studied hemoglobin from single cells on fine polyacrylamide fibers of 50 μm diameter [22]. Recently, the adaption of gel electrophoresis to capillary electrophoresis has been used for the analysis of oligonucleotides [23, 24], oligosaccharides [25], and proteins.

In capillary gel electrophoresis (CGE) mode, the capillary is filled with an anticonvection medium (e.g. polyacrylamide or agarose) and the electroosmotic flow is suppressed. Analytes are separated based on size due to the molecular sieving effect of the gel.

Capillary Isoelectric Focusing (CIEF)

Capillary isoelectric focusing is a powerful CE mode for separations of proteins and polypeptides [26]. Isoelectric focusing means that a molecule will migrate as long as it is charged and will stop migrating when it becomes neutral in an electric field. Zwitterionic chemicals are used as carrier ampholytes to provide a pH gradient where the pH is low at the anode and high at the cathode.

In CIEF, the first step is to load the capillary with a sample solution mixed with carrier ampholytes. When a high voltage is applied across the capillary, a pH gradient is established through the migration of positively charged ampholytes toward the cathode and that of negatively charged ampholytes toward the anode. At the same time, the protein sample components also migrate toward the points in the capillary where the pHs are equal to their isoelectric points (pI). Proteins with pIs different by less than 0.02 pH unit can be separated into discrete zones [27]. After isoelectric focusing separation, a salt (or sodium hydroxide/salt mixture) can be added into either the cathodic buffer or the anodic buffer. A high voltage is reapplied, the anions or cations of the added salt(s) compete with hydroxyl/hydronium ion migration, resulting in a pH gradient change and migration of both ampholytes and protein sample components toward the end of the capillary within the buffer reservoir with added salt.

Capillary Isotachopheresis (CITP)

In capillary isotachopheresis, separation is performed at zero electroosmotic flow and the buffer is heterogeneous. The capillary is filled with two different electrolytes: a leading electrolyte with higher electrophoretic mobility (in a reservoir) and a terminating electrolyte (in another reservoir) with lower electrophoretic mobility than any of the sample components. The sample is inserted between the leading and terminating electrolytes. During the separation process, sample components present in low concentrations are focused into concentrated narrow bands based on the individual electrophoretic mobilities of the sample components. Cations and anions can be determined in two separate runs. The separated component zones can be detected by conductivity or

concentration gradient detectors [28]. The self-concentrating effect in CITP can also be employed as a simple preconcentration method for other capillary electrophoresis separation techniques [29].

1.1.8 Micellar Electrokinetic Capillary Chromatography (MECC)

Armstrong and Herry reported their pioneering work of using micellar solutions as mobile phases in high performance liquid chromatography in 1980 [30]. Micellar electrokinetic capillary chromatography (MECC), also called as micellar capillary electrophoresis, was first reported by Terabe in 1984 [31] to extend the use of the separation power of capillary electrophoresis to electrically neutral analytes. Terabe's extensive study of MECC has demonstrated the separation power of MECC for both neutral and ionic analytes.

1.1.8A The Formation of Micelles

In the MECC separation mode, an ionic surfactant is added to the separation buffer at a concentration above its critical micelle concentration (cmc). A surfactant molecule has a hydrophobic "tail" (e.g. non-polar hydrocarbon chain) and an ionic hydrophilic "head" (e.g. polar functional group or ionic group). In an aqueous buffer solution, the monomers of the surfactant form roughly spherical micelles in a way that the hydrophobic tails of the surfactant molecules are oriented toward the center of the micelle forming a pseudo hydrophobic phase, whereas the hydrophilic heads of the molecules point toward the surface of the micelle. The number of surfactant molecules making up a micelle is called the aggregation number, which is typically in the range of 50-100 and the diameters of micelles are in the range of 3 to 6 nm [18].

1.1.8B Separation Principle

Micelles are dynamic structures and provide a pseudo-phase for liquid-liquid partition. Analytes, in particular neutral analytes, will partition between the micelles and the aqueous buffer solution within the capillary. The electroosmotic flow of the buffer solution and the electrophoretic migration of the ionic micelles make possible separation between analytes having different micellar solubilities. The rate of an analyte partitioning between micelles and the aqueous buffer must be fast enough so that zone broadening is minimized. Micellar electrokinetic capillary chromatography allows the high separation efficiency of capillary electrophoresis to be applied to neutral analytes. MECC can also improve separation of ionic analytes that even have identical mobilities [32]. The micelle can affect the electrophoretic migration of ionic species through the partitioning of the ions between the micelle and the aqueous buffer solution. All ions bound to a micelle or free in the aqueous buffer solution are subject to electrophoretic migration due to their own charges. The combination of electrophoretic and chromatographic separation mechanisms makes it hard to predict the migration time of the ionic analyte in MECC.

1.1.8C Important Parameters in MECC

The Capacity Factor (k')

To describe the distribution of a neutral analyte between micelles and the bulk aqueous buffer solution, the capacity factor, k' , is defined for MECC in a similar way as that for chromatography:

$$k' = \frac{n_{mc}}{n_{aq}} \quad (1.11)$$

where n_{mc} and n_{aq} are the amount of the analyte incorporated into the micelle and that in the aqueous buffer solution, respectively. The migration time of the neutral analyte, t_r , can be related to the capacity factor as [31]

$$t_r = \frac{1 + k'}{1 + \left(\frac{t_0}{t_{mc}}\right) k'} t_0 \quad (1.12)$$

where t_0 is the migration time of the aqueous buffer solution and t_{mc} is the migration time of the micelle. The migration time of the neutral analyte is equal to t_0 when $k' = 0$, or when the analyte does not interact with the micelle at all; the migration time is equal to t_{mc} when k' is infinity, or the analyte is totally incorporated into the micelle. An analyte that stays longer in micelles migrates at a slower velocity toward the cathode when an anionic surfactant is used. The migration time of neutral analyte is limited between the migration time window of t_0 to t_{mc} .

The migration times t_0 and t_{mc} can be determined experimentally. The marker used to indicate the migration time of the bulk buffer solution must be electrically neutral as well as totally excluded from the micelle. Methanol is usually chosen as a marker for t_0 due to its negligible incorporation into the micelle. Methanol can be detected by ultraviolet-visible absorption detectors due to a change in refractive index as it passes through the detection window. The marker for measuring the micelle migration time must be totally incorporated into the micelle. Sudan III (an organic dye), or quinine hydrochloride can be used for t_{mc} measurement. From t_0 , t_{mc} , and t_r , the capacity factor can be calculated through the above equation.

Resolution in MECC

Resolution of two adjacent peaks in MECC can be expressed [33] as:

$$R = \frac{N_2^{\frac{1}{2}}}{4} \left(\frac{\alpha - 1}{\alpha} \right) \left(\frac{k'_2}{1 + k'_2} \right) \left[\frac{1 - t_0/t_{mc}}{1 + (t_0/t_{mc}) k'_1} \right] \quad (1.13)$$

where α is the separation factor (k'_2/k'_1), and k'_1 and k'_2 are the capacity factors of peak 1 and peak 2, respectively. The factors that could affect the separation factor of a neutral analyte include applied voltage, pH of the buffer, surfactant concentration [34], and surfactant type. All the variables except surfactant type have very little effect. For neutral analytes in MECC with a given surfactant, the selectivity factors are determined almost exclusively by the micelle/aqueous buffer partition coefficients [35].

1.1.8D Selectivity Manipulation in MECC

The parameters that can effectively affect the partition coefficients include 1) temperature of the separation buffer with a surfactant; 2) the type of the surfactant and the type of micelles; 3) modification of the aqueous buffer phase.

The partition coefficient depends on temperature. An increase in temperature causes a decrease in partition coefficient and in viscosity, which results in shorter migration time. Since the dependence of the distribution coefficient on temperature is different among analytes, temperature can affect separation selectivity. But the temperature effect on selectivity is not dramatic in MECC [36].

The simplest way to modify selectivity is to try different surfactants (cationic or anionic). The use of different types of surfactants can provide

moderate changes in the separation selectivity [32]. Since most analytes interact with the surfaces of micelles, the ionic hydrophilic head is more important in terms of selectivity modification. In the case of ionic analytes, hydrophobicity and charge affect the partition coefficient. Therefore, the use of a cationic surfactant will result in an entirely different selectivity than when an anionic surfactant is used for the separation of ionic analytes. The partition coefficient can be affected by adding a second (non-ionic) surfactant as a co-surfactant to form a mixed micelle. The addition of non-ionic surfactant molecules into the original ionic micelles causes a lower surface charge and a larger size, which results in a narrower migration time window [34].

Modification of the aqueous buffer solution is another effective way to manipulate selectivity. The buffer pH plays an important role in affecting the partition coefficients of ionizable analytes by changing both the charges on the analyte molecules and their electroosmotic velocity. The partition coefficients of analytes can be altered by addition of additives to aqueous buffer solution. The possible additives are organic modifiers (solvents), urea, cyclodextrins, crown ethers, and metal ions.

1.1.8E Sodium Dodecyl Sulfate (SDS)

Sodium dodecyl sulfate is the most popular surfactant for micellar electrokinetic capillary chromatography. Sodium dodecyl sulfate, $\text{CH}_3(\text{CH}_2)_{11}\text{OSO}_3\text{Na}$, is an anionic surfactant that forms micelles at concentrations above its critical micelle concentration (8 mM). The aggregation number of SDS micelle is 62. **Figure 1.4** shows a schematic diagram of the separation principle of MECC using SDS.

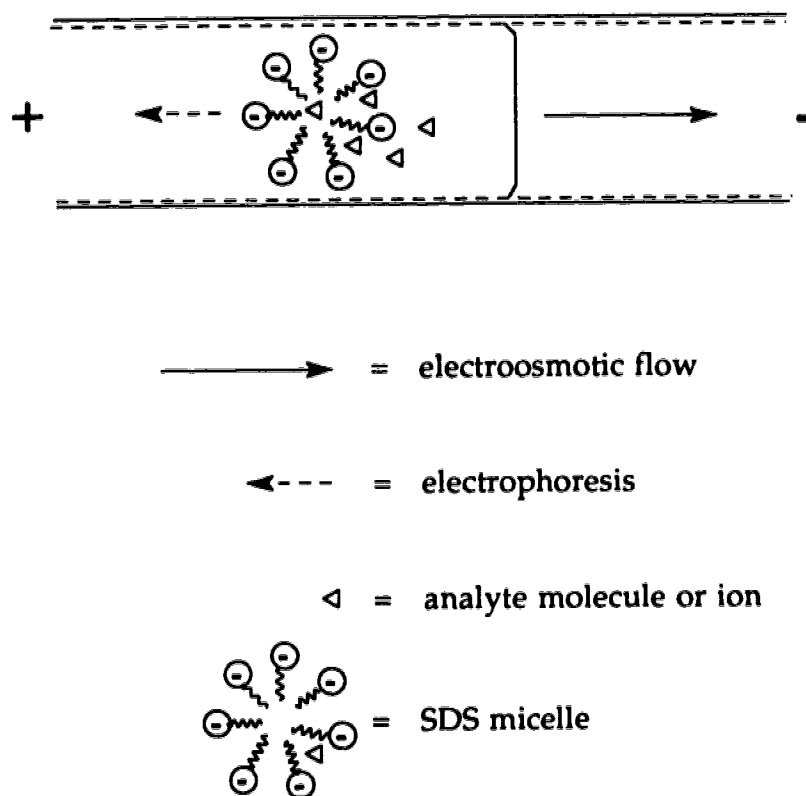


Figure 1.4 Micellar electrokinetic capillary chromatography using sodium dodecyl sulfate (SDS)

The hydrocarbon ends of the SDS molecules are oriented toward the center of the micelle forming a pseudo hydrophobic phase, whereas the negatively-charged ends of the SDS molecules leave a large number of net negative charges on the micelle surface. When an electric field is applied, the micelles tend to move toward the anode. But the strong electroosmotic flow drags the micelles toward the cathode. The net effect of electrophoretic flow and electroosmotic flow is to move micelles out of the capillary at a characteristic velocity.

1.1.9 Detection Methods

Detection sensitivity is an important issue in capillary electrophoresis. To retain high resolution separation, it is necessary to minimize both the concentration and volume of analyte injected onto the capillary. A variety of detection schemes have been developed for capillary electrophoresis. Both on-column detection and post-column detection can be coupled with capillary electrophoresis.

On-column detection

Polyimide coating near the detection end of the capillary can be removed to provide a small optical window for on-column light-based detection including UV absorbance [31, 37, 38], fluorescence [7, 8, 39-41], refractive index measurements [42, 43], and other spectroscopic methods [44].

UV absorption remains the most popular method of detection even with its rather limited sensitivity, which is due to the short path length across the capillary diameter. The mass detection limits are typically of 100 femtomoles , i.e.

10^{-13} moles, injected for low molecular weight analyte in capillary electrophoresis [45]. Fluorescence detection provides the highest sensitivity for capillary electrophoresis. Other on-column detectors include electrochemical-based (e.g. conductivity, or amperometric) [46] and radioactivity-based detection [47, 48].

Post-column detection

The analyte molecules eluting out of the detection end of the capillary can also be detected by post-column techniques such as fluorescence [24, 49-51], chemiluminescence [45, 52] and mass spectrometry (MS) [53, 54]. Capillary electrophoresis has been successfully coupled with mass spectrometry using atmospheric pressure ionization sources (i.e., electrospray and ion spray) [55]. CE-MS is becoming an increasingly popular method of obtaining characteristic information about peptide and protein mixtures [56, 57].

1.1.10 Detection Limits

Limit of detection (LOD) or detection limit may be defined as the smallest amount of an analyte that can give a signal three times higher than the standard deviation (s) of the gross blank signal. The background noise can be measured using sensitive voltage meters over a certain period of time and the standard deviation can be calculated. But like chromatography, detection limits in capillary electrophoresis may be more conveniently calculated by Knoll's method [58]; the electropherogram baseline is inspected over a time period given by 10-100 times the full peak-width in terms of time ($w_{1/2}$) at one-half peak height. The

maximum deviation (h_n) from the average of the baseline is used to estimate the 3σ detection limit:

$$C_{\text{LOD}} = K_{\text{LOD}} h_n C_s / h_s \quad (1.14)$$

where C_{LOD} is the concentration limit of detection, h_s/C_s is the analyte peak height/unit amount of analyte, K_{LOD} is a constant that is determined for the time period employed. Values of K are listed in **Table 1.1**:

Table 1.1 Multiplier constants for limit of detection of Knoll's method

peak width multiple	10	20	50	100
K_{LOD}	1.9718	1.4309	0.9194	0.6536

This technique, based on the Tchebycheff inequality, relies on robust statistics. Very weak assumptions are made on the underlying noise distribution in the data. More importantly, correlation introduced between adjacent datum due to filtering does not artificially underestimate the standard deviation of the baseline. Relatively precise estimates of the detection limit are produced by inspecting the baseline over a large number of samples.

To calculate detection limit in capillary electrophoresis, the peak height (h_s) and the maximum deviation (h_n) are obtained from the electropherogram of a very diluted sample (C_s). The number of moles of analyte corresponding to the limit of detection can be calculated through the following equations:

$$\text{capillary volume:} \quad V_c = \pi r^2 L_c \quad (1.15)$$

$$\text{injection volume:} \quad V_{inj} = V_c \left(\frac{t_{inj}}{t_r} \right) \left(\frac{\text{injection voltage}}{\text{CE voltage}} \right) \quad (1.16)$$

$$\text{number of moles injected:} \quad n_{inj} = C_s V_{inj} \quad (1.17)$$

$$\text{detection limit:} \quad n_{LOD} = K_{LOD} n_{inj} (h_n / h_s) \quad (1.18)$$

The spectacular low detection limits in capillary electrophoresis can be described using the following units: femtomole (10^{-15} mole), attomole (10^{-18} mole), zeptomole (10^{-21} mole), and yoctomole (10^{-24} mole).

1.2 POST-COLUMN LASER-INDUCED FLUORESCENCE (LIF) DETECTION

1.2.1 General Introduction

Detection limits in fluorescence measurements are usually determined by shot-noise in the background signal. Parker lists four sources of background signal in fluorescence: 1) Fluorescence from solvent impurities, 2) fluorescence from cuvette windows, 3) Raman and Rayleigh scatter from the solvent, and 4) light scatter at the cuvette-sample interface [59]. Detector dark current is a fifth source of background. To produce excellent detection limits, each of these sources of background signal must be minimized. Solvent impurities are minimized by scrupulous care in sample and buffer preparation. Disposable plastic-ware is used for sample preparation; buffers are kept in special glassware,

and a clean-air hood is used to provide a dust-free environment for sample and buffer preparation. Detection limits for my system often corresponded to 10^{-12} M analyte; a nanogram of contaminant in a liter of water would have generated a background signal that swamped the analyte signal.

Laser-induced fluorescence (LIF) is well suited for detection in capillary electrophoresis and is the most sensitive detection scheme for capillary electrophoresis. As monochromatic excitation light sources, lasers have made spectacular improvements in detection limits in fluorescence measurements. The high spatial coherence of a laser allows very small sample volumes to be probed with high efficiency. This coherence allows the use of capillaries with very small diameter, as low as 10 μm . When coupled with efficient collection and detection, minute amounts of analyte may be detected.

In 1985, Zare's research group reported the first application of on-column laser-induced fluorescence detection in capillary electrophoresis [60]. Femtomole amounts of dansyl labeled amino acids were detected. On-column laser-induced fluorescence detection requires removal of the polyimide coating outside of the fused silica capillary to provide a small on-column transparent window near the exit end of the capillary. A laser beam is focused onto the detection window to induce fluorescence within the capillary. Fluorescence collection is accomplished at right angles to both the incident laser beam and the sample stream flowing in the capillary. On-column laser-induced fluorescence detection has an advantage of no extra column bandbroadening, but suffers from a relatively large amount of light scatter, which generates a large amount of background signal due to reflection and refraction at the cylindrical capillary walls.

Post-column laser-induced fluorescence detection requires careful design to minimize undesirable extra column band broadening. An ideal way to reduce

the background noise from light scattering is to measure fluorescence in a post-column flow chamber with flat windows providing good optical quality. A post-column laser-induced fluorescence detector using a sheath flow cuvette was developed to provide extremely high sensitivity for capillary electrophoresis by Dovichi's group. Detection limits have been improved from sub-attomole (10^{-18} mole) in 1988 [49], low zeptomole (10^{-21} mole) range in 1992 [61] to yoctomole (10^{-24} mole) in 1993. Single molecule detection of highly fluorescent sulforhodamine 101 has been achieved with a low-cost green helium-neon laser operated at 594 nm with 8 mW power [13].

1.2.2 Instrumentation

1.2.2A Sheath Flow Cuvette

Light scatter at the solvent windows is eliminated by eliminating the refractive index discontinuity associated with the sample-window interface. A sheath flow cuvette, **Figure 1.5**, taken from a flow cytometer, is interfaced with capillary electrophoresis as a post-column fluorescence detector [62-67]. The cuvette is made from optically flat quartz. Typically, the cuvette has 2-mm thick windows and a 200- μm square hole in the center. A specially designed metal holder is used to hold the cuvette and provide inlet for sheath flow. The exit of a capillary with outer diameter less than 200- μm is inserted into the square flow chamber. A sheath buffer, which is identical to the separation buffer, is supplied with a high-precision syringe pump to flow through the cuvette. A simple alternative way to provide sheath flow is to form a siphon by raising the sheath buffer level a few centimeters above the solution level in the waste vial.

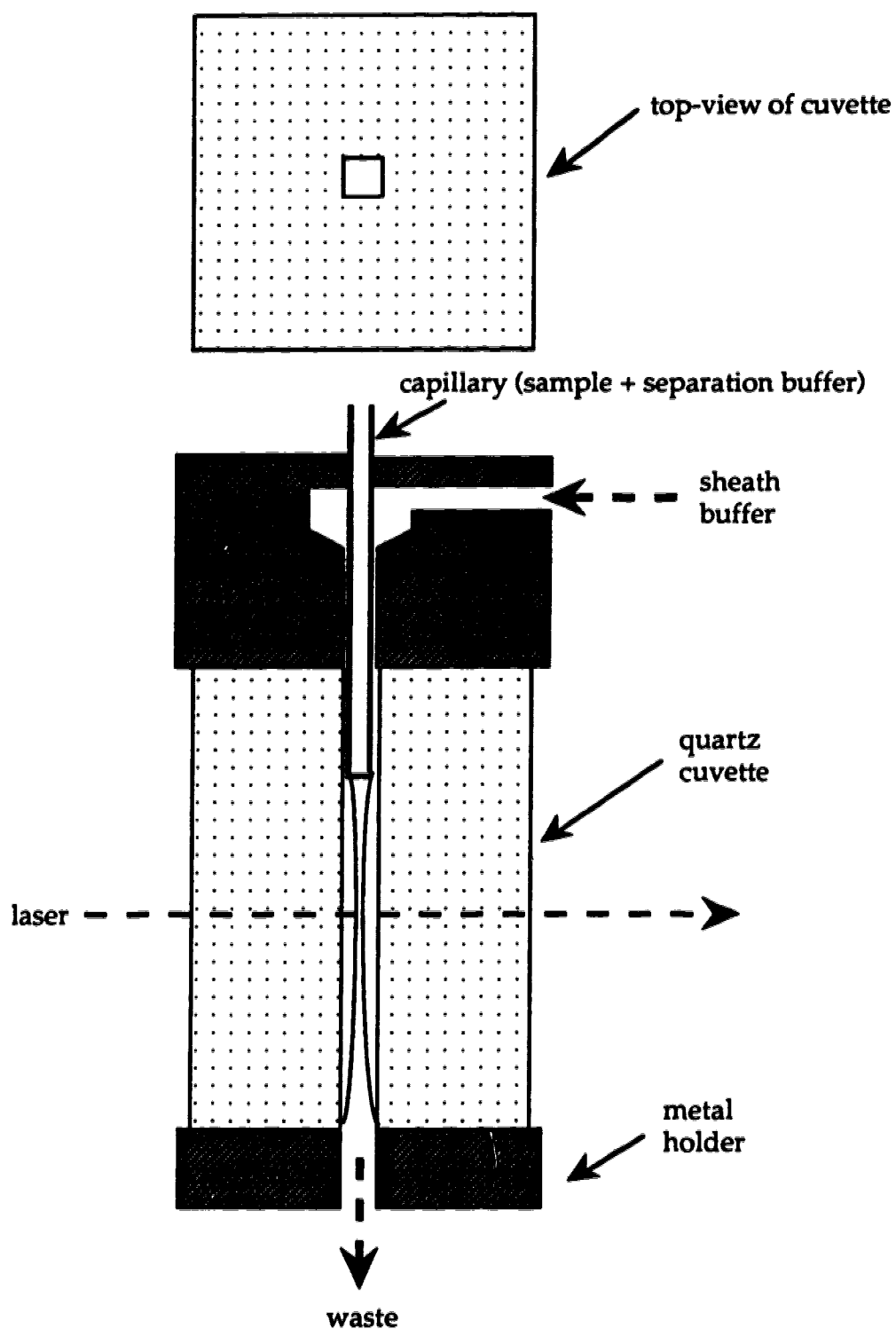


Figure 1.5 Sheath flow cuvette as a post-column laser-induced fluorescence detector for capillary electrophoresis

In this detector, the solution coming out of the capillary at a low linear velocity is dynamically focused into a fine stream in the center of a sheath stream flowing at a much higher linear velocity. Because the sample solution is surrounded by buffer of identical refractive index, there is no light scatter generated at the sample-sheath interface. The square-walled detection chamber provides high optical quality windows for low background fluorescence measurements.

1.2.2B Lasers

A laser beam provides several important properties as an excitation light source, including spectral purity, high power, temporal coherence and spatial coherence. Continuous wave (cw) gas lasers are chosen as light sources due to their excellent spatial coherence and long lifetime. The excellent spatial coherence makes it possible to focus a laser beam into a small (a few mm) spot, which matches the size of the sample stream in the sheath flow cuvette to minimize the detector volume.

The choice of laser is first based on the spectral properties of the analyte. The wavelength of the laser must match well the maximum absorbance of the analyte. In practice, if more than one component is present in the sample, it is possible to optimize the laser wavelength by labeling the components with the same fluorescent molecules. For example, tetramethylrhodamine isothiocyanate can be used to label amine-containing analytes such as amino acids, peptides and proteins. The maximum absorbance of tetramethylrhodamine isothiocyanate derivatives is at about 550 nm, which is matched by the 543.5-nm line of the recently commercialized green helium-neon laser.

In well designed fluorescence detectors, Raman scatter from the solvent is the major source of background signal. Water has two Raman bands, one at about 1650 cm^{-1} and the other ranging from 3100 to about 3700 cm^{-1} . There are also two minor Raman bands at 1640 and 2200 cm^{-1} . To avoid Raman scatter from water, the excitation wavelength should be chosen so that the analyte emission wavelength occurs where the Raman signal is relatively weak [68].

Laser power and stability are also important parameters in choosing a laser as excitation source in laser-induced fluorescence measurements. A high-stability laser is required to obtain shot-noise limited performance. Under shot-noise conditions, the noise in the background increases with the square root of laser power while the fluorescence signal gains linearly with the laser power. The high irradiance of a focused laser beam results in better detection limits than can be produced by an incoherent light source. But extremely high laser power and irradiance are limited in use because optical saturation of the absorbance transition and photo degradation of the analyte molecules occur. For highly fluorescent molecules, the laser irradiance should be held to a value less than 10^5 W cm^{-2} to avoid saturation. Both saturation and photo degradation limit the utility of pulsed lasers for fluorescence excitation in capillary electrophoresis. Instead, moderate to low power continuous wave lasers are suited for high sensitivity fluorescence detection for capillary electrophoresis. Examples are argon ion and helium-neon lasers.

1.2.2C Focusing Optics

The laser beam is directed by mirrors to the sheath flow cuvette at right angles to the cuvette walls. Inexpensive and high quality microscope objectives

may be used to focus the laser beam into a spot where the laser beam excites the analyte molecules.

1.2.2D Fluorescence Collection

Careful optical design of high efficiency collection of fluorescence can maximize the number of fluorescence photons reaching the photo detector and minimize the background signal intensity to improve detection limits. Fluorescence is collected at right angles to both the sample stream and the laser beam with a good numerical aperture microscope objective. The collection efficiency is related to the numerical aperture, N.A., and the refractive index of the surrounding medium, n , as the following equation:

$$\text{collection efficiency} = \sin^2 \left[\frac{\arcsin (\text{N.A.}/n)}{2} \right] \quad (1.19)$$

where a collection of 1 implies that the lens collects all of the photons emitted by a fluorescent molecule. Because the lens is usually surrounded by air and $n = 1.0$, a high collection efficiency requires a lens of very high numerical aperture. Table 1.2 lists the collection efficiencies of lenses with different numerical apertures [68].

Table 1.2 Collection efficiency of microscope objectives ($n = 1.0$)

numerical aperture	1.0	0.9	0.8	0.7	0.6	0.5	0.4	0.3	0.2	0.1
collection efficiency	0.500	0.280	0.200	0.140	0.100	0.067	0.042	0.023	0.010	0.003

A lens with a numerical aperture of 1.0 will collect half of the light emitted by the illuminated sample. To collect fluorescence signal in the sheath flow cuvette, the working distance (the distance from the exit of the lens to the illuminated sample) of the lens has to be greater than 2 mm because of the 2-mm thickness of the cuvette windows.

The microscope objective images the illuminated sample stream onto a pinhole that acts as a mask to block scattered laser light from the cuvette walls. The size of the pinhole is matched to the size of the sample image. Either a pinhole with fixed size or an iris with adjustable pinhole size may be employed for the above purpose.

1.2.2E Spectral Filters

After the spatial mask and before the photo detector, a spectral filter may be used to reject both the Rayleigh scattered light at the laser wavelength and the Stokes-shifted Raman scatter while maximizing transmission of fluorescence. The spectral filter provides higher throughput (> 50% transmission) and much easier alignment compared with the use of a monochromator.

1.2.2F Photo Detectors

A photo detector, which only sees the fluorescence from the illuminated sample stream, responds to the fluorescence signal and converts it into an electrical signal with high efficiency. Conventionally, a photomultiplier tube (PMT) is used in fluorescence detection.

1.2.3 Fluorescent Derivatization of Analytes

Two major limitations of laser-induced fluorescence detection are the limited available wavelengths of lasers and the non-fluorescent nature of most analytes of interest. But the extremely high sensitivity provided by laser-induced fluorescence detection has drawn considerable interest in the development of methods for such compounds. Both pre-column and post-column derivatization have been used to introduce fluorescent dyes that react with the analytes of interest.

Pre-column derivatization

Before injecting into the capillary for electrophoresis separation, analytes react with fluorescent dyes to form fluorescent derivatives using conventional chemical apparatus. Pre-column derivatization has a number of general advantages. First, no specialized apparatus or techniques are required. The labeling reaction conditions can be modified in any manner required to maximize conversion to fluorescent derivatives. Second, the labeling reactions need not to be rapid to be useful. Third, side products or excess fluorescent reagents can be separated from the reaction mixture, either by a procedure prior to injection of the derivatized sample into the capillary or by capillary electrophoresis separation.

There are two disadvantages of most pre-column derivatization methods for capillary electrophoresis separation. First, after derivatization the differences in size between similar compounds becomes smaller, which may require considerable effort to optimize the separations. Second, multifunctional analyte molecules may produce two or more fluorescent products that are likely to

exhibit different migration times, which will make the interpretation of the electropherogram difficult.

Post-column derivatization

After separation by capillary electrophoresis, the analytes enter a mixing chamber where they react with the fluorescent probes in a short period of time and the fluorescent derivatives of the analytes are detected by laser-induced fluorescence detectors. Post-column derivatization requires sufficiently fast labeling reactions and carefully designed apparatus to carry out the reaction, which are necessary to minimize degradation of the high efficiency separation by capillary electrophoresis and to keep the % derivatized consistent from run to run.

1.2.3A Criteria for Choosing Fluorescent Dyes

The criteria for choosing a fluorescent dye are based both on the spectral properties of the chromophore and the reactivity between the modification probe and the analyte:

- 1) The fluorescent dye must be excited easily with an available laser source,
- 2) The fluorescent dye must have a reasonably high fluorescent quantum yield and low photodestruction rate,
- 3) The fluorescent dye must have a reactive functional group to react with the analyte of interest,
- 4) The fluorescent dye must be stable and reacts quickly with analytes to produce stable derivatives.

Fluorophors

Fluorescein and rhodamine are two very useful fluorophors. The maximum absorption wavelength (490 nm) of fluorescein closely matches the 488 nm line of the argon ion laser and the maximum absorption wavelength (550 nm) of rhodamine closely matches the 543.5 nm line of the green helium-neon laser. In general, long-wavelength excitation generates low background signal because the scattered light intensity scales roughly as λ^{-4} and relatively few impurity molecules absorb long-wavelength light.

Reactive Probes for Amine Groups

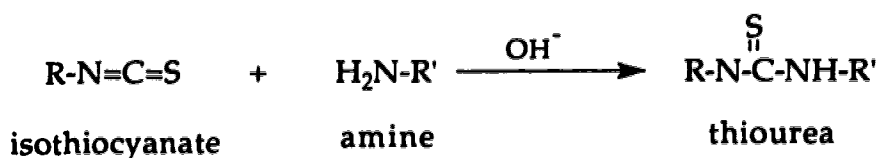
As one of the commonly found groups in biomolecules, primary amines can be reliably modified in aqueous solution. There are three major classes of labeling reagents commonly used for amine modification: isothiocyanates, succinimidyl esters, and sulfonyl halides. The reactions of an amine with a probe through an acylation reaction form thioureas, carboxamides, or sulfonamides [69].

One important application of capillary electrophoresis is the separation and characterization of amino acids, peptides and proteins, and carbohydrates. To use high sensitivity laser-induced fluorescence detection, those biomolecules have to be labeled with fluorescent dye molecules. Virtually all proteins have lysine residues that contain ϵ -amine groups and most have a free amine terminus. Non-amino carbohydrates can be reductively aminated [70].

Reactivity is most significantly affected by the class of the amine and its basicity. The acylation of an amine with a probe requires the non-protonated

form of the amine. Aliphatic amines are moderately basic. The reaction of aliphatic amine with an acylation probe is strongly pH dependent. The concentration of the free base form of ϵ -amino group of lysine is very low below pH 8, but the α -amino group at the N-terminus of a peptide usually has a pKa of ~ 7 . The pH range usually used to carry out the acylation reactions is from neutral to 9.5, since higher pH will cause faster degradation of the acylation reagent in the presence of water. The non-basic "amines" found in nucleotides such as adenosine or guanosine and the amide group of peptides are virtually non-reactive with these reagents in aqueous solution.

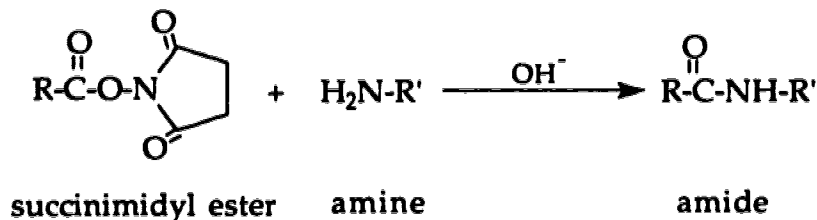
Isothiocyanates (R-N=C=S) Isothiocyanates react selectively with primary amines to form thioureas:



where R is a fluorophore and R' can be any function group. Sodium bicarbonate or borate buffer (0.1-0.2 M) at pH 9.0 is recommended for carrying out the conjugation between isothiocyanates and amine-containing analytes [71].

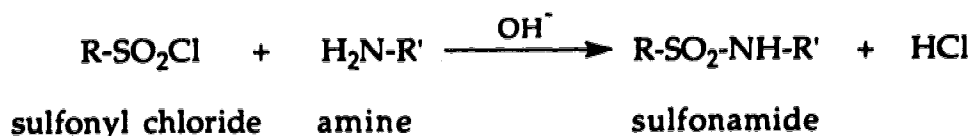
The isothiocyanates are moderately reactive. The thiourea group is reasonably stable for a short period of time, but then deteriorates. Fluorescein isothiocyanate (FITC) and tetramethylrhodamine isothiocyanate (TRITC) are the most widely used fluorescent dyes for labeling amine-containing biomolecules and in the preparation of fluorescent antibody conjugates. The labeling reactions must be carried out in the dark for several hours.

Succinimidyl esters These reagents are excellent labeling reagents for amine modification, since they have good reactivity with aliphatic amines and the amide derivatives formed are as stable as peptide bonds. Succinimidyl ester stock solutions can be prepared in dry dimethylformamide (DMF) or dimethylsulfoxide (DMSO). The best pH for labeling reaction is 7.5-8.5. The recommended buffer is 0.1-0.2 M sodium bicarbonate without correction of pH (approximately 8.3). The labeling reaction, as shown below, can be carried out at room temperature in the dark for less than one hour.



Once mixed with aqueous buffer, succinimidyl esters will experience hydrolysis that competes with the labeling reactions. Fortunately, the hydrolysis is usually slow below pH 9.

Sulfonyl halides As highly reactive probes, sulfonyl halides react with aliphatic amines to form extremely stable sulfonamides that are resistant to hydrolysis under the conditions required for amino acid analysis of proteins. Sulfonyl halides are unstable in DMSO, but can be dissolved in dry DMF. The sulfonyl chloride labeling reaction is shown below:



The recommended buffer for the above reaction is 0.1-0.2 M sodium bicarbonate or borate at pH 9. The labeling reactions are usually very fast.

Like succinimidyl esters, sulfonyl halides are unstable in water, especially at the higher pH required for the amine labeling reaction to happen. The rapid hydrolysis of sulfonyl halides makes difficult the labeling of small molecules such as amino acids. But, sulfonyl halides are useful in protein conjugation, since excess amounts of fluorescent sulfonyl halides can be separated from the conjugates through column gel filtration.

1.2.3B Fluorescent Dyes

Three fluorescent dyes used in this thesis are fluorescein isothiocyanate (FITC), tetramethylrhodamine isothiocyanate (TRITC), and 5-carboxytetramethylrhodamine succinimidyl ester (TRSE). Their structures are shown in Figure 2.1 and Figure 4.1. Some spectral and experimental parameters of these three fluorescent dyes are listed in Table 1.3.

Table 1.3 Parameters of three fluorescent dyes

dye	FITC	TRITC	TRSE
solvent buffer pH	9	9	9
ϵ ($M^{-1} cm^{-1}$)	7.7×10^4	10.0×10^4	8.0×10^4
maximum absorbance	494	555	552
laser	Ar+ (488 nm)	He-Ne (543.5 nm)	He-Ne (543.5 nm)
maximum emission	518 nm	579 nm	570 nm
spectral filter	515DF20	580DF40	580DF40

1.3 CHEMILUMINESCENCE (CL) DETECTION FOR CE

1.3.1 General Introduction

The phenomenon of chemiluminescence was first named and described by Eilhard Weidemann in 1888 [72] as "light emission occurring as a result of chemical processes". Chemiluminescence still remains a very active research area as a sensitive method for chemical analysis.

Chemiluminescence (CL) is the light-emission produced by a chemical reaction without any associated generation of heat. In a chemiluminescence reaction, an electronically excited state is produced that emits light as it returns to its ground state. Three conditions are required for CL to occur: 1) The chemical reaction must release sufficient energy to populate an excited energy state; 2) the reaction pathway must favor the formation of excited state product; and 3) the excited state product must be capable of emitting a photon itself (direct CL) or transferring its energy to another molecule that can emit (indirect, energy transfer, or sensitized CL). The light emission intensity in a CL reaction are determined both by the chemical reaction rate and by chemiluminescence quantum yield. The CL quantum yield is defined as the ratio of the number of photons emitted to the number of molecules reacted. It is the product of the excitation quantum yield (i.e. the ratio of the number of molecules at excited state to the number of molecules reacted) and the emission quantum yield (i.e. the ratio of the number of photons emitted to the number of molecules at excited state).

CL offers some advantages for chemical analysis. First of all, CL is an extremely sensitive technique; detection limits less than 10^{-12} M were reported

for diethylisoluminol [73]. Like fluorescence, quantitation is based on detection of light; through use of high efficiency photo detectors, extremely high sensitivity detection is possible. Unlike fluorescence, the detection limit is usually determined by reagent purity rather than unavoidable Raman scatter. Also, unlike fluorescence, a maximum of one photon is produced for each analyte molecule. Second, CL detection does not require an excitation light source, which greatly simplifies the detector design and can decrease the detector cost compared with fluorescence. The instrumentation for CL detection consists of a system to mix reagents with analytes and a light detector.

Many of the early analytical applications of CL were focused on trace transition metal ions based on their catalytic or enhancing action on the chemiluminescence signal. Chemiluminescence detection has been used in flow injection systems.

The chemiluminescence literature inevitably states that the detection limit is set by noise in the background signal produced by contaminants in the solution. If this holds for liquid chromatography, then the detection limit (expressed in units of moles) will scale linearly with sample volume. Capillary zone electrophoresis utilizes nanoliters of sample for separation; detection limits are expected to fall near one attomole.

1.3.2 Chemiluminescence Reactions

Luminol: The chemiluminescence from the oxidations of luminol (5-amino-2,3-dihydrophthalazine-1,4-dione) in alkaline solutions was first observed in 1928 [74]. As one of the best known and most efficient chemiluminescence reactions, the oxidation reaction of luminol with the most useful oxidant,

hydrogen peroxide, requires a catalyst in an alkaline solution and produces 3-aminophthalate, with the emission of blue light that is centered at about 425 nm, **Figure 1.6.**

Other oxidants that can be used in the luminol CL reaction include permanganate, hypochlorite, and iodine. Typical catalysts are transition metal ions (e.g., Co^+ , Cu^{2+} , Fe^{3+}), ferricyanide, peroxidase, and hemin [75].

Several features of the luminol CL reaction make it suitable for use as a detection for capillary electrophoresis [45]. First, the reaction is fast at room temperature. Second, luminol has very high chemiluminescence quantum yields, ranging from 0.01 to 0.05 depending on conditions in the reaction solution [76]. Third, there is commercially available isoluminol isothiocyanate that can be used as a chemiluminescence derivatizing reagent for amine-containing analytes [77].

Acridinium: The reaction of acridinium ester with hydrogen peroxide in the presence of a base is another chemiluminescence reaction used for capillary electrophoresis [52]. This CL reaction has a high CL efficiency and a reasonable fast reaction rate. There are modified acridiniums with functional groups suitable for derivatizing biomolecules [78].

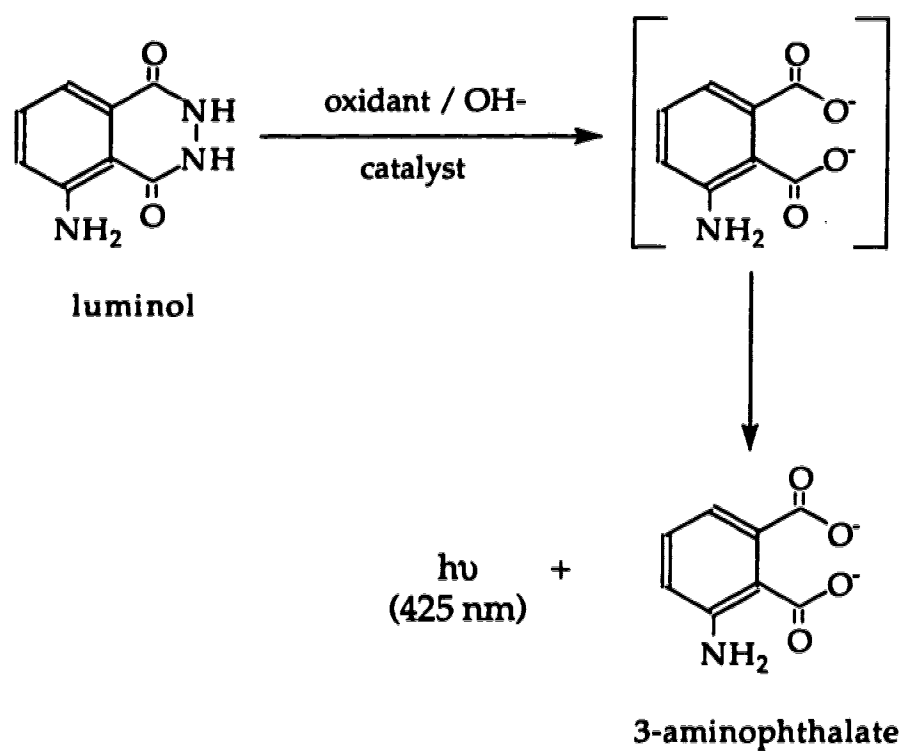


Figure 1.6 Luminol chemiluminescence reaction with hydrogen peroxide

REFERENCES

1. B. M. Turner, *Mikrochim. Acta* **III**, 305-318 (1958).
2. B. M. Turner, *Nature* , **179**, 964-965 (1957).
3. S. Hjerten, *Chromatographic Reviews* , **9**, 122-219 (1967).
4. F. E. P. Mikkers, F. M. Everaerts, T. P. E. M. Verheggen, *J. Chromatogr.* , **169**, 1-10 (1979).
5. F. E. P. Mikkers, F. M. Everaerts, T. P. E. M. Verheggen, *J. Chromatogr.* , **169**, 11-20 (1979).
6. J. W. Jorgenson, K. D. Lukacs, *Clin. Chem.* , **27**, 1551-1553 (1981).
7. J. W. Jorgenson, K. D. Lukacs, *Anal. Chem.* , **53**, 1298-1302 (1981).
8. J. W. Jorgenson, K. D. Lukacs, *Science* , **222**, 266-272 (1983).
9. M. J. Eby, *Bio/technology* , **7**, 903-911 (1989).
10. X. Huang, M. J. Gordon, R. N. Zare, *Anal. Chem.* , **60**, 375-377 (1988).
11. S. Honda, S. Iwase, S. Fujiwara, *J. Chromatogr.* , **404**, 313-320 (1987).
12. J. McCabe, *Canadian Chemical News* , **February**, 16-18 (1991).
13. D. Y. Chen, Ph. D. Thesis in Chemistry, University of Alberta (1993).
14. T. Tsuda, T. Mizuno, J. Akiyama, *Anal. Chem.* , **59**, 799-800 (1987).
15. R. A. Wallingford, A. G. Ewing, *Anal. Chem.* , **59**, 678-681 (1987).
16. R. A. Wallingford, A. G. Ewing, *Anal. Chem.* , **60**, 1972-1975 (1988).
17. M. Deml, F. Foret, P. Bocek, *J. Chromatogr.* , **320**, 159-165 (1985).
18. *Introduction to capillary electrophoresis* , (Beckman Instruments, Inc., 1992).
19. W. J. Lambert, D. L. Middleton, *Anal. Chem.* , **62**, 1585-1587 (1990).
20. J. E. Edstrom, *Nature* , **172**, 809 (1953).

21. J. E. Edstrom, *Biochim Biophys Acta* , **22**, 378-388 (1956).
22. G. T. Mاتيoli, H. B. Niewisch, *Science* , **150**, 1824-1826 (1965).
23. D. Y. Chen, H. R. Harke, N. J. Dovichi, *Nucleic Acids Research* , **20**, 4873-4880 (1992).
24. H. Swerdlow, et al., *Anal. Chem.* , **63**, 2835-2841 (1991).
25. J. Liu, O. Shiota, M. Novotny, *J. Chromatogr.* , **559**, 223-235 (1991).
26. J. Wu, J. Pawliszyn, *J. Microcol. Sep.* , **4**, 419-422 (1993).
27. M. Zhu, R. Rodriguez, T. Wehr, *J. Chromatogr.* , **559**, 479 (1991).
28. J. Wu, J. Pawliszyn, *J. Microcol. Sep.* , **5**, 217-222 (1993).
29. F. Foret, V. Sustacek, P. Bocek, *J. Microcol. Sep.* , **2**, 229 (1990).
30. D. W. Armstrong, S. J. Herry, *J. Liq. Chromatogr.* , **3**, 657-662 (1980).
31. S. Terabe, K. Otsuka, K. Ichikawa, A. Tsuchiya, T. Ando, *Anal. Chem.* , **56**, 111-113 (1984).
32. K. Otsuka, S. Terabe, T. Ando, *J. Chromatogr.* , **332**, 219-226 (1985).
33. S. Terabe, k. Otsuka, T. Ando, *Anal. Chem.* , **57**, 834-841 (1985).
34. E. L. Little, J. P. Foley, *J. Microcol. Sep.* , **4**, 145-154 (1992).
35. J. P. Foley, *Anal. Chem.* , **62**, 1302-1308 (1990).
36. A. T. Balchunas, M. J. Sepaniak, *Anal. Chem.* , **60**, 617-621 (1988).
37. Y. Walbroehl, J. W. Jorgenson, *J. Chromatogr.* , **315**, 135-143 (1984).
38. M. Yu, N. J. Dovichi, *Anal. Chem.* , **61**, 37-40 (1989).
39. J. S. Green, J. W. Jorgenson, *J. Chromatogr.* , **352**, 337-343 (1986).
40. W. G. Kuhr, E. S. Yeung, *Anal. Chem.* , **60**, 2642-2644 (1988).

41. M. Albin, R. Weinberger, E. Sapp, S. Moring, *Anal. Chem.* , **63**, 417-422 (1991).
42. J. Wu, T. Otake, T. Kitamori, T. Sawada, *Anal. Chem.* , **63**, 2216-2218 (1991).
43. A. E. Bruno, B. Krattiger, F. Maystre, H. M. Widmer, *Anal. Chem.* , **63**, 2689-2697 (1991).
44. W. G. Kuhr, C. A. Monnig, *Anal. Chem* , **64**, 389R-407R (1992).
45. R. Dadoo, L. A. Colon, R. N. Zare, *J. High Resolut. Chromatogr.* , **15**, 133-135 (1992).
46. P. D. Curry, S. C. E. Engstrom, A. G. Ewing, *Electroanalysis* , **3**, 587-596 (1991).
47. S. L. J. Pentoney, R. N. Zare, J. F. Quint, *Anal. Chem.* , **61**, 1642-1647 (1989).
48. K. D. Altria, C. F. Simpson, A. K. Bharij, A. E. Theobald, *Electrophoresis* , **11**, 732 (1990).
49. Y. F. Cheng, N. J. Dovichi, *Science* , **242**, 562-564 (1988).
50. Y. F. Cheng, S. Wu, D. Y. Chen, N. J. Dovichi, *Anal. Chem.* , **62**, 496-503 (1990).
51. E. Arriaga, D. Y. Chen, X. L. Cheng, N. J. Dovichi, *J. Chromatogr.* , **652**, 347-353 (1993).
52. M. A. Ruberto, M. L. Grayeski, *Anal. Chem.* , **64**, 2758-2762 (1992).
53. M. J. F. Suter, B. B. DaGue, W. T. Moore, S. N. Lin, R. M. Caprioli, *J. Chromatogr.* , **553**, 101-116 (1991).
54. Z. Deyl, R. Struzinsky, *J. Chromatogr.* , **569**, 63-122 (1991).

55. R. D. Smith, J. A. Olivares, N. T. Nguyen, H. R. Udseth, *Anal. Chem.* , **60**, 436-441 (1988).
56. P. Thibault, S. Pleasance, *Rapid Commun. Mass Spectrom.* , **5**, 484-490 (1991).
57. I. M. Johannson, E. C. Huang, J. D. Henion, *J. Chromatogr.* , **554**, 311-327 (1991).
58. J. E. Knoll, *J. Chrom. Sci.* **23**, 422-425 (1985).
59. C. A. Parker, *Photoluminescence of Solutions*, New york: Elsevier, Section 5C (1968)
60. E. Gassmann, J. E. Kuo, R. N. Zare, *Science* , **230**, 813-815 (1985).
61. J. Y. Zhao, D. Y. Chen, N. J. Dovichi, *J. Chromatogr.* , **608**, 117-120 (1992).
62. D. C. Nguyen, R. A. Keller, J. H. Jett, J. C. Martin, *Anal. Chem.* , **59**, 2158-2160 (1987).
63. P. Tempst, L. Rivier, *Anal. Biochem.* , **183**, 290-300 (1989).
64. M. R. Melamed, P. F. Mullaney, M. L. Mendelsohn, *Flow Cytometry and Sorting*, New York: Wiley (1979).
65. D. Pinkle, *Anal. Chem.* , **54**, 503A-519A (1982).
66. L. W. Hershberger, J. B. Callis, G. D. Christian, *Anal. Chem.* , **51**, 1444-1446 (1979).
67. T. A. Kelly, G. D. Christian, *Anal. Chem.* , **53**, 2110-2114 (1981).
68. S. Wu, N. J. Dovichi, *J. Chromatogr.* , **480**, 141-155 (1989).
69. R. P. Haugland, *Molecular Probes: Handbook of Fluorescent Probes and Research Chemicals*, K. D. Larison, Eds., (Molecular Probes, Inc., Eugene, OR, 1992).

70. J. Liu, O. Shirota, D. Wiesler, M. Novotny, *Proc. Natl. Acad. Sci.* , **88**, 2302-2306 (1991).
71. Personal communication with Molecular Probe, Inc., (1992),
72. E. Weidemann, *Ann. Phys. Chem.* , **175**, 5-130 (1988).
73. H. R. Schroeder, P. O. Volgelhut, *Anal. Chem.* , **51**, 1583-1585 (1979).
74. H. O. Albrecht, *Phys. Chem.* , **136**, 321 (1928).
75. H. R. Schroeder, F. M. Yeager, *Anal. Chem.* , **50**, 1114-1120 (1978).
76. U. Isacsson, G. Wettermark, *Analytica Chimica Acta* , **68**, 339-362 (1974).
77. S. R. Spurlin, M. M. Cooper, *Anal. Lett.* , **19**, 2277-2283 (1986).
78. I. Weeks, I. Beheshti, F. McCapra, A. K. Campbell, J. S. Woodhead, *Clin. Chem.* , **29**, 1474-1479 (1983).

CHAPTER 2

LOW-COST LASER-INDUCED FLUORESCENCE DETECTION FOR MICELLAR CAPILLARY ELECTROPHORESIS: ZEPTOMOLE DETECTION OF TETRAMETHYLRHODAMINE THIOCARBAMYL AMINO ACID DERIVATIVES*

* A version of this chapter has been published. *J. Chromatogr.*, **608**, 117-120 (1992)

2.1 INTRODUCTION

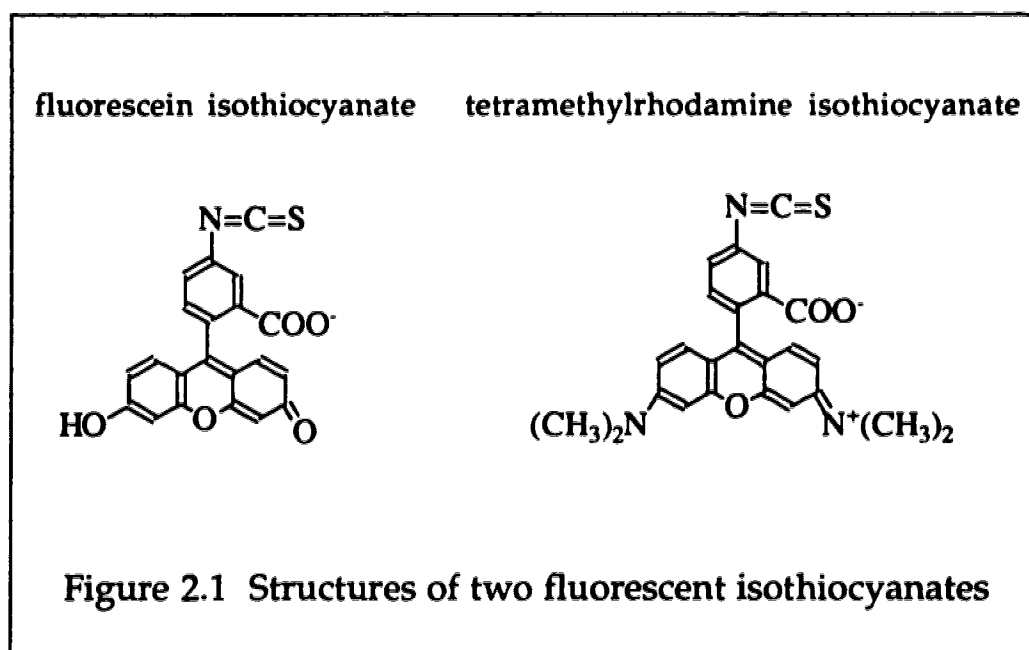
Capillary electrophoresis provides unrivaled separation of biological materials; theoretical plate counts exceed 10^6 for small molecules and exceed 10^7 for oligonucleotides [1, 2]. Just as capillary electrophoresis provides unrivaled separation efficiency, laser-induced fluorescence detection provides unrivaled sensitivity. For example, Keller's group has demonstrated the detection of individual fluorescent molecules in flowing streams [3, 4]. The combination of the separation efficiency of capillary electrophoresis with the detection sensitivity of the laser-induced fluorescence system produces analytical instrumentation with unrivaled performance: complex mixtures containing hundreds of components may be separated and identified at the zeptomole (10^{-21} mole) level [2].

Isothiocyanate derivatives of amino acids are of interest in Edman degradation sequence determination of proteins. The classic Edman reagent, phenylisothiocyanate (PITC), is universally used in commercial protein sequencers [5]. Conventional approaches to amino acid determination for protein sequencing use liquid chromatography separation and ultraviolet absorbance detection of the products of the sequencing reaction, phenylthiohydantoin (PTH) derivatives of amino acids, at picomole (10^{-12} mole) levels [6]. The PTH derivatives of amino acids have been separated by capillary electrophoresis and detected by ultraviolet absorbance [7]. Detection limits are about 100 femtomoles (10^{-13} moles) of the PTH derivatives with UV transmission detection. Other isothiocyanates may be used in the sequencing reaction. For example, dimethylaminoazobenzene isothiocyanate is used to produce the non-fluorescent dimethylaminoazobenzene thiohydantoin (DABTH) derivatives that absorb in

the blue portion of the spectrum, with detection limits of about 100 fmol with liquid chromatography separation and transmission detection. Sub-femtomole detection limits are produced for the PTH and DABTH derivatives with capillary electrophoretic separation and thermo-optical absorbance detection [8, 9].

Fluorescent isothiocyanates demonstrate excellent detection limits for amino acids, roughly eight orders of magnitude superior to classic absorbance detection limits. This research group has described high-sensitivity detection of fluorescein isothiocyanate (FITC) derivatives of amino acids [1, 8, 10]. Fluorescein has a strong absorbance at the argon ion laser emission wavelength of 488 nm, has a high fluorescent quantum efficiency (~ 0.5), but suffers from mediocre photobleaching properties [11]. The best detection limits reported by Dovichi's laboratory for fluorescein thiohydantoin and thiocarbamyl derivatives of amino acids range from 1 to 2 zeptomole of derivative injected onto the capillary. Recently, other laboratories have reported detection limits of 10-20 zeptomoles for fluorescein thiocarbamyl amino acid derivatives [12, 13].

Tetramethylrhodamine isothiocyanate (TRITC) is an interesting modified Edman degradation reagent. Figure 2.1 shows the structures of fluorescein isothiocyanate and tetramethylrhodamine isothiocyanate. The TRITC dye molecule has similar structure to FITC and should have similar reaction characteristics. TRITC absorbs strongly in the green portion of the spectrum and emits in the red. The red emission of TRITC contrasts nicely with the green portion of FITC in double-labeling experiments. The same chromophore is used by Applied Biosystems as their TAMRA-labeled primer for DNA sequencing.



TRITC offers useful spectroscopic properties for ultrasensitive detection. The molar absorptivity is greater than $100,000 \text{ L mol}^{-1} \text{ cm}^{-1}$ at 540 nm and the emission maximum is at 567 nm [14]. Soper *et al.* [15] have reported a fluorescence quantum yield of 15% and a photodestruction rate of 5×10^{-6} in aqueous solutions. From a practical standpoint, the most important property of the dye is that it is conveniently excited by the recently commercialized green helium-neon laser, which produces a 0.75 mW beam at 543.5 nm. The longer wavelength excitation, compared with 488 nm excitation of fluorescein, should produce a decrease in background signal due to the λ^{-4} property of light scatter. This green helium-neon laser is similar in construction to the conventional red helium-neon laser and should have similar lifetime, cost, and power.

TRITC was first used as a fluorescent label in immunology in 1962 [16]. In 1975, Brandtzaeg demonstrated the advantages of TRITC to conjugate with IgG

over fluorescein isothiocyanate, rhodamine B isothiocyanate, RB200SC (lissamine rhodamine B sulfonyl chloride) [17]. TRITC has also been used to label immunological reagents for histological applications [14]. While Dovichi's research group has produced zeptomole detection limits for TAMRA-labeled DNA fragments separated by capillary gel electrophoresis [18, 19], there is no research report on applications of the fluorophore for determination of small molecules by electrophoresis. In this research project, TRITC is used to label the 20 common amino acids, Figure 2.2, for micellar electrokinetic capillary chromatography separation. The excitation of TRITC-labeled thiocarbamyl derivative analyte with the recently commercialized green helium-neon laser results in a low-cost fluorescence detector with zeptomole detection limits, which is 1,000,000,000 times superior to conventional techniques for amino acid analysis.

2.2 EXPERIMENTAL

2.2.1 Capillary Electrophoresis Setup

The capillary electrophoresis system was constructed with post-column laser-induced fluorescence detection in a sheath flow cuvette. Figure 2.3 shows the schematic diagram of the capillary electrophoresis system, which consisted of a fused silica capillary coated outside with a thin layer of polyimide to strengthen the tube, a high voltage (HV) power supply (Spellman high voltage electronics, Plainview, NY, USA) providing up to +30 kV for capillary zone electrophoresis, and two buffer reservoirs.

The capillary was filled with separation buffer and the injection end was

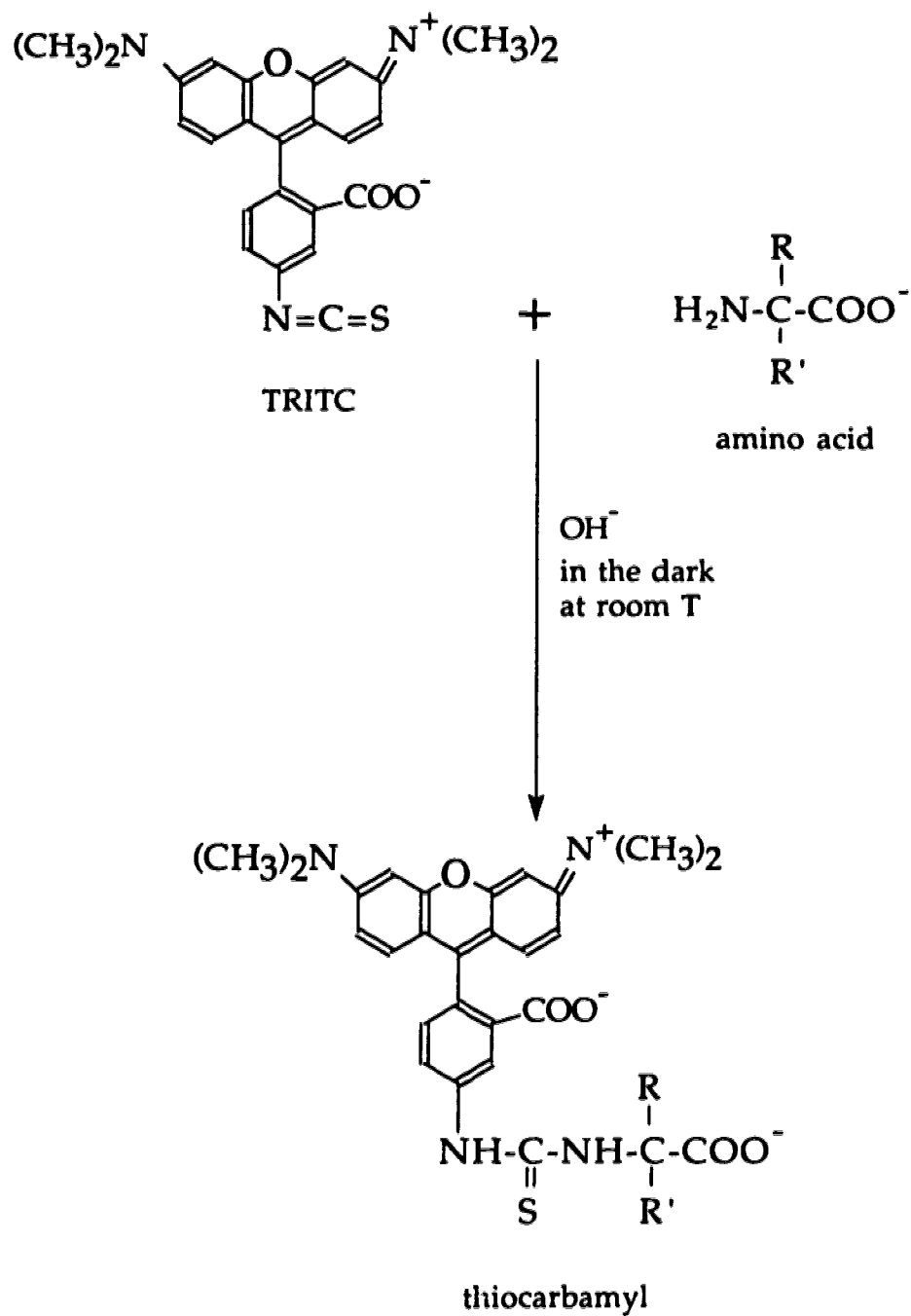


Figure 2.2 TRITC and amino acid labeling reaction

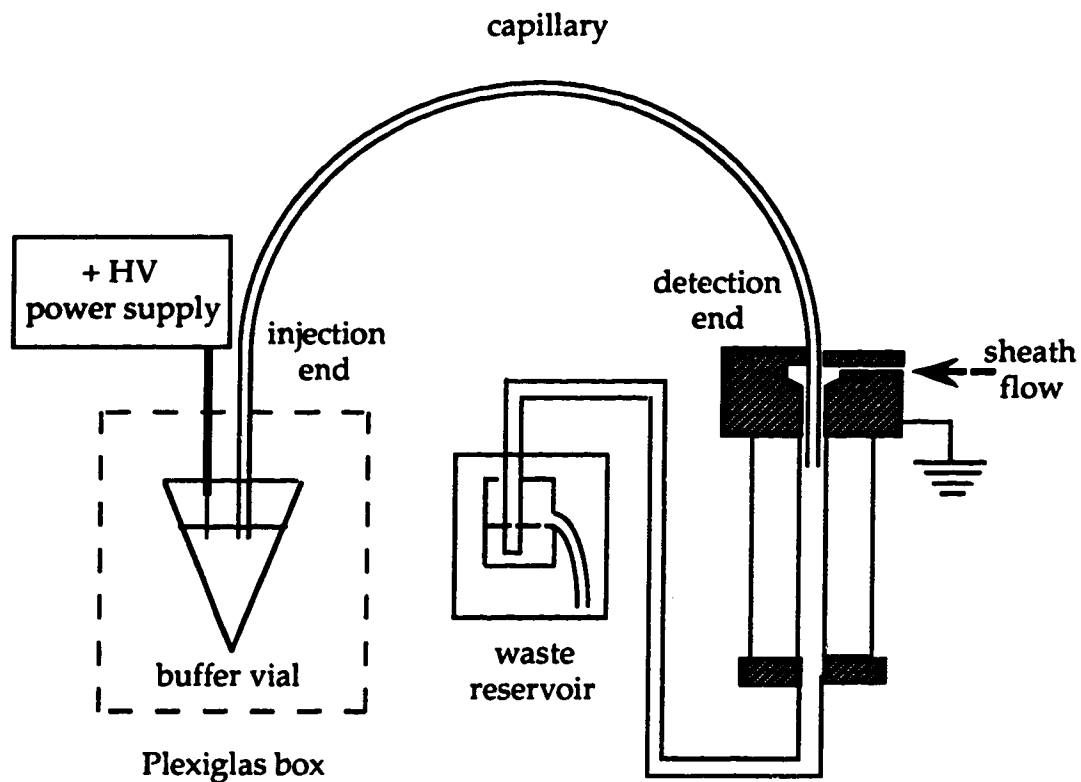


Figure 2.3 Schematic diagram of the capillary electrophoresis system with post-column detection in a sheath flow cuvette

dipped in the separation buffer contained in a 1.5-mL disposable polypropylene vial (Fisher Scientific). The detection end of the capillary was inserted into a sheath flow cuvette. The specially designed waste container kept the waste solution level the same as that in the separation buffer reservoir to prevent hydrodynamic flow from occurring in the capillary. A platinum electrode was put in contact with the separation buffer at the injection end of the capillary. To avoid electrical hazard, the high voltage end of the capillary was enclosed in a safety interlock equipped Plexiglas box. The metal holder for the sheath flow cuvette was held at ground potential to complete the circuit for capillary electrophoresis. A resistor was used to convert the electric current flowing through the capillary into voltage.

2.2.2 Laser-Induced Fluorescence Detector

Figure 2.4 shows the schematic diagram of the system setup for capillary electrophoresis with post-column laser-induced fluorescence detection in a sheath flow cuvette.

Laser and Focusing Microscope Objective

Helium-neon lasers produce monochromatic beams of coherent light with non-ionizing output radiation at wavelengths in the green (543.5 nm), red (632.8 nm), and infrared (1.523 μ m) portion of the spectrum. Both linearly polarized and randomly polarized versions of helium-neon lasers are available. These lasers have a good reputation for being reliable, easy to use, low-cost, small in size, and having long-lifetime.

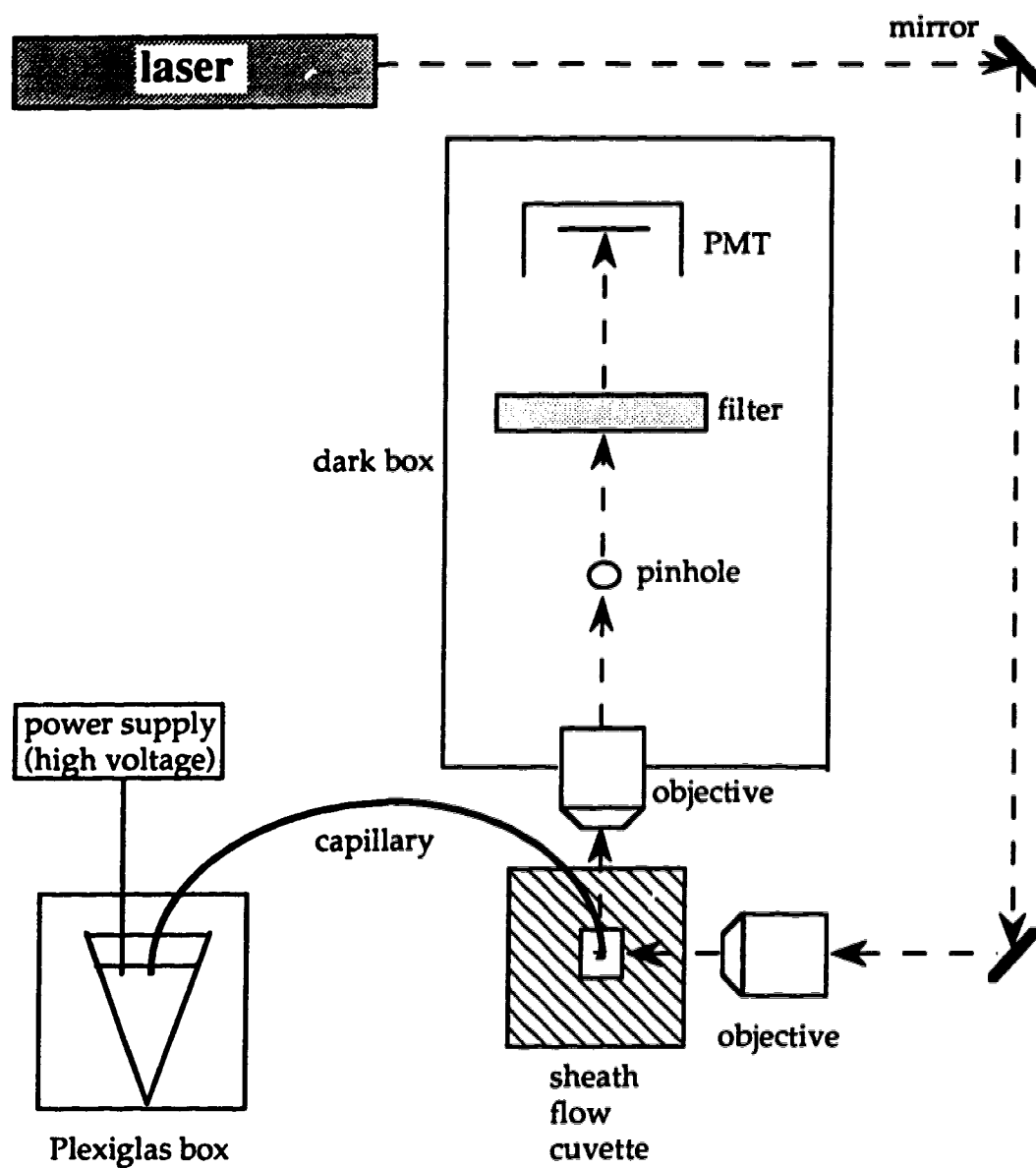


Figure 2.4 Schematic diagram of instrumentation for capillary electrophoresis with post-column laser-induced fluorescence detection

In this laser-induced fluorescence detector, a randomly polarized green helium-neon laser, GreNe (05LGR173 from Melles Griot), in a cylindrical housing with a separate power supply was used. The laser beam provided a low power (0.75 mW) excitation wavelength at 543.5 nm that closely matched the maximum absorption wavelength (~555 nm) of TRITC. Some properties of the GreNe laser are listed in Table 2.1.

The green helium-neon laser was directed by mirrors and focused with a 5x (25-mm focal length) microscope objective (Melles Griot), which provided an irradiance of about 100 W cm^{-2} . The irradiance may not have been the optimized value for maximum fluorescence signal, but it produced a very low background that was beneficial for low detection limits. The microscope objective was mounted on translation stages, which positioned the laser beam about $200 \mu\text{m}$ below the exit of the capillary in a post-column fluorescence flow chamber. The laser beam was perpendicular to both the cuvette windows and the sample stream coming out of the capillary.

Sheath Flow Cuvette

The fluorescence detector was based on a sheath flow cuvette. The locally assembled cuvette had a $200\text{-}\mu\text{m}$ square flow chamber (NSG-Precision Cells, Farmingdale, NY, USA) and 2-mm thick windows made of good optical quality quartz. A fused silica capillary with an outer diameter of about $189 \mu\text{m}$ fitted snugly within the square quartz flow chamber. A sheath stream, of identical composition as the separation buffer and provided by a high stability syringe pump, surrounded the sample stream at the exit of the capillary. At the very low flow rates employed in electrophoresis, the flow profile was laminar with a typical diameter of $10 \mu\text{m}$.

Table 2.1 Properties of the green helium-neon laser

model number	05LGR173
wavelength (nm)	543.5
TEM ₀₀ power (mW)	0.75
beam diameter at $1/e^2$ (mm)	0.75
beam divergence (mrad, full)	0.92
beam amplitude noise (%RMS, 0-100 Hz)	0.5
beam amplitude stability (\pm % in a day)	2.5
operating current (mA)	6.5
operating voltage (\pm 100 V _{dc})	2650
polarization	random

Fluorescence Collection Optics

Fluorescence signal from the illuminated sample stream (fluorescent or fluorescently labeled) was collected at right angles both to the sample stream and the laser beam with an 18x, 0.45 numerical aperture (N.A.) objective (Melles Griot, ON, Canada) and imaged onto an 800- μm diameter pinhole, which acted as a spatial filter to get rid of stray light from both room lights and the scattered laser light.

Spectral Filter

A single interference filter, Model 590DF40 (Omega Optical, Inc., Brattleboro, VT, USA), was placed in front of the photomultiplier tube to block scattered laser light while still passing much of the fluorescence. The spectrum of the filter is shown in Figure 2.5.

The bandpass of the filter is from 570 to 610 nm, centered at 590 nm. The spectral filter completely blocks the Rayleigh scattered light at the wavelength (543.5 nm) of the green helium-neon laser and the Raman scattering from the solvent (water) at 700 nm.

Photomultiplier Tube (PMT)

Fluorescence was detected with a Hamamatsu R1477 photomultiplier tube (Hamamatsu Corporation, San Jose, CA, USA), operated at 1000 V. The current output from the photomultiplier tube was passed through a 0.1 second RC low-pass filter and converted into voltage signal that was displayed onto a strip-chart recorder.

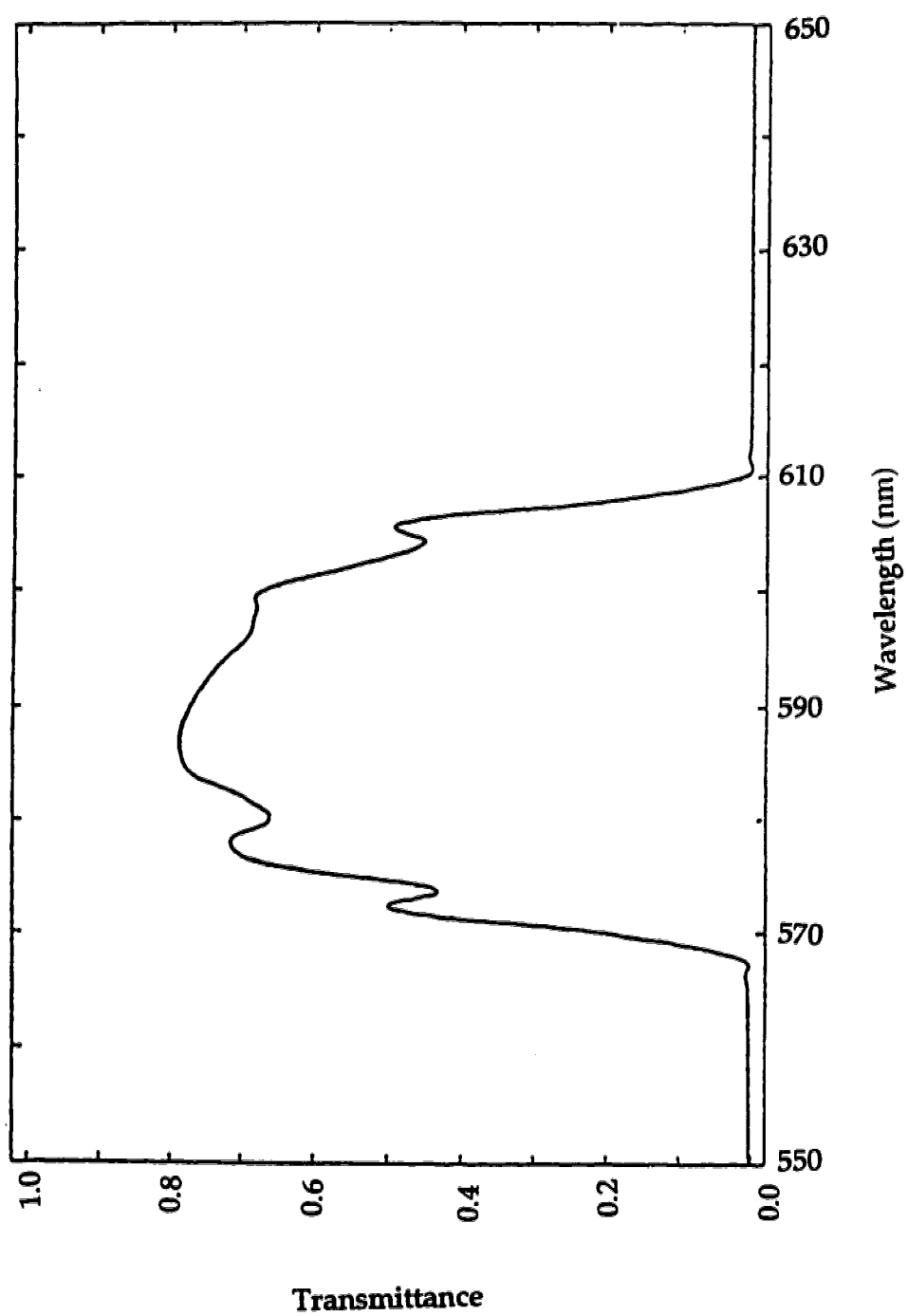


Figure 2.5 Spectrum of the interference filter 590DF40

The laser used to excite fluorescence had low power (0.75 mW) and produced very low background signals in the sheath flow cuvette. As a result, the dark current of the PMT dominates the background signal. The photomultiplier tube was cooled to -25 °C with a Products for Research (Massachusetts, USA) PMT cooler, which greatly reduced the PMT dark current and improved the detection limits.

System setup

The capillary electrophoresis with laser-induced fluorescence detection system was setup on a 3 by 4 feet optical breadboard ((Newport, Irvine, CA, USA) that provided a vibration-free surface for mounting all of the mechanical and optical components. The fluorescence collection and detection optics including the collection microscope objective, pinhole, spectral filter, and photomultiplier tube were covered with an aluminum box painted black to prevent background from room light and laser light from reaching the PMT. To make alignment easier, all of the centers of the optical components were positioned 6 inches above the optical breadboard.

Alignment of the Fluorescence Detection System

The purposes of aligning the fluorescence detection system are to maximize the collection of fluorescence signal and minimize the background signal in order to achieve high sensitivities. Experimentally, a relatively high concentration (10^{-6} M) of tetramethylrhodamine isothiocyanate solution was run continuously through the capillary by electrophoresis and the sheath flow rate was set at 0.48 ml per hour. First, the laser beam was focused to a small spot that

matched the sample stream size in the sheath flow cuvette. Second, the positions of the collection optics within the dark box were adjusted to image the fluorescence spot nicely onto the PMT. Third, the cuvette was moved carefully using the three translation stages to produce the maximum fluorescence signal.

2.2.3 Stock Solutions

2.2.3A Preparation of Borate Buffers

The deionized water used to prepare these solutions was from a Barnstead NANOpure system.

(1) Boric Acid (H_3BO_3) Stock Solution: 0.202 M

The 0.20M boric acid stock solution was prepared by dissolving 2.50 g boric acid (Fisher Scientific Company, Fair Lawn, NJ, USA) in 200 ml deionized water in a glass volumetric flask.

(2) Sodium Borate Stock Solution: 0.0500 M borax ($\text{Na}_2\text{B}_4\text{O}_7 \cdot 10\text{H}_2\text{O}$) or 0.202 M in terms of sodium borate

A 0.200 M borate stock solution was prepared by dissolving 3.81 g sodium borate (Fisher Scientific Company, Fair Lawn, NJ, USA) in 200 ml deionized water in a glass volumetric flask.

(3) Borate Buffer: 0.2 M, pH = 8.6

A 0.2 M borate buffer was prepared by mixing 850 ml of solution (1) with 900 ml of solution (2) and filtered with 0.22 μm pore-size membranes (Millipore).

(4) Borate Buffer: 5 mM, pH = 8.4

A 5 mM borate buffer was prepared by diluting 250 ml of 0.2 M borate buffer to 1000 ml with deionized water.

2.2.3B Preparation of Borate / SDS Buffer

A 5 mM borate buffer with 10 mM sodium dodecyl sulfate (Aldrich Chemical Company, Milwaukee, WI, USA) was prepared by dissolving SDS in 5 mM borate buffer and the pH was adjusted to 8.6 by 0.1 M sodium hydroxide solution.

2.2.3C Amino Acid Stock Solutions

The structures of the 20 common amino acids of proteins are shown in **Table 2.2**. Stock solutions of these amino acids (Fluka ChemieAG, CH-9470 Buchs, Switzerland) were prepared by dissolving individual amino acids in 0.2 M borate buffer. The concentration range varied from 1.0 to 3.6 mM, **Table 2.3**. The stock solutions were stored at 4°C.

2.2.3D TRITC Stock Solution

The molecular weight of tetramethylrhodamine isothiocyanate (Molecular Probes, Inc., Eugene, OR, USA) is 479 g/mole. TRITC stock solution, 7×10^{-5} M, was prepared in 50 ml HPLC grade acetone and stored at 4°C in the dark.

2.2.4 Labeling Reactions

Tetramethylrhodamine thiocarbamyl derivatives were produced by mixing 800 μ L of 7×10^{-5} M tetramethylrhodamine isothiocyanate stock in acetone with 500 μ L of each of the 1 to 3.6 mM amino acid stock solution. The labeling reactions were allowed to react at room temperature for a few hours in

Table 2.2 Structures of 20 common amino acids

Aliphatic	Aromatic
$\begin{array}{c} \text{H} \\ \\ \text{H}_3\text{N}^+ - \text{CH} - \text{COO}^- \\ \text{Glycine} \end{array}$ $\begin{array}{c} \text{CH}_3 \\ \\ \text{H}_3\text{N}^+ - \text{CH} - \text{COO}^- \\ \text{Alanine} \end{array}$	$\begin{array}{c} \text{C}_6\text{H}_5 \\ \\ \text{CH}_2 \\ \\ \text{H}_3\text{N}^+ - \text{CH} - \text{COO}^- \\ \text{Phenylalanine} \end{array}$ $\begin{array}{c} \text{OH} \\ \\ \text{C}_6\text{H}_4 \\ \\ \text{CH}_2 \\ \\ \text{H}_3\text{N}^+ - \text{CH} - \text{COO}^- \\ \text{Tyrosine} \end{array}$
$\begin{array}{c} \text{H}_3\text{C} \quad \text{CH}_3 \\ \quad \\ \text{CH} \\ \\ \text{CH}_2 \\ \\ \text{H}_3\text{N}^+ - \text{CH} - \text{COO}^- \\ \text{Leucine} \end{array}$ $\begin{array}{c} \text{H}_3\text{C} \quad \text{CH}_3 \\ \quad \\ \text{CH} \\ \\ \text{H}_3\text{N}^+ - \text{CH} - \text{COO}^- \\ \text{Valine} \end{array}$	$\begin{array}{c} \text{C}_8\text{H}_6\text{N}_2 \\ \\ \text{CH}_2 \\ \\ \text{H}_3\text{N}^+ - \text{CH} - \text{COO}^- \\ \text{Tryptophan} \end{array}$
$\begin{array}{c} \text{CH}_3 \\ \\ \text{CH}_2 \\ \\ \text{H}_3\text{C} - \text{CH} \\ \\ \text{H}_3\text{N}^+ - \text{CH} - \text{COO}^- \\ \text{Isoleucine} \end{array}$	
Hydroxyl	Sulfur-Containing
$\begin{array}{c} \text{OH} \\ \\ \text{CH}_2 \\ \\ \text{H}_3\text{N}^+ - \text{CH} - \text{COO}^- \\ \text{Serine} \end{array}$ $\begin{array}{c} \text{CH}_3 \\ \\ \text{CH} - \text{OH} \\ \\ \text{H}_3\text{N}^+ - \text{CH} - \text{COO}^- \\ \text{Threonine} \end{array}$	$\begin{array}{c} \text{SH} \\ \\ \text{CH}_2 \\ \\ \text{H}_3\text{N}^+ - \text{CH} - \text{COO}^- \\ \text{Cysteine} \end{array}$ $\begin{array}{c} \text{CH}_3 \\ \\ \text{S} \\ \\ \text{CH}_2 \\ \\ \text{CH}_2 \\ \\ \text{H}_3\text{N}^+ - \text{CH} - \text{COO}^- \\ \text{Methionine} \end{array}$
Acidic	Amidic
$\begin{array}{c} \text{COOH} \\ \\ \text{CH}_2 \\ \\ \text{H}_3\text{N}^+ - \text{CH} - \text{COO}^- \\ \text{Aspartic acid} \end{array}$ $\begin{array}{c} \text{COOH} \\ \\ \text{CH}_2 \\ \\ \text{CH}_2 \\ \\ \text{H}_3\text{N}^+ - \text{CH} - \text{COO}^- \\ \text{Glutamic acid} \end{array}$	$\begin{array}{c} \text{H}_2\text{N} - \text{CO} \\ \\ \text{CH}_2 \\ \\ \text{H}_3\text{N}^+ - \text{CH} - \text{COO}^- \\ \text{Asparagine} \end{array}$ $\begin{array}{c} \text{H}_2\text{N} - \text{CO} \\ \\ \text{CH}_2 \\ \\ \text{CH}_2 \\ \\ \text{H}_3\text{N}^+ - \text{CH} - \text{COO}^- \\ \text{Glutamine} \end{array}$
Basic	Cyclic
$\begin{array}{c} \text{H}_2\text{N} - \text{C} = \text{NH} \\ \\ \text{NH} \\ \\ \text{CH}_2 \\ \\ \text{CH}_2 \\ \\ \text{H}_3\text{N}^+ - \text{CH} - \text{COO}^- \\ \text{Arginine} \end{array}$ $\begin{array}{c} \text{NH}_2 \\ \\ \text{CH}_2 \\ \\ \text{CH}_2 \\ \\ \text{CH}_2 \\ \\ \text{H}_3\text{N}^+ - \text{CH} - \text{COO}^- \\ \text{Lysine} \end{array}$	$\begin{array}{c} \text{CH}_2 \\ / \quad \backslash \\ \text{CH}_2 \quad \text{CH}_2 \\ \quad \\ \text{H}_2\text{N}^+ - \text{CH} - \text{COO}^- \\ \text{Proline} \end{array}$
$\begin{array}{c} \text{HN} \quad \text{N} \\ \backslash \quad / \\ \text{CH} \\ \\ \text{CH}_2 \\ \\ \text{H}_3\text{N}^+ - \text{CH} - \text{COO}^- \\ \text{Histidine} \end{array}$	

Table 2.3 The 20 Amino Acid Stock Solutions

No.	amino acid	abbreviation		MWt	pK _a [*]	stock solution
				(g/mole)	(α-NH ₃ ⁺)	(mM)
1	Alanine	Ala	A	89.10	9.7	1.2
2	Arginine	Arg	R	210.67	9.0	1.0
3	Asparagine	Asn	N	132.12	8.8	1.2
4	Aspartic acid	Asp	D	133.11	9.8	2.0
5	Cysteine	Cys	C	121.16	10.8	1.4
6	Glutamic acid	Glu	E	147.13	9.7	1.0
7	Glutamine	Gln	Q	146.15	9.1	1.5
8	Glycine	Gly	G	75.07	9.6	2.1
9	Histidine	His	H	209.63	9.2	3.6
10	Isoleucine	Ile	I	131.18	9.7	2.8
11	Leucine	Leu	L	131.18	9.6	1.2
12	Lysine	Lys	K	182.65	9.0	1.4
13	Methionine	Met	M	149.21	9.2	1.7
14	Phenylalanine	Phe	F	165.19	9.1	2.5
15	Proline	Pro	P	115.13	10.6	1.3
16	Serine	Ser	S	105.09	9.2	1.8
17	Threonine	Thr	T	119.12	10.4	1.1
18	Tryptophan	Trp	W	204.23	9.4	1.0
19	Tyrosine	Tyr	Y	181.19	9.1	1.2
20	Valine	Val	V	117.15	9.6	1.2

* C.K. Mathews and K.E. van Holde, *Biochemistry*, Page 137 (1990), The Benjamin/cummings Publishing Company, Inc., Redwood City, CA, USA.

the dark. TRITC stock solution, 800 μ L was mixed with 500 μ L 0.2 M borate buffer to serve as the reaction blank. The reaction mixtures of TRITC and amino acids were diluted to the desired concentrations for capillary electrophoresis with the separation buffer in 1.5-ml polypropylene microcentrifuge vials (Fisher Scientific Company, Pittsburgh, PA, USA).

2.2.5 Capillary Electrophoresis Conditions

Separation was carried out using fused silica capillaries of 50 μ m inner diameter and 190 μ m outer diameter (Polymicro Technologies, Phoenix, AZ, USA). The separation buffer was 5 mM, pH 9.0 borate solution in deionized water with 10 mM sodium dodecyl sulfate. The sheath flow rate was 0.48 ml/hour. The sample was injected electrokinetically at 1 kV for 10 seconds. Electrophoresis was driven at +30 kV by a high voltage power supply (Spellman, Plainview, NY, USA).

2.3. RESULTS AND DISCUSSION

2.3.1 Spectral Properties of Tetramethylrhodamine Isothiocyanate

Unlike fluorescein isothiocyanate, tetramethylrhodamine isothiocyanate does not dissolve easily in acetone. An ultrasonic bath was used to help TRITC dissolve in HPLC grade acetone. The bright purple solution was sensitive to light and temperature and was stored at 4°C in the dark.

The absorption spectrum, **Figure 2.6**, of tetramethylrhodamine isothiocyanate in 5 mM borate buffer (pH 9) was measured with a UV-Vis

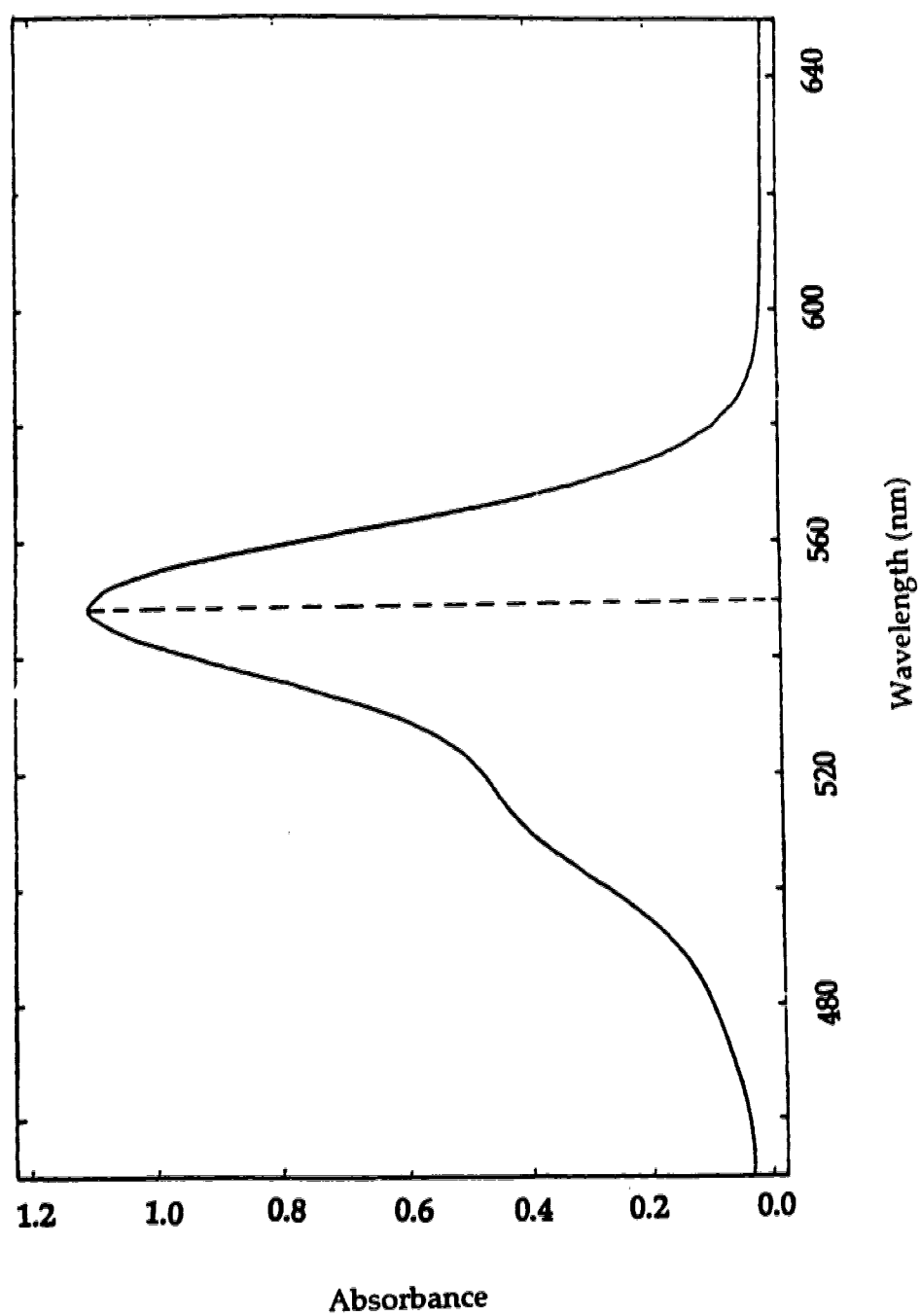


Figure 2.6 Absorbance spectrum of TRITC

spectrophotometer (8451A Diode Array Spectrophotometer, Hewlett Packard). The maximum absorption occurs at about 555 nm with a molar absorptivity of about $85,000 \text{ L mol}^{-1} \text{ cm}^{-1}$. The fluorescence spectrum of the TRITC molecule is shown in Figure 2.7 and was measured with a fluorescence detector (Heath) when the excitation wavelength was set at 555 nm. The maximum fluorescence is centered at 573 nm.

The electropherogram of tetramethylrhodamine isothiocyanate showed only one peak. After mixing with the separation borate buffer, the TRITC peak decreased gradually over time, which shows that the TRITC molecules are not stable in basic aqueous solutions.

2.3.2 Labeling Reaction: Time Effect

The reaction of TRITC with amino acids is rather sluggish at room temperature. Mixtures of TRITC and glycine were allowed to react over a 10 hour period. A small amount of the sample was removed from the reaction mixture periodically and analyzed by capillary electrophoresis with laser-induced fluorescence detection. The experimental data of reaction times and the TRITC and TRITC labeled glycine (TRITC-Gly) peak heights are listed in Table 2.4.

Figure 2.8 shows a typical electrophorogram of TRITC labeled glycine. The average of two or three determinations of the TRITC or TRITC-glycine peak heights is plotted in Figure 2.9. The squares correspond to the production of TRITC-glycine while the circles correspond to unreacted TRITC. In this reaction, the amino acid was present in nearly 18-fold excess, so that consumption of TRITC and production of TRITC-amino acid were expected to follow the first-order kinetics with the same rate constant. Instead, TRITC disappeared more

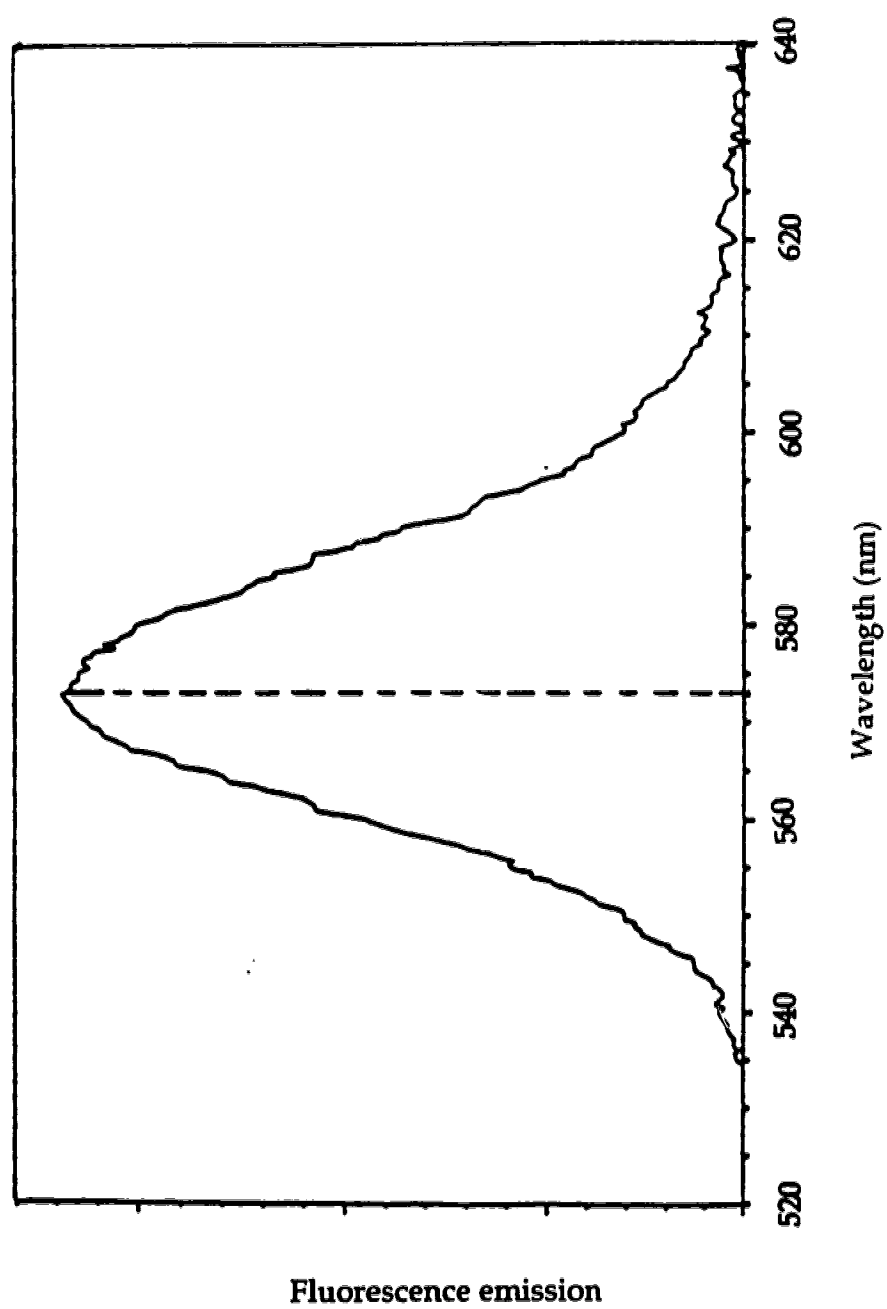


Figure 2.7 Fluorescence emission spectrum of TRITC

Table 2.4 Experimental data of reaction times and peak heights

reaction time (hour)	TRITC peak height (mm)	TRITC-Gly peak (mm)
0.5	123.8	77.7
1.0	61.5	103.3
1.5	41.2	138.2
2.0	29.0	155.3
2.5	19.7	165.3
3.0	16.5	178.4
3.5	13.0	196.5
4.0	11.5	205.3
5.0	9.5	233.2
6.0	9.0	256.5
7.0	6.7	258.8
8.0	6.2	253.5
9.0	6.5	250.4
10.0	6.0	246.4

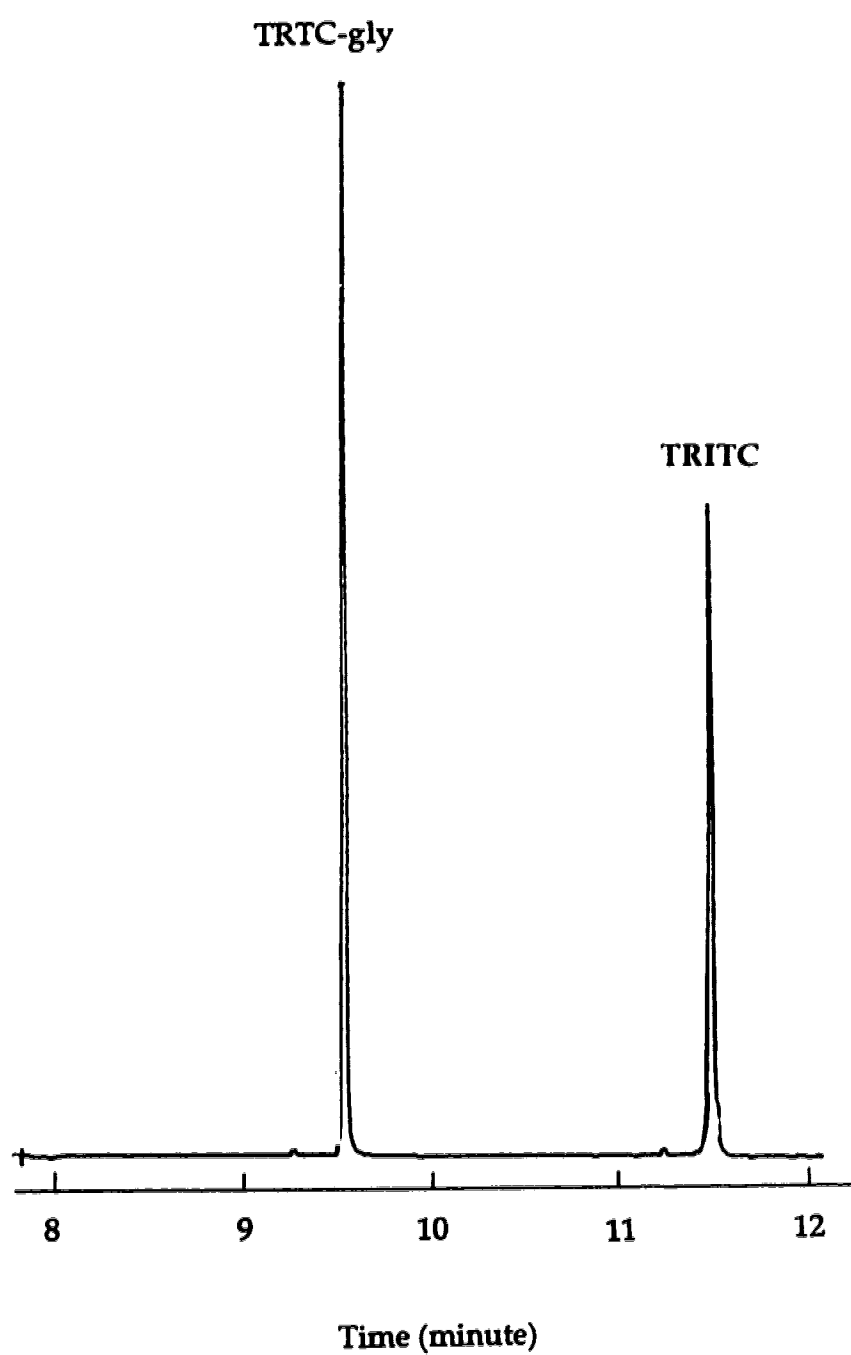


Figure 2.8 Electropherogram of TRITC labeled glycine

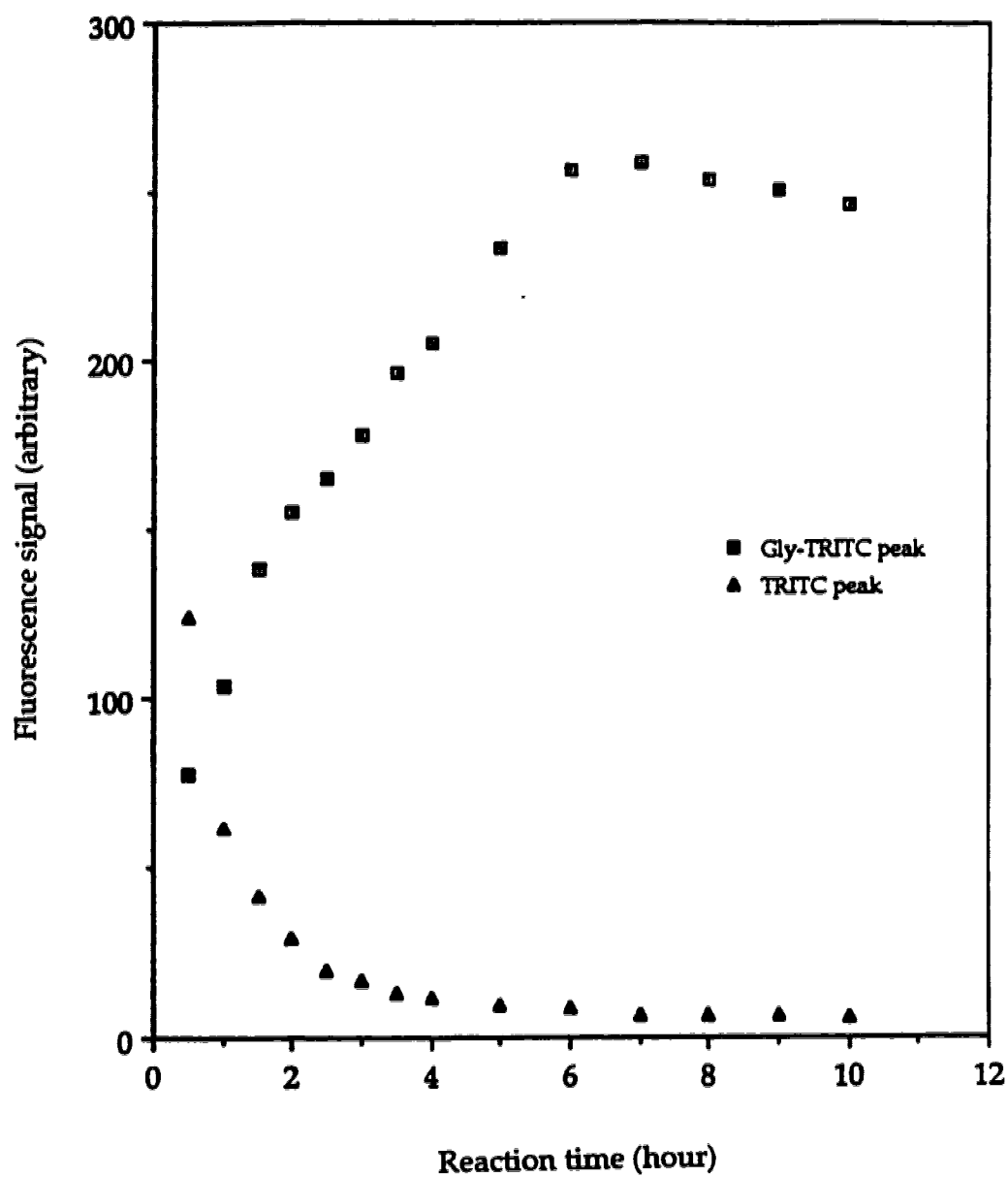


Figure 2.9 Fluorescence peak height vs. reaction time

rapidly than TRITC-glycine was produced. It appears that TRITC undergoes both reaction with amino acid and decomposition. Similar behavior has been observed in this laboratory for FITC reaction with amino acids. The isothiocyanates are not particularly stable in protic solvents, presumably undergoing hydrolysis to generate non-fluorescent products. At room temperature, TRITC disappears after about 6-8 hours in a borate buffer of pH 9. Analyte concentrations were calculated based on TRITC as the limiting reagent and the assumption that the reaction went to completion. As a result, the instrumental detection limits quoted below must be interpreted as the upper boundary for actual detection limits.

2.3.3 Detection Limits

Detection limits were calculated by the method of Knoll [20]; the baseline was inspected over a time period given by 50 times the peak-width. The maximum deviation from the average of the baseline was used to estimate the 3σ detection limit. Relatively precise estimates of the detection limits were produced by inspecting the baseline over a large number of samples. The 3σ concentration detection limit for TRITC-glycine was 1×10^{-12} M, injected onto the capillary. Injection volume was estimated to be 1 nL for this amino acid, so that the mass detection limit corresponds to 1 zeptomole of amino acid injected onto the capillary. One zeptomole of analyte corresponds to 1,200 analyte molecules. The detection volume, defined by the intersection of the laser beam and sample stream, was estimated to be 10 pL. There were 5 analyte molecules present on average in the detection volume at the detection limit.

2.3.4 Separation of 20 Tetramethylrhodamine Isothiocyanate Labeled Amino Acid Thiocarbamyl Derivatives

The separation of six TRITC labeled amino acids (Ala, Gly, Leu, Ile, Phe, Val) was first tried with 5 mM borate buffer (pH 9). The electropherogram showed poor separation of six TRITC-amino acids, indicating that capillary zone electrophoresis (CZE) was not good enough to separate a mixture of 20 amino acids labeled with TRITC.

The next step was to add some anionic surfactant (SDS) to the separation buffer. **Figure 2.10** presents the electropherogram of twenty TRITC labeled amino acids separated by micellar electrokinetic capillary chromatography with laser-induced fluorescence detection. The capillary used for the separation was 92 cm long. The total TRITC concentration in the mixture was 2.5×10^{-7} M. The PMT power supply was set at 1060 V. As is typical for zone electrophoresis separation of other thiocarbamyl derivatives of amino acids, separation was not complete; alanine and proline co-eluted as did lysine, arginine and TRITC. However, the separation of the remaining amino acids was good and the total separation time was 12 minutes. On the other hand, the number of theoretical plate count calculated for TRITC-amino acid peaks were on the order of 2 million. This separation demonstrates that high plate counts do not automatically translate into high resolution. The large size of the derivatizing reagent dwarfs small differences in the size of amino acids. The size- to-charge ratio of each of the TRITC-amino acid derivatives is quite similar and base-line separation was not achieved using 5 mM borate buffer with 10 mM SDS.

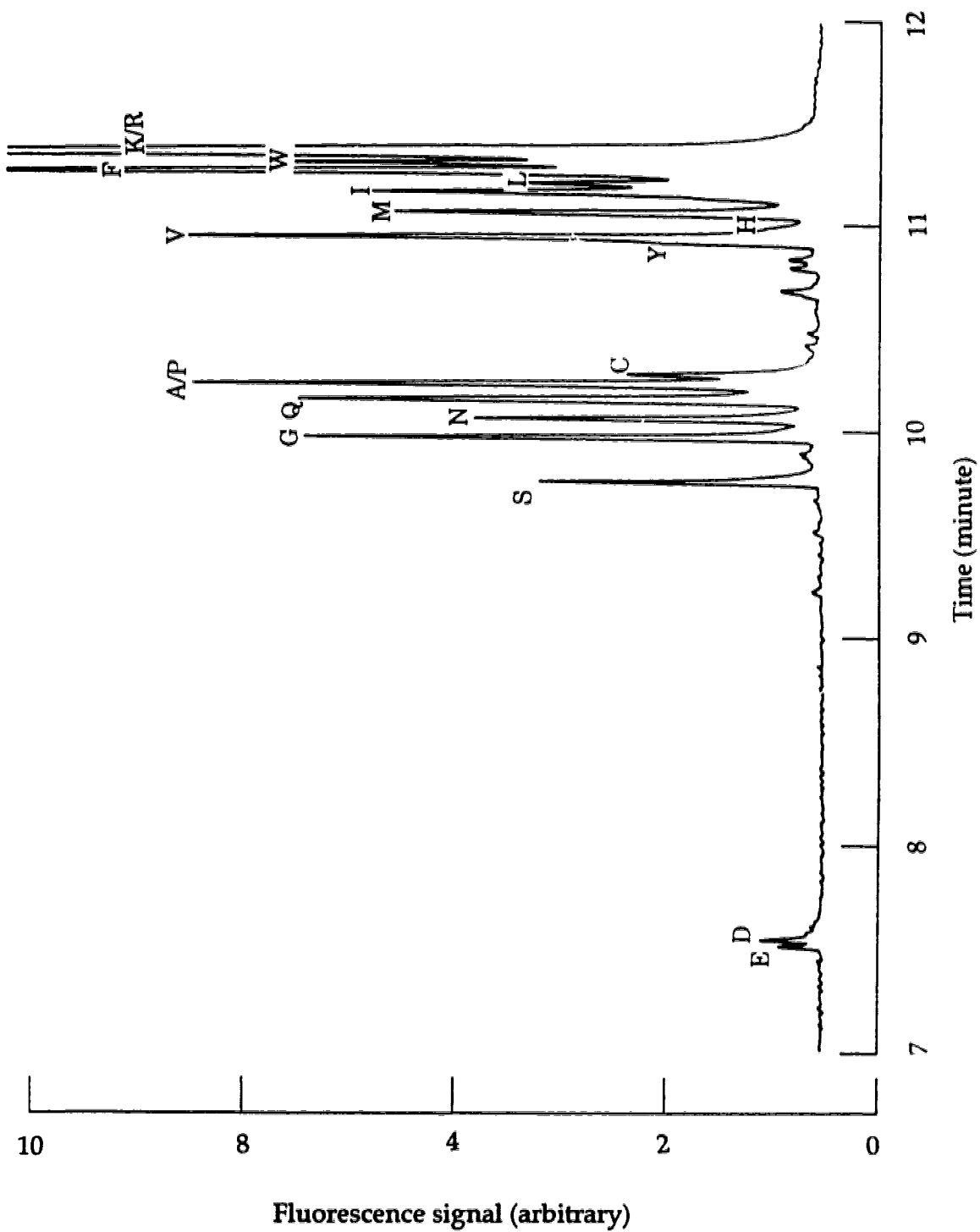


Figure 2.10 Electropherogram of 20 TRITC labeled amino acids

2.4 CONCLUSIONS

Tetramethylrhodamine isothiocyanate may be used to label amino acids at room temperature in the dark, producing thiocarbamyl derivatives. These derivatives may be separated by micellar electrokinetic capillary chromatography and detected with high sensitivity by a low-cost laser-induced fluorescence system. The detection limit for TRITC-glycine injected onto the capillary was 1 zeptomole.

Tetramethylrhodamine isothiocyanate reacts relatively slowly with amino acids; the reaction rate is far too sluggish for routine use in protein sequencing. The classic Edman reagent, phenylisothiocyanate (PITC), will react in less than 30 minutes. Instead, equal concentration mixtures of PITC and TRITC can be used in a double coupling sequencing reaction. The PITC is not detected but instead used to scavenge any unreacted N-terminal amino acids. The reaction with both reagents will yield a large excess of the phenyl thiohydantoin and a small amount of tetramethylrhodamine thiohydantoin after each step in the Edman cycle. The tetramethylrhodamine labeled amino acids can be detected with exquisite sensitivity as shown in the results presented in this chapter. Even if the tetramethylrhodamine isothiocyanate reaction efficiency is 0.1% of the reaction of phenyl isothiocyanate, proteins may be sequenced with attomole sensitivity.

However, given the slow nature of the isothiocyanate reaction between TRITC and amino acids, other derivatizing reagents are of interest for general amino acid analysis. The most interesting reagents are those that absorb strongly at the excitation wavelengths of readily available lasers [21]. Derivatizing reagents that have been coupled with laser-induced fluorescence detection include o-phthalaldehyde excited by an argon ion laser operating in the

ultraviolet at 351 and 363 nm [22], DANSYL excited by a helium-cadmium laser at 325 nm [23], naphthalenedialdehyde (NDA) excited by the 457.9 nm line of an argon ion laser [24], fluorescamine labeled amino acids excited at 325 nm with a mercury lamp [25], and 3-(4-carboxybenzoyl)-2-quinolinecarboxaldehyde excited at 442 nm with a helium-cadmium laser [26].

REFERENCES

1. Y. F. Cheng, S. Wu, D. Y. Chen, N. J. Dovichi, *Anal. Chem.* , **62**, 496-503 (1990).
2. H. P. Swerdlow, S. Wu, H. R. Harke, N. Dovichi, *J. Chromatogr.* , **516**, 61-67 (1990).
3. N. J. Dovichi, J. C. Martin, J. H. Jett, R. A. Keller, *Science.* , **219**, 845-847 (1983).
4. D. C. Nguyen, R. A. Keller, J. H. Jett, J. C. Martin, *Anal. Chem.* , **59**, 2158-2160 (1987).
5. P. Edman, *Acta Chem. Scand.* , **4**, 277-283 (1950).
6. P. Tempst, L. Rivier, *Anal. Biochem.* , **183**, 290-300 (1989).
7. K. Otsuka, S. Terabe, T. Ando, *J. Chromatogr.* , **332**, 219-226 (1985).
8. K. C. Waldron, S. Wu, C. W. Earle, H. R. Harke, N. J. Dovichi, *Electrophoresis*, **11**, 777-780 (1990).
9. K. C. Waldron, N. J. Dovichi, *Anal. Chem.* , **64**, 1396-1399 (1992).
10. Y. F. Cheng, N. J. Dovichi, *Science* , **242**, 562-564 (1988).
11. S. Wu, N. J. Dovichi, *J. Chromatogr.* , **480**, 141-155 (1989).
12. J. V. Sweedler, J. B. Shear, H. A. Fishman, R. N. Zare, *Anal. Chem.* , **63**, 496-502 (1991).
13. C. A. Monnig, J. W. Jorgenson, *Anal. Chem.* , **63**, 802-807 (1991).
14. R. P. Haugland, *Handbook of Fluorescent Probes and Research Chemicals*, K. D. Larison, Ed., (Molecular Probes, Inc., Eugene, OR, 1989).
15. S. A. Soper, et al., *Proc. SPIE* , **1435**, 168 (1991).

16. M. L. Smith, T. R. Carski, C. W. Griffin, *J. Bacteriol.* , **83**, 1358-1359 (1962).
17. P. Brandtzaeg, *Annals New York Academy of Sciences* , **254**, 35 (1975).
18. D. Y. Chen, H. P. Swerdlow, H. R. Harke, J. Z. Zhang, N. J. Dovichi, *J. Chromatogr.* , **559**, 237-246 (1991).
19. H. Swerdlow, J. Z. Zhang, D. Y. Chen, H. R. Harke, G. Ronda, S. Wu, N. J. Dovichi, and F. Carl, *Anal. Chem.* , **63**, 2835-2841 (1991).
20. J. E. Knoll, *J. Chrom. Sci.* , **23**, 422-425 (1985).
21. J. Gluckman, D. Shelly, M. Novotny, *J. Chromatogr.* , **317**, 443-453 (1984).
22. H. Todoriki, T. Hayashi, H. Naruse, *J. Chromatogr.* , **276**, 45-54 (1983).
23. E. Gassmann, J. E. Kuo, R. N. Zare, *Science* , **230**, 813-815 (1985).
24. M. C. Roach, M. D. Harmony, *Anal. Chem.* , **59**, 411-415 (1987).
25. R. A. Wallingford, A. G. Ewing, *Anal. Chem.* , **59**, 678-681 (1987).
26. J. Liu, Y. Z. Hsieh, D. Wiesler, M. Novotny, *Anal. Chem.* , **63**, 408-412 (1991).

CHAPTER 3

ATTACHMENT OF A SINGLE FLUORESCENT LABEL TO PEPTIDES FOR DETERMINATION BY CAPILLARY ZONE ELECTROPHORESIS*

* A version of this chapter has been published. *J. Chromatogr.*, **608**, 239-242 (1992)

3.1 INTRODUCTION

Capillary zone electrophoresis is a particularly powerful technique for the separation and analysis of complex protein mixtures [1]. To avoid column overloading, only small amounts of dilute sample can be introduced onto the capillary without degrading the separation efficiency. For example, injection of 1 nL of a 10^{-6} M protein solution corresponds to the introduction of one femtomole (10^{-15} mole) of protein. Conventional ultraviolet absorbance detection is problematic at low femtomole sample loadings. Universal detection, for example based on refractive index gradient detection, is useful in the analysis of unlabeled peptides [2]. Again, detection limits are in the low femtomole range. Alternatively, post-column derivatization may be used to label proteins for fluorescent detection, albeit with limited sensitivity and reduced separation efficiency [3, 4].

Fluorescence detection provides outstanding detection limits for capillary electrophoresis. Pre-column labeled amino acids and DNA sequencing fragments may be detected at the low to sub-zeptomole level [5, 6]. While pre-column fluorescent labeling is useful in amino acid and DNA analysis, it is not always useful in peptide analysis. The difficulty is straightforward: protein labeling reactions inevitably rely on reagents that attack the N-terminal α -amino group. Simultaneously, the ϵ -amino groups associated with lysine residues will also react. Unfortunately, most fluorescent labels are bulky and labeling does not go to completion. The labeling reaction produces a complex mixture of products, corresponding to attachment of different number of labels at different sites [7]. Each of the reaction products has a slightly different migration rate, giving rise to a complicated and uninterpretable electropherogram.

The number of possible reaction products may be calculated from simple combinatorial analysis. If there is no lysine residue, there is only one possible reaction product, that labeled at the N-terminal amino group. If there is one lysine group, there are three possible labeled products: one labeled only at the N-terminal α -amino group, one labeled only at the lysine ϵ -amino group, and one with both sites labeled. If there are n primary amino groups that can be labeled, then there are

$$\sum_{m=1}^n \frac{(n)!}{m! (n-m)!} = 2^n - 1 \quad (3.0)$$

different labeled products possible. For peptides and proteins with more than a few primary amino groups, the number of reaction products becomes very large. A peptide with three primary amino groups has seven possible labeled reaction products while a protein with 10 primary amino groups has 1023 possible products. Analysis of a mixture of peptides that are incompletely labeled is not practical; instead of observing a single peak for each peptide, many tens or hundreds of peaks are observed for each peptide and protein.

To ensure that only the N-terminal amino group is labeled, the peptide may be taken through one cycle of the Edman degradation reaction before the labeling reaction [8]. This method first treats the sample with phenylisothiocyanate (PITC), the classic Edman degradation reagent [9]. PITC is relatively small and efficiently reacts under basic conditions with all primary and secondary amines present in the peptide. Under acidic conditions, the N-terminal amino acid is cleaved, exposing an unreacted primary amine. This peptide, now truncated by one residue, may be labeled with an appropriate fluorescent (or chromophoric) reagent.

In this chapter, fluorescein isothiocyanate (FITC) is chosen as the labeling reagent, but other isothiocyanates or sulfonyl halides could be used. The product of the reaction is the peptide with the original N-terminal amino acid removed, with all ϵ -amino lysine groups converted to the phenyl thiocarbamyl, and with a single fluorescent label at the N-terminus of the truncated peptide.

3.2 EXPERIMENTAL

3.2.1 Labeling Peptide Directly

Peptide 8656 (Peninsula Labs, Belmont, CA, USA) has a primary structure Arg-Lys-Arg-Ala-Arg-Lys-Glu. A 10^{-4} M solution was prepared in a 0.2 M pH 9.2 borate buffer. The fluorescein isothiocyanate derivative was prepared by mixing 100 μ L of 4.7×10^{-4} M FITC (Molecular Probes, Oregon, USA) solution prepared in HPLC grade acetone with 100 μ L of the peptide solution. The reaction proceeded at room temperature in the dark for 8 hours in a 1.5-ml disposable polypropylene vial (Fisher Scientific Company, Pittsburgh, PA, USA).

3.2.2 Manual Edmon Degradation Procedure

The manual Edman degradation procedure was similar to that reported by Edman and Henschen [10]. Approximately 2 mg of the peptide was dissolved in 1 ml buffer in a stoppered glass test tube; the buffer was 0.4 M triethylamine (Anachemica, Montreal, PQ, Canada) in 3 : 2 (V:V) 1-propanol : water, adjusted to pH 9.6 with 1 M trifluoroacetic acid (TFA) (Sigma Chemical Co., St. Louis, MO, USA). 50 μ L of PITC (Sigma Chemical Co., St. Louis, MO, USA) was added to the peptide solution, the tube was flushed with N_2 and incubated at 55 $^{\circ}$ C for 20

minutes in a water bath with occasional agitation. The solution was extracted with five 2-ml aliquots of benzene with centrifugation to separate the phases. The benzene layers were discarded and the aqueous layer was freeze dried. The residue was extracted three times with 0.5 ml aliquots of ethyl acetate (Caledon Laboratories, Georgetown, ON, Canada). The ethyl acetate had been passed through an alumina column and filtered before use. The ethyl acetate extract was dried under a stream of N₂. A portion of 100 µL of anhydrous TFA (Protein Sequencing Grade, Sigma Chemical Co., St. Louis, MO, USA) was added and the solution was incubated at 40 °C for 15 minutes in a water bath with occasional agitation. The residue was dried under vacuum for about 10 minutes. Three ml of 1,2-dichloroethane (Caledon Laboratories) was added and the solution was centrifuged to separate the layers. The dichloroethane layer was discarded, and 1 mL more dichloroethane was added. The residue was macerated with a glass stirring rod. The mixture was centrifuged and the dichloroethane layer was discarded. The aqueous layer was dried under vacuum and stored in a desiccator at 4 °C until further use.

3.2.3 Labeling Truncated Peptide

The dried, truncated peptide was dissolved in 1.00 ml of a 0.2 M pH 9.2 borate buffer with a concentration $\sim 10^{-5}$ M. To label the truncated peptide, 10 µL of 4.7×10^{-4} M fluorescein isothiocyanate solution prepared in HPLC grade acetone was mixed with 100 µL of the truncated peptide solution in a 1.5-ml disposable polypropylene vial (Fisher Scientific Company, Pittsburgh, PA, USA). The reaction proceeded for 8 hours in the dark at room temperature. Solutions were diluted to a total FITC concentration of 10^{-6} M with 5 mM borate buffer (pH 9.2) before injection onto the capillary.

3.2.4 Instrument Setup

The system setup of capillary electrophoresis with laser-induced fluorescence detection was similar to the one described in chapter 2 and the optical components were specially chosen for detection of fluorescein isothiocyanate. A low-power (50 mW, air-cooled) argon ion laser (Uniphase, CA, USA) operating at $\lambda = 488$ nm was focused with a 2.5x microscope objective into the center of a sheath flow cuvette (200- μ m square chamber and 2-mm thick windows). Fluorescence was collected at right angles to both the sample stream and the incident laser beam with a 32x, 0.65 numerical aperture microscope objective. The illuminated sample was imaged onto a 600 μ m diameter pinhole, which acts as a mask to block scattered laser light. An interference filter (Omega optical, Inc., Brattleboro, VT, USA) with a 525 nm center wavelength and a 40 nm bandpass was used to reject Rayleigh and Raman scatter while maximizing the transmission of fluorescence. A R1477 photomultiplier tube (Hamamatsu Corporation, San Jose, CA, USA) detected the fluorescence signal. After passing through a low-pass filter, the current from the photomultiplier tube was converted into voltage signal and recorded with a Macintosh IIsi computer.

3.2.5 Capillary Electrophoresis Conditions

A 44 cm long, 50 μ m inner diameter and 190 μ m outer diameter fused silica capillary (Polymicro Technologies, Phoenix, AZ, USA) was used for separations. The separation buffer was 5 mM, pH 9.2 borate buffer. Samples were injected electrokinetically for 5 seconds at 2 kV; separation proceeded at 13 kV provided by a high voltage power supply (Spellman high voltage electronics, Plainview, NY, USA).

3.3 RESULTS AND DISCUSSION

The primary structure of this peptide is Arg-Lys-Arg-Ala-Arg-Lys-Glu. The peptide used in this example has two lysine residues in addition to the N-terminal arginine residue. When labeled with fluorescein isothiocyanate, a total of seven fluorescent products are possible. The separation of the labeled peptide is shown in Figure 3.1. In addition to the unreacted FITC peak, there are at least seven peaks present, corresponding to the different products of the labeling reaction. Comparison with the electropherogram for the single label peptide suggests that the second peak in this electropherogram contains a single label at the α -amino group. The relatively close spacing of the other peaks is not surprising. Conversion of the ϵ -amino group to the phenyl thiocarbamyl derivative increases the size of the peptide slightly but should not change its charge.

If the peptide is taken through one cycle of the Edman degradation reaction, the N-terminal amino acid (Arginine) is removed; the primary structure of the truncated peptide is Lys-Arg-Ala-Arg-Lys-Glu. In the Edman degradation step, the amine-containing side chains of the lysine residues are converted to the ϵ -phenylthiocarbamyl derivative. By protecting the ϵ -amino groups and cleaving the N-terminal amino acid, only one amine is available for further labeling. The reaction mixture shows two peaks, Figure 3.2, one corresponding to the labeled peptide and the other to unreacted fluorescein isothiocyanate. The Edman treatment appears to be quite efficient; no peaks corresponding to multiple labeling are detected.

A small impurity is noted in the reaction product, with an elution time of about 5.25 min. This impurity was undetectable for the labeled native peptid

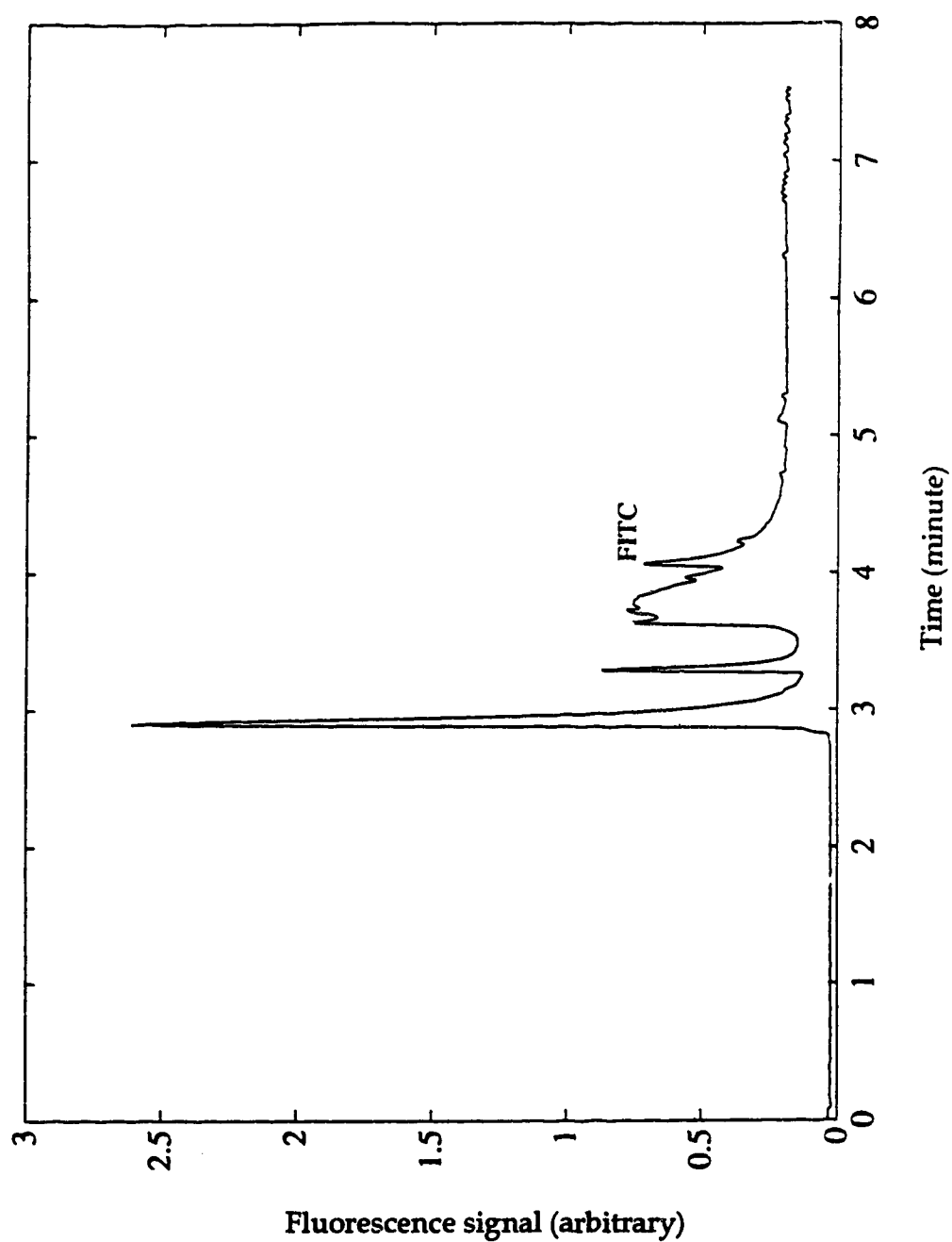


Figure 3.1 Multiple labeling: electropherogram of direct fluorescein isothiocyanate labeled peptide 8656; peak labeled with FITC is the unreacted derivatizing reagent

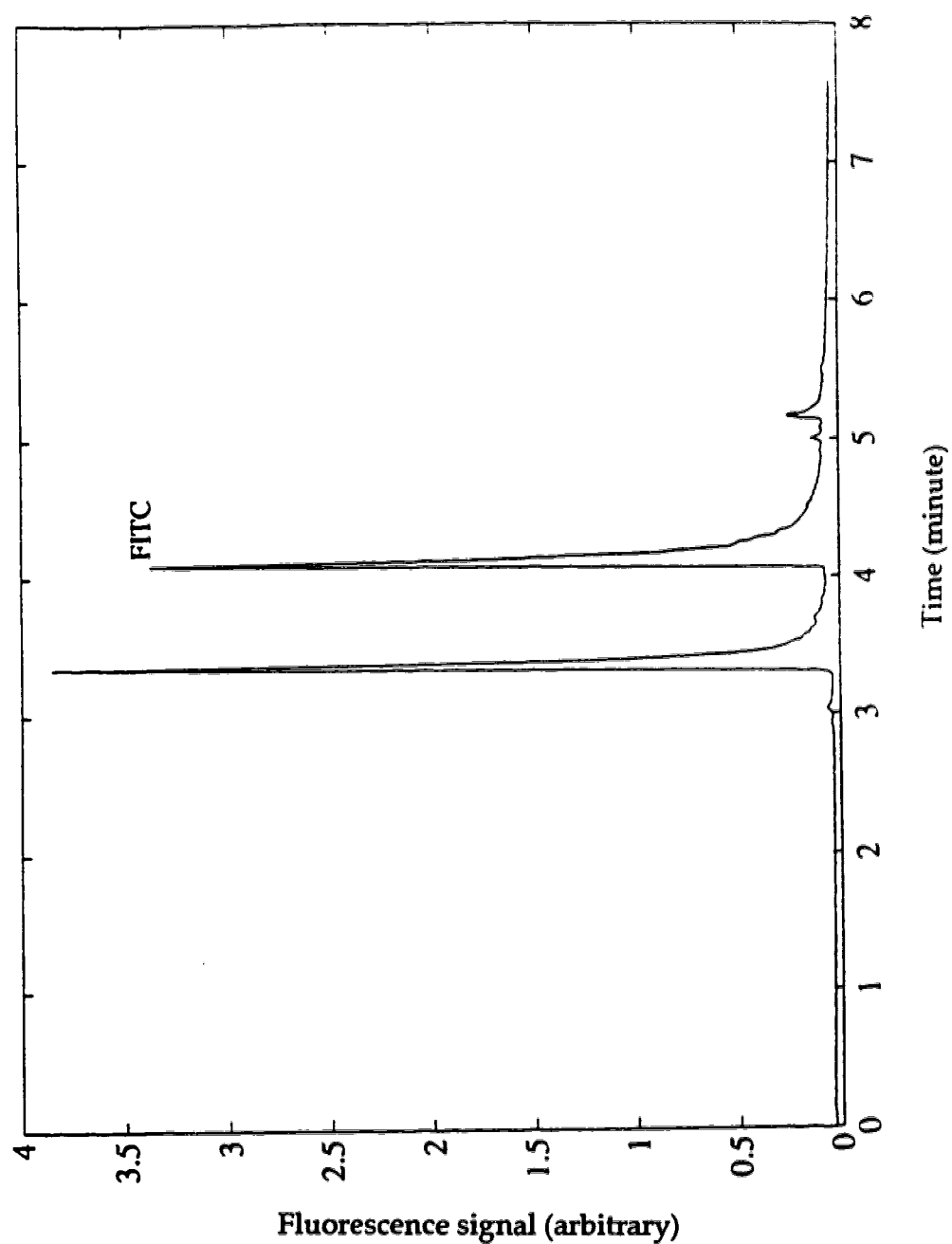


Figure 3.2 Single labeling: electropherogram of truncated peptide 8656; peak labeled with FITC is the unreacted derivatizing reagent

because of the complex reaction mixture. However, by ensuring that only one label is attached to the peptide, the electropherogram is simplified so that the minor contaminant can be detected.

3.4 CONCLUSIONS

Pre-column fluorescent labeling is convenient for high sensitivity peptide analysis in capillary electrophoresis. When pre-column derivatization is employed, incomplete multiple labeling is problematic, producing a complicated mixture from a single analyte. A single label can be attached to the peptide by first taking the peptide through one cycle of the Edman degradation reaction; because of its small size and high reactivity, phenyl isothiocyanate quickly and efficiently labels all free amino groups in the peptide. All ϵ -amino groups on lysine residues are converted to the ϵ -phenyl thiocarbamyl, and can not partake in the labeling FITC reaction; only the N-terminal amino group is available for further labeling.

As a limitation to this technology, only unblocked peptides can be labeled. N-terminal acetylated peptides do not have a free α -amino group. While various chemical unblocking procedures, such as cyanogen bromide cleavage, can be employed, they can produce a number of reaction products, defeating the purpose of this labeling protocol. Also, the procedure removes the N-terminal amino acid; two peptides that differ only at the N-terminal amino acid will be indistinguishable after this labeling procedure.

This reaction was performed by use of the manual Edman reaction at relatively high concentration. It would be much more efficient to use an automated protein sequencer to perform this reaction; picomoles of protein could

be prepared at 10^{-8} M concentration for fluorescent labeling [11]. However, the sequencer must be modified to allow facile recovery of the treated peptide; a strong solvent could be used to remove the peptide from a Polybrene treated solid phase sequencing disk.

Last, this reaction was demonstrated with phenyl isothiocyanate as the protecting reagent and fluorescein isothiocyanate as the labeling reagent. It may prove possible to use smaller protecting reagents, such as methyl isothiocyanate, which should react more quickly than PITC. Other fluorescent reagents could be used. As always, the labeling chemistry should be chosen to provide a good match to the excitation source [12]. As an attractive reagent, the 3-(4-carboxybenzoyl)-2-quinolinecarboxaldehyde derivative absorbs strongly in the blue and appears to react quickly with primary amines [7].

REFERENCES

1. J. W. Jorgenson, K. D. Lukacs, *Science* , **222**, 266-272 (1983).
2. T. McDonnell, J. Pawliszyn, *J. Chromatogr.* , **559**, 489 (1991).
3. S. L. J. Pentoney, X. Huang, D. S. Burgi, R. N. Zare, *Anal. Chem.* , **60**, 2625-2629 (1988).
4. D. J. Rose, J. W. Jorgenson, *J. Chromatogr.* , **447**, 117-131 (1988).
5. Y. F. Cheng, N. J. Dovichi, *Science* , **242**, 562-564 (1988).
6. J. Y. Zhao, D. Y. Chen, N. J. Dovichi, *J. Chromatogr.* , **608**, 117-120 (1992).
7. J. Liu, Y. Z. Hsieh, D. Wiesler, M. Novotny, *Anal. Chem.* , **63**, 408-412 (1991).
8. R. A. Jue, R. F. Doolittle, *A novel approach to amino acid sequencing*. A. S. Bhowan, Eds., Protein/peptide sequence Analysis: Current methodologies (CRC Press INC, 1988).
9. P. Edman, *Arch. Biochem. Biophys.* , **22**, 475 (1949).
10. P. Edman, A. Henschen, *Protein Sequence Determination*. S. B. Needleman, Eds., Springer, Berlin, 1975).
11. P. Tempst, L. Rivier, *Anal. Biochem.* , **183**, 290-300 (1989).
12. J. Gluckman, D. Shelly, M. Novotny, *J. Chromatogr.* , **317**, 443-453 (1984).

CHAPTER 4

SEPARATION OF AMINATED MONOSACCHARIDES FOR OLIGOSACCHARIDE SEQUENCING BY MICELLAR CAPILLARY ELECTROPHORESIS WITH LASER-INDUCED FLUORESCENCE DETECTION*

* A version of this chapter has been accepted for publication. *J. Chromatogr.*, (1994)

4.1 INTRODUCTION

The study of carbohydrates is a very important area of molecular biology in which great investment has been placed so as to understand more fully what the functions of carbohydrates are, and how we can manipulate them to our advantage. Carbohydrates have been shown to play essential roles in biology such as cell/cell recognition, hormone receptors, virus binding sites, inflammation processes and various other biological functions. Because of their importance to biological systems, it is of importance for us to be able to determine the primary structure of carbohydrate chains, i.e. oligosaccharide sequencing, which play monumental roles in cell function and interaction.

The first step to sequence an oligosaccharide is to determine the composition of the chain. This requires a good separation technique because of the many types of monomers involved, some of which are isomers. The second step of sequencing an oligosaccharide chain is to develop a strategy to degrade the chain specifically. Because of the variety of linkage between the monomers, an oligosaccharide primary structure can be branched. This makes it more difficult to sequence oligosaccharides than proteins and DNA. So far no single method has been devised for oligosaccharide sequencing like the Edman degradation of polypeptides.

In the past and even today, analysis of oligosaccharide chains has proceeded by methods such as methylation analysis, enzymatic degradation, and mass spectrometry in association with nuclear resonance spectroscopy [1]. However, in biological system the raw amount of these oligosaccharide chains is minuscule in comparison to the amounts the procedures mentioned above require. Because of this, these methods are impractical for analysis of the

oligosaccharides contained on cell surfaces. Thus, a different method with great separation power and high sensitivity is required to identify and quantify the monosaccharide fragments for oligosaccharide sequencing.

Capillary electrophoresis offers excellent separation efficiency. Also, the small dimensions of the capillary tubes offer substantial opportunities for the analysis of extremely small amount of samples. Normally, the solution volume required by capillary electrophoresis is at the order of nanoliter or less. The excellent separation efficiency of capillary electrophoresis with possible high sensitivity detection has been applied successfully for the analysis of peptides, proteins, and oligonucleotides. But as one of the important classes of biomolecules, carbohydrates did not attract much attention in the field of CE separation until 1989, mainly due to the lack of chromophores for high sensitivity detection. Since Honda and co-workers [2] reported the capillary electrophoresis results of monosaccharides as their N-(2-pyridyl)glycamines with UV detection in 1989, there is now a growing research interest in carbohydrates using capillary electrophoresis as reviewed recently by Kuhr and Monnig [3].

Because carbohydrates are usually neutral, it is often necessary to convert them into charged species for capillary zone electrophoresis separation. Fortunately, carbohydrates can interact with ionic species including anionic complexes with sodium borate, sodium stannate [4], sulphonated benzene boronic acid [5], sodium germanate [6], sodium tungstate [7] and cationic complexes with lead acetate, cations of alkali and alkaline earth metals [8]. Borate buffer is the most commonly used buffer for the electrophoretic separation of carbohydrates. Recently, a detailed study of the influence of borate complexation on the electrophoretic behavior of underivatized carbohydrates in capillary electrophoresis has been reported by Hoffstetter-Kuhn *et al.* [9].

Micellar electrokinetic capillary chromatography (MECC) is a useful CE mode in separating neutral analytes as well as ionic species. Even though borate complexation with carbohydrates makes capillary zone electrophoresis applicable to carbohydrate separation, it has been found that the MECC mode can improve separation efficiency in complicated sugar analysis [10]. Capillary gel electrophoresis (CGE) is also another choice for carbohydrate separation [11].

There are two kinds of detection strategies for carbohydrate determination using capillary electrophoresis. One is to detect the sugars directly without any derivatization [9, 12, 13, 14]. But because carbohydrates have a very low UV absorbance, direct UV absorbance detection is limited to the nanomole (10^{-9} mole) range, even with a 2-20 fold increase in the UV absorbance at 195 nm by adding borate to underivatized carbohydrates [14]. An indirect UV detection system using sorbic acid as both carrier electrolyte and chromophore for carbohydrate determination improved detection limits to the picomole (10^{-12} mole) range. Detection of underivatized carbohydrates (both aldoses and ketoses) in the femtomole (10^{-15} mole) range was achieved using indirect fluorescence detection with visible laser excitation [13]. Another class of detection is to introduce a chromophore to carbohydrates in order to achieve high sensitivity. A report on the derivatization of reducing mono- and oligosaccharides to N-2-pyridylglycamines demonstrated a significant increase in sensitivity to the low picomole level using on-column UV detection of these derivatives at 240 nm [15]. Laser-induced fluorescence detection provides the highest sensitivity for capillary electrophoresis. It is necessary to introduce an active functional group to a carbohydrate molecule as a suitable precursor for derivatization with fluorescent dyes. Reductive amination is a well established procedure for introducing primary amine groups to carbohydrates [16]. With

reductive amination, mono- or oligosaccharide derivatives of 3-(4-carboxybenzoyl)-2-quinolinecarboxaldehyde (CBQCA) have detection limits in the low attomole (10^{-18} mole) range [11, 17].

Post-column laser-induced fluorescence detection in a sheath flow cuvette has been developed as a remarkable sensitive technique for capillary electrophoresis with detection limits at the order of zeptomole (i.e. 10^{-21} mole) or less [18, 19]. If this system is used to determine monosaccharide fragments from oligosaccharide sequencing, an ultra-sensitive oligosaccharide sequencer may be developed.

New methods being developed for oligosaccharide sequencing involve labeling of the reducing end of a carbohydrate chain followed by enzymatic degradation from the non-reducing ends. Alternatively, it may be possible to chemically degrade the sugar chains from their reducing ends. Model compounds are required to explore these sequencing strategies.

In this chapter, the six neutral reducing monosaccharides found in mammalian carbohydrates were chosen to serve as standards for oligosaccharide sequencing: glucose, galactose, mannose, fucose, N-acetylglucosamine and N-acetylgalactosamine. The derivatization of glucose, galactose, mannose, fucose into their 1-amino-1-deoxy alditols and N-acetylglucosamine and N-acetylgalactosamine into their 2-amino-2-deoxy alditols is described. 5-carboxytetramethylrhodamine N-hydroxysuccinimidyl ester (TRSE) was used to label the aminated monosaccharides because the low-cost and high-sensitivity detector developed in chapter 2 can be used and zeptomole or better detection limits of TRSE labeled monosaccharides are possible. Figure 4.1 shows the structure of the fluorescent dye molecule. The labeling reaction between a primary amine and a succinimidyl ester was described in chapter 1.

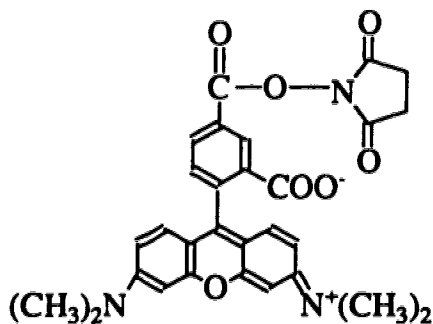


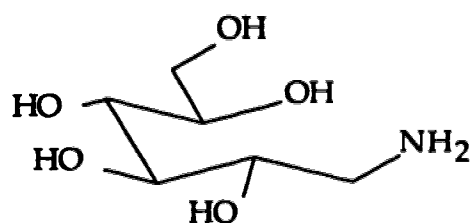
Figure 4.1 Structure of 5-carboxytetramethylrhodamine succinimidyl ester

4.2 EXPERIMENTAL

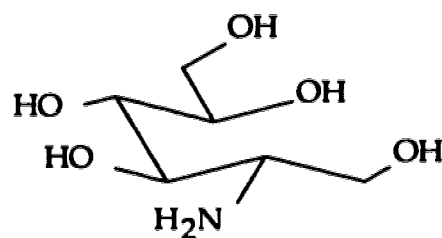
4.2.1 Synthesis of Six Standards of Aminated Monosaccharides (by Paul Diedrich from Dr. Ole Hindsgaul's group)

The standards for glucose, galactose, mannose, and fucose are 1-amino-1-deoxy alditols while the standards for N-acetylglucosamine and N-acetylgalactosamine are 2-amino-2-deoxy alditols. The structures of these standards are shown in Figure 4.2.

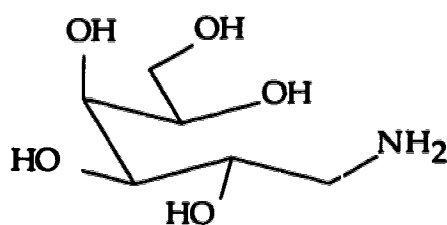
In the past, methods for the synthesis of free amine derivatives of reducing sugars such as glucamine include the reduction of glucose in methanolic ammonia [20], the catalytic reduction of glucose in the presence of hydrazine [21], and the reduction of glucose over Raney nickel in liquid



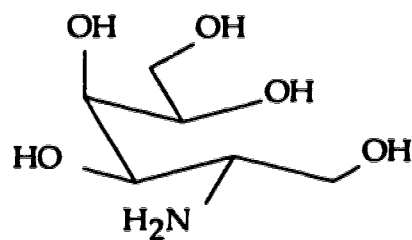
1-amino-1-deoxy-D-glucitol
(GlcNH₂)



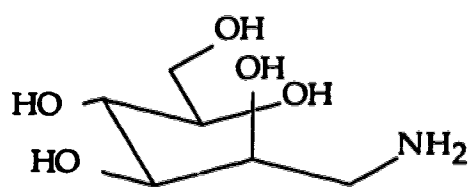
2-amino-2-deoxy-D-glucitol
(2-GlcNH₂)



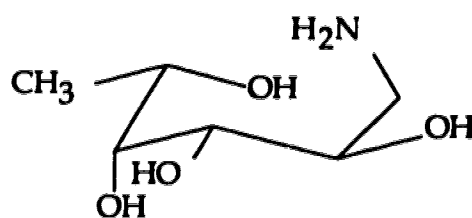
1-amino-1-deoxy-D-galactitol
(GalNH₂)



2-amino-2-deoxy-D-galactitol
(2-GalNH₂)



1-amino-1-deoxy-D-mannitol
(ManNH₂)



1-amino-1-deoxy-L-fucitol
(FucNH₂)

Figure 4.2 Structures of six aminated monosaccharides

ammonia [22]. These methods, however, are designed for large scale industrial production. The initial approach to synthesize milligram-scale reductively aminated monosaccharides was to try the method of Borch *et al.* [16], which made use of the selective reducing agent sodium cyanoborohydride. The one-pot reaction allowed that all reagents could be added at once as the cyanoborohydride selectively reduces the imine (an intermediate) much faster than the carbonyl group. Thus the aldehyde, formed during mutarotation, could react with ammonium acetate to yield the imine which would be then reduced to the free amine. The difficulty with this method came during isolation of the product when ion exchange columns were to be used to separate the 1-amino-1-deoxy-D-glucitol formed from the salts present in the reaction. An alternative method of synthesis was therefore sought to overcome this difficulty.

The method adopted for adding a free amine group to a reducing monosaccharide was based on the scheme described by Bock *et al.* [23]. Certain modifications were incorporated which afforded a product of high purity in reasonable yields. Glucose, galactose, mannose, or fucose was reductively aminated, see Figure 4.3 as an example. The first step is the reaction of a concentrated sugar solution with excess benzylamine until full conversion of reducing sugar to imine product was indicated by thin layer chromatography. This process typically required 4-6 hours at a temperature of about 50°C. Next the reduction of the imine by sodium borohydride yielded the 1-benzylamino-1-deoxy derivatives. As the benzylamine is in excess the aqueous solution is quite basic, it was possible to remove the excess benzylamine by extracting the aqueous solution with dichloromethane. The completion of this process was also monitored by thin layer chromatography. Dilution of the aqueous layer with methanol followed by acidification and evaporation removed borate esters

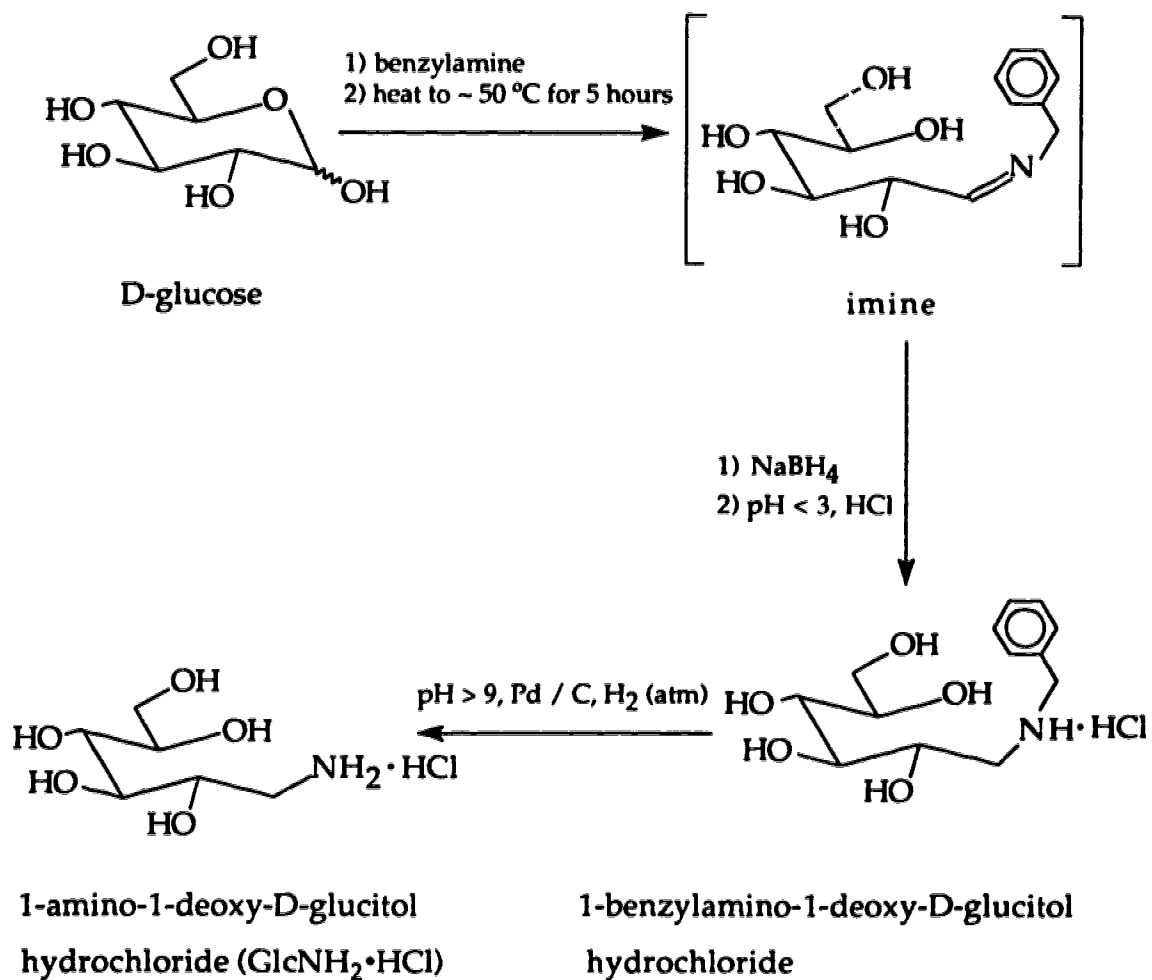


Figure 4.3 Reductive amination of D-glucose

from the product.

The N-benzyl intermediate typically was isolated, recrystallized and characterized with a portion of the recrystallized product being used for the reduction. De-benzylation proceeded by catalytic reduction of the benzylamino intermediate under atmospheric hydrogen using palladium on carbon as the catalyst. This reduction was carried out overnight and yielded the free amine at the 1 position of the reducing sugar.

The synthesis of standards for N-acetylglucosamine and N-acetylgalactosamine using the above method yielded mixtures that resisted purification. An alternative way, as shown in Figure 4.4, was to reduce glucosamine or galactosamine and to use the existing free amine for fluorescent labeling. The solution of the sugar (glucosamine or galactosamine) was added dropwise to a concentrated basic solution of sodium borohydride over a period of approximately 2 hours at a temperature of 45°C. After reduction of the amine sugar, the solution was then acidified and concentrated in vacuo with methanol three times to remove borate esters. The collected products were recrystallized and yielded pure 2-amino-2-deoxy alditols.

Thin layer chromatography was performed on silica gel (Merck, 60-F254) with detection by quenching of fluorescence and/or by charring with sulfuric acid. All chemicals used were reagent grade and solvents used were distilled. Water was distilled and deionized using the Millipore milli-Q water system. ^1H NMR spectra were recorded at 300 MHz (Bruker AM-300) or 360 MHz (Bruker WM-360) in D_2O . ^{13}C -NMR spectra were recorded at 75 MHz (D_2O). Mass spectra were carried out by low resolution positive fast atom bombardment in Clelland matrix. The ^{13}C NMR and mass spectrum data are listed in Table 4.1.

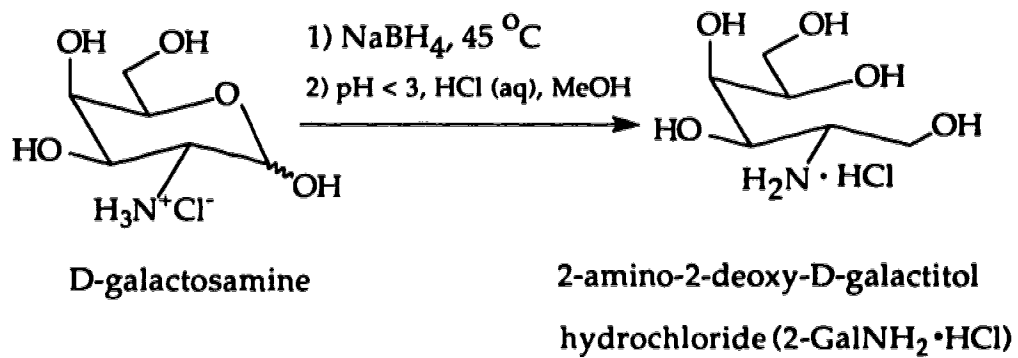
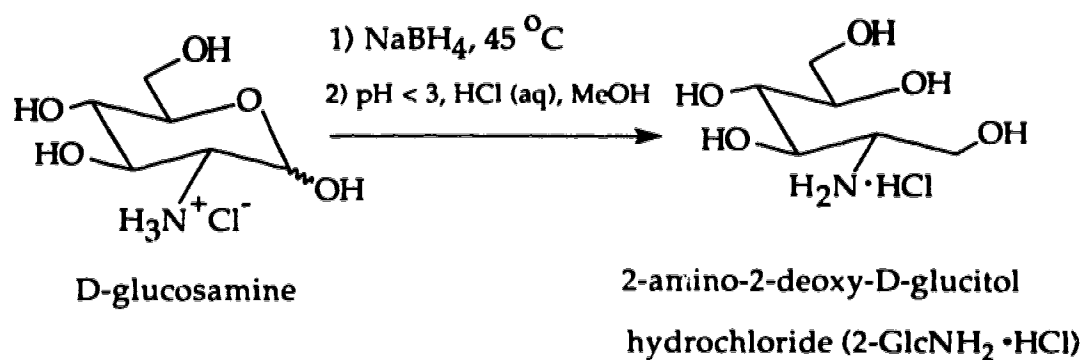


Figure 4.4 Reduction of D-glucosamine and D-galactosamine

Table 4.1 ^{13}C NMR (shift in ppm) and mass spectrum data

standard	C-1	C-2	C-3	C-4	C-5	C-6	mass peak
1-amino glucitol	42.6	69.8	71.8	71.5	71.6	63.5	181.1
1-amino galactitol	43.6	67.3	71.3	70.1	70.7	64.0	181.1
1-amino mannitol	43.4	68.0	71.7	69.8	71.5	63.9	181.1
1-amino fucitol	43.6	66.6	73.5	67.5	71.7	19.5	165.0
2-amino glucitol	59.8	56.3	71.7	66.9	71.4	63.7	181.1
2-amino galactitol	60.8	54.9	71.8	67.7	71.1	63.8	181.1

4.2.2 Labeling Reactions

Stock Solutions

5-carboxytetramethylrhodamine N-hydroxysuccinimidyl ester (Molecular Probes, Inc., Eugene, OR, USA) was dissolved in dimethylformamide (DMF) to make 1.28×10^{-3} M stock solution (dark purple) and stored in freezer. Stock solutions of alanine and the aminated sugars were prepared 2×10^{-2} M in 0.185 M NaHCO_3 buffer (pH = 8.3) and stored in a refrigerator (4°C).

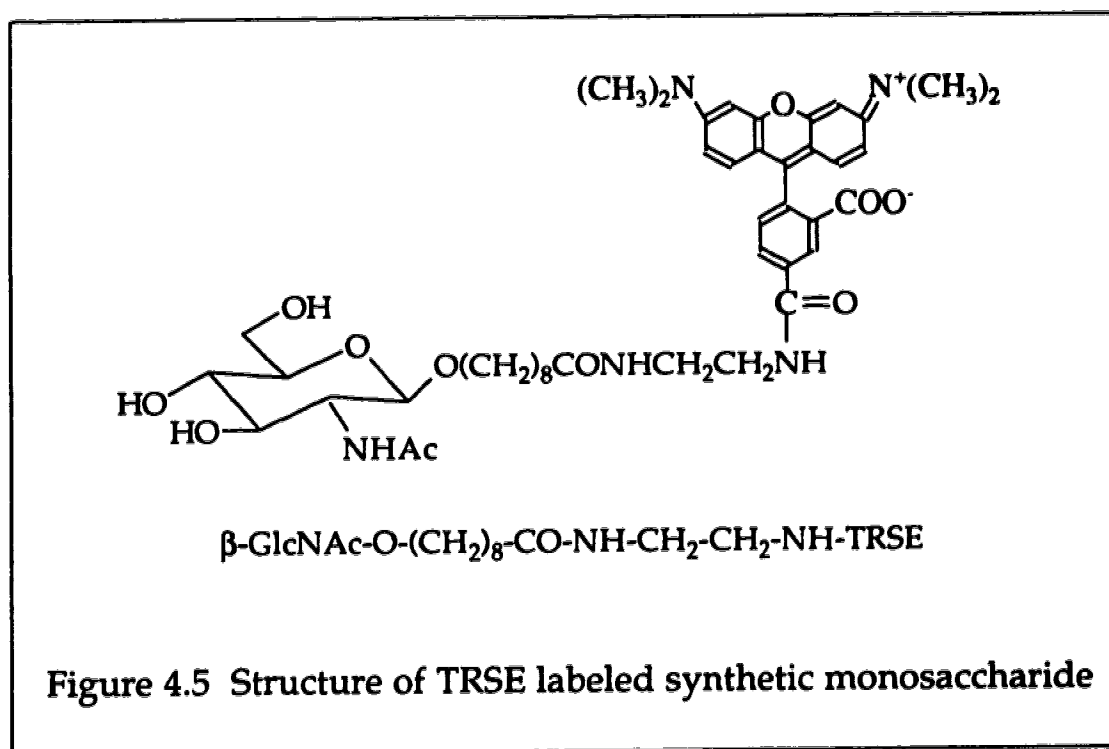
Labeling Reactions

Alanine or sugar stock solution (30 μL) was mixed with 5 μL TRSE stock solution in a 1.5-ml dark brown polypropylene vial (Fisher Scientific, Pittsburgh, PA, USA). The mixtures were vortexed and centrifuged a few times during the one hour reaction period. The labeling reaction was carried out at room temperature in the dark. Then the reaction mixtures were stored in a refrigerator

(4°C) for future use. A blank solution was prepared by mixing 30 μL 0.185 M NaHCO_3 buffer with 5 μL TRSE stock.

4.2.3 Standard for Detection Limit and Calibration Curve

Synthetic 8-methoxycarbonyloctyl β -D-N-acetylglucosamine was reacted with ethylenediamine to produce β -GlcNAc-O-(CH₂)₈-CO-NH-CH₂-CH₂-NH₂. The free primary amine group was labeled with TRSE. The labeled derivative, as shown in Figure 4.5,



was purified and used as a standard to determine the linear dynamic range and detection limit of the capillary electrophoresis system with laser-induced fluorescence detection in a sheath flow cuvette described below. A 2.4×10^{-4} M

stock solution of this standard was prepared in water. The solution was diluted to a series of concentrations by a buffer containing 10 mM Na_2HPO_4 , 10 mM borate and 10 mM SDS (pH = 9.3) for micellar electrokinetic capillary chromatography with laser-induced fluorescence detection in a sheath flow cuvette. The peak heights were used to construct a calibration curve and to calculate the detection limit of the instrument.

4.2.4 Instrument Setup

The capillary electrophoresis system with laser-induced fluorescence detection was described in Chapter 2 [19]. An inexpensive helium-neon laser was used to provide 0.75-mW beam at the wavelength of 543.5 nm (Melles Griot, ON, Canada). The beam was focused with a 10x microscope objective about 200 μm below the exit of the capillary which was fixed one end inside the 200- μm square chamber of the sheath flow cuvette. Post-column laser-induced fluorescence was collected at right angles with an 50x, 0.60 numerical aperture (Melles Griot) onto an Iris with adjustable pinhole diameter. The interference filter was 580DF40 (580 nm center, 40 nm band pass, Omega optical, Inc., Brattleboro, VT, USA). A Hamamatsu R1477 photomultiplier tube (Hamamatsu Corporation, San Jose, CA, USA) was operated at 1200 V at room temperature. The photomultiplier tube output was passed through a 0.1 second RC low-pass filter and recorded with a Macintosh IIsi computer.

4.2.5 Electrophoresis Conditions

A 74.4 cm long, 10- μm inner diameter and 145- μm outer diameter uncoated open-tube fused silica capillary (Polymicro Technologies, Phoenix, AZ,

USA) was used for separations. Sample injections were performed electrokinetically at 2500 V for 5 seconds. Electrophoresis was driven at 29 kV with a high voltage power supply (Spellman CZE 1000R, Spellman high voltage electronics, Plainview, NY, USA).

4.2.6 Separation Buffers

Stock buffer solutions were prepared in deionized water (from a Barnstead NANOpure system) and filtered with 0.22- μ m pore-size membranes. These aqueous stock solutions included 0.2 M Na₂HPO₄, 0.1 M phenyl boronic acid, 0.2 M borate and 0.556 M sodium dodecyl sulfate. Separation buffers were prepared by mixing these stock solutions. For example, most separations were performed with a buffer of 10 mM Na₂HPO₄, 18 mM phenylboronic acid, 10 mM borate and 10 mM sodium dodecyl sulfate (pH 9.3).

4.3 RESULTS AND DISCUSSION

4.3.1 The Fluorescent Dye: TRSE

Spectral Properties

Figure 4.6 presents the absorbance spectra of 2.4×10^{-6} M 5-carboxytetramethylrhodamine N-hydroxysuccinimidyl ester in methanol and in 10 mM borate buffer, and Figure 4.7 shows the absorbance spectrum of TRSE labeled β -GlcNAc-O-(CH₂)₈-CO-NH-CH₂-CH₂-NH₂ in methanol. All of the absorbance spectra were measured with a UV-Vis spectrophotometer (8451A Diode Array Spectrophotometer, Hewlett Packard). TRSE has a maximum

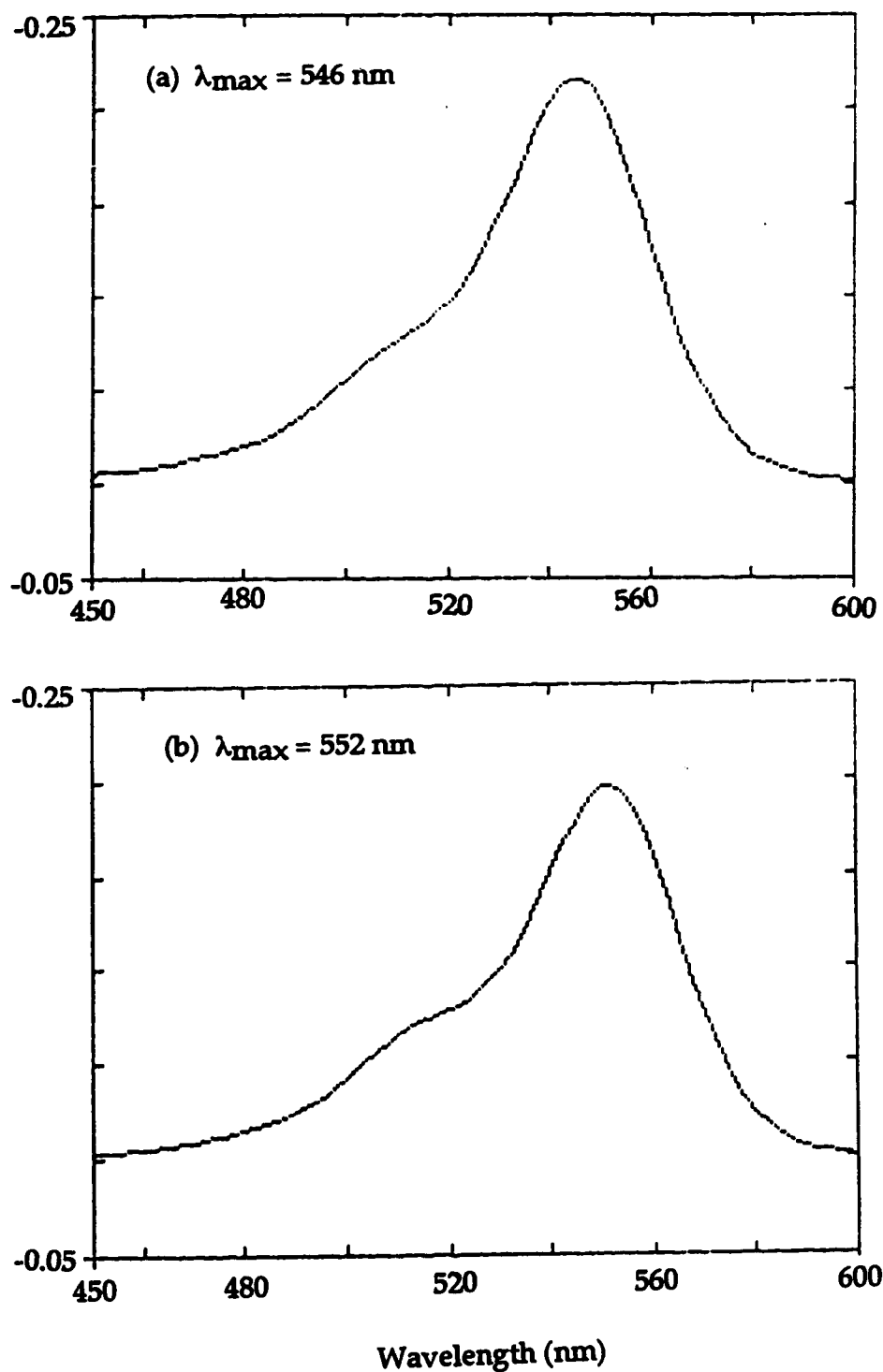


Figure 4.6 Absorbance spectra of TRSE ($2.4 \times 10^{-6} \text{ M}$) in (a) methanol and (b) 10 mM borate buffer

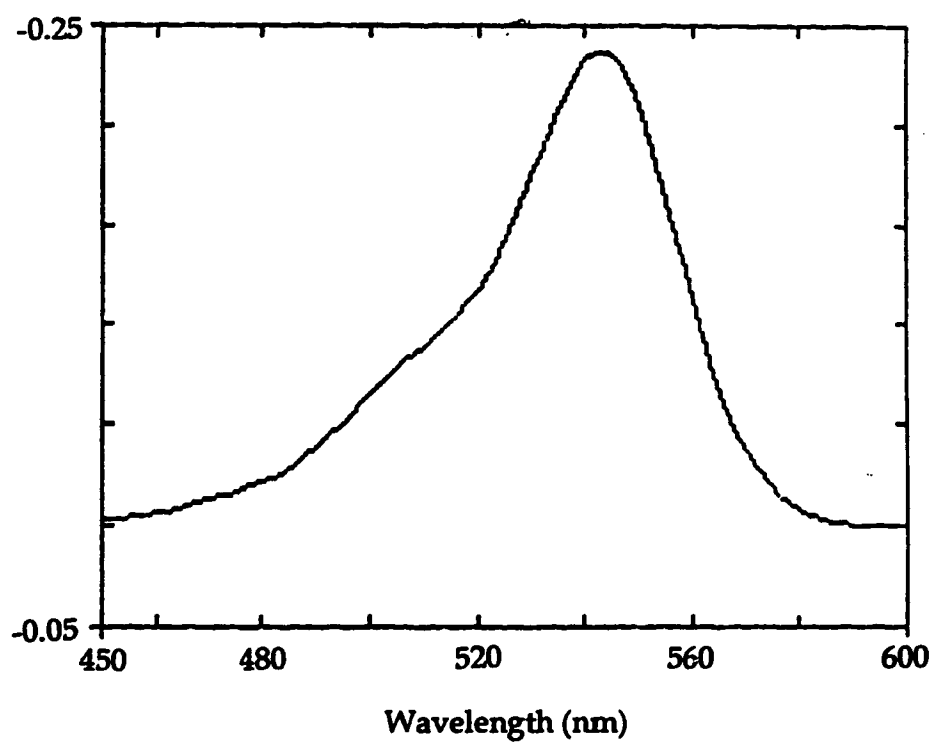


Figure 4.7 Absorbance spectrum of TRSE labeled synthetic sugar
 β -GlcNAc-O-(CH₂)₈-CO-NH-CH₂-CH₂-NH₂
(2.4×10^{-6} M in methanol)

absorbance at 546 nm in methanol with a molar absorptivity of $8.8 \times 10^4 \text{ M}^{-1}\text{cm}^{-1}$ and 552 nm in 10 mM borate buffer with a molar absorptivity of $8.1 \times 10^4 \text{ M}^{-1}\text{cm}^{-1}$. The maximum absorbance of TRSE labeled $\beta\text{-GlcNAc-O-(CH}_2)_8\text{-CO-NH-CH}_2\text{-CH}_2\text{-NH}_2$ occurs at wavelength of 542 nm.

The fluorescence emission spectrum of the TRSE labeled $\beta\text{-GlcNAc-O-(CH}_2)_8\text{-CO-NH-CH}_2\text{-CH}_2\text{-NH}_2$ is shown in Figure 4.8 and was measured with a fluorescence detector (Spectrofluorometer MK2, Andor Scientific Ltd.) when the excitation wavelength was set at 543 nm. The gain was set at 1 and the scan increment was 40 nm. The maximum fluorescence is centered at about 570 nm.

Electropherograms

Figures 4.9 and 4.10 present the electropherograms of the dye diluted from its stock solution in DMF by the 10 mM borate buffer with 10 mM SDS (pH 9.3). Figure 4.9 shows the electropherogram generated immediately after dilution of TRSE from its stock solution. The fused silica capillary used was 73.8 cm long and had an inner diameter of 50 μm ; injection voltage was 2 kV for 5 seconds, electrophoresis voltage was 29 kv, and the voltage of PMT power supply was 1200 V. There are three peaks in the electropherogram. The last peak (peak 1) corresponds to the succinimidyl ester of the dye, while the other two peaks (peak 2 and peak 3) are generated by the hydrolysis products of the dye in the pH 9.3 buffer. The electropherogram shown in Figure 4.10 was generated 22 hours after dilution of TRSE from its stock solution. The experimental conditions were the same as those used for generating Figure 4.9. The increases in the peak heights of the hydrolysis products and the decrease in the TRSE peak height indicate the poor stability of the succinimidyl ester in the basic buffer.

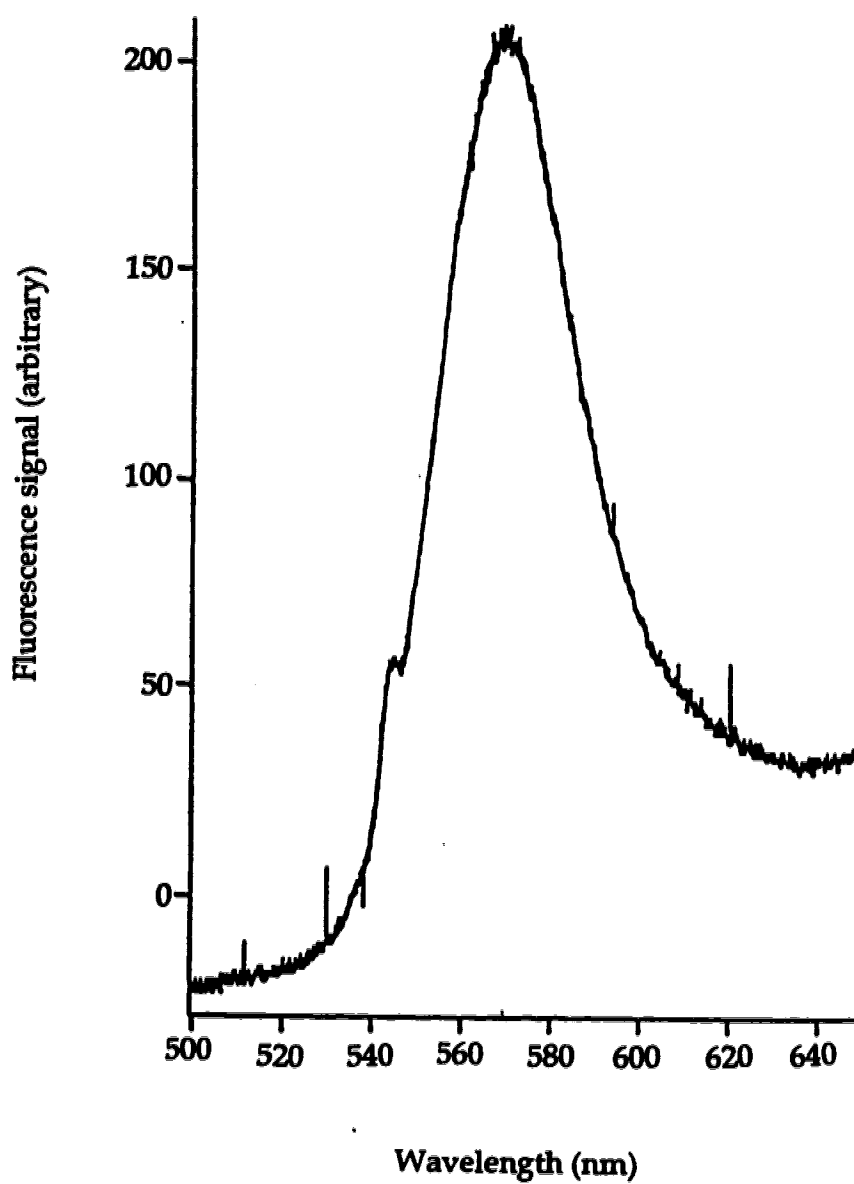


Figure 4.8 Fluorescence emission spectrum of TRSE labeled
 β -GlcNAc-O-(CH₂)₈-CO-NH-CH₂-CH₂-NH₂
(2.4×10^{-6} M in methanol)

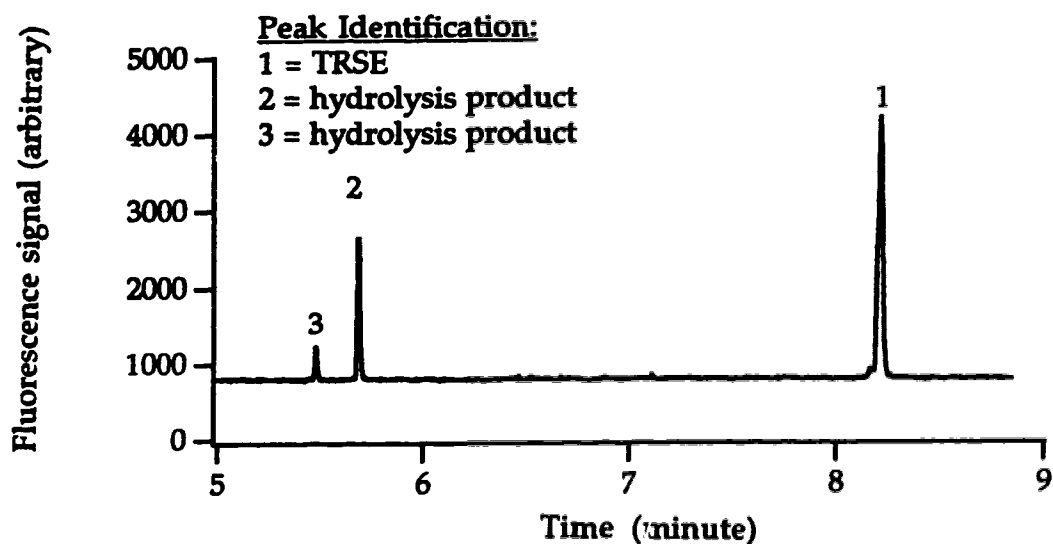


Figure 4.9 Electropherogram of TRSE (immediately after dilution from its stock solution by 10 mM borate buffer with 10 mM SDS)

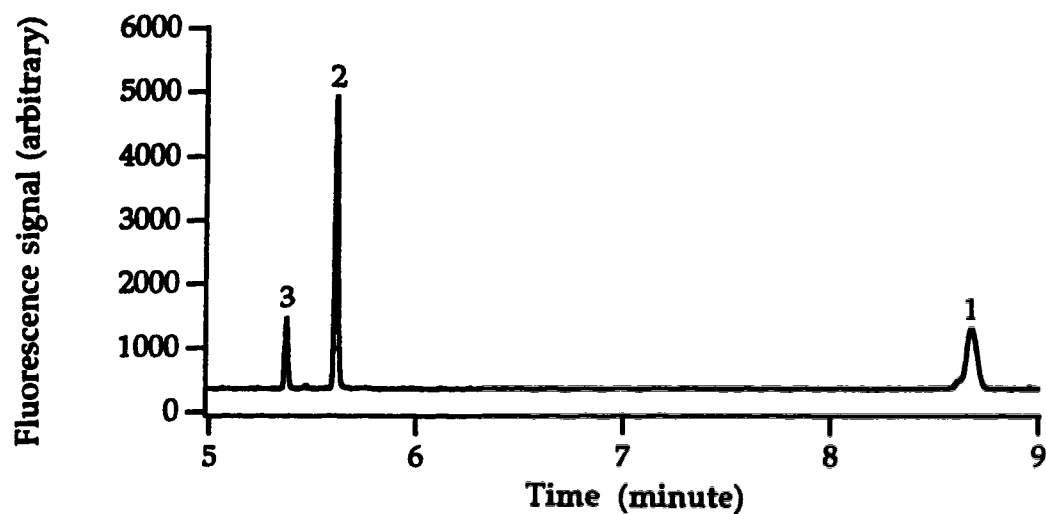


Figure 4.10 Electropherogram of TRSE (22 hours at room temperature after dilution from its stock solution by 10 mM borate buffer with 10 mM SDS)

4.3.2 Calibration Curve and Detection Limit

Table 4.2 lists the calibration curve data from the electropherograms of the synthetic sugar standard at different concentrations. A calibration curve, Figure 4.11, is constructed using $\log(\text{sugar peak height})$ vs. $\log([\text{sugar}], \text{M})$. The calibration curve shows a linear dynamic range of at least three orders of magnitude.

Table 4.2 Calibration curve data

[sugar], M	$\log([\text{sugar}], \text{M})$	sugar peak height	$\log(\text{sugar peak height})$
4.8×10^{-8}	-7.3	9.4034	0.9733
4.8×10^{-9}	-8.3	0.8671	-0.0618
4.8×10^{-10}	-9.3	0.0957	-1.1018
4.8×10^{-11}	-10.3	0.0109	-1.9593

Figure 4.12 shows the electropherogram of the synthesized sugar labeled with TRSE. The capillary used was 74.4 cm long and had an 10 μm inner diameter of 10 μm . Nine picoliters of the 4.8×10^{-11} M solution was injected (800 V for 5 seconds). which corresponds to 4.4×10^{-22} mole or 260 analyte molecules. The bottom panel of the figure shows the smoothed version of the data, where the data have been convoluted with a 0.6 second wide Gaussian shaped filter. According to Knoll's method [24], the calculated detection limit of the instrument is 60 molecules.

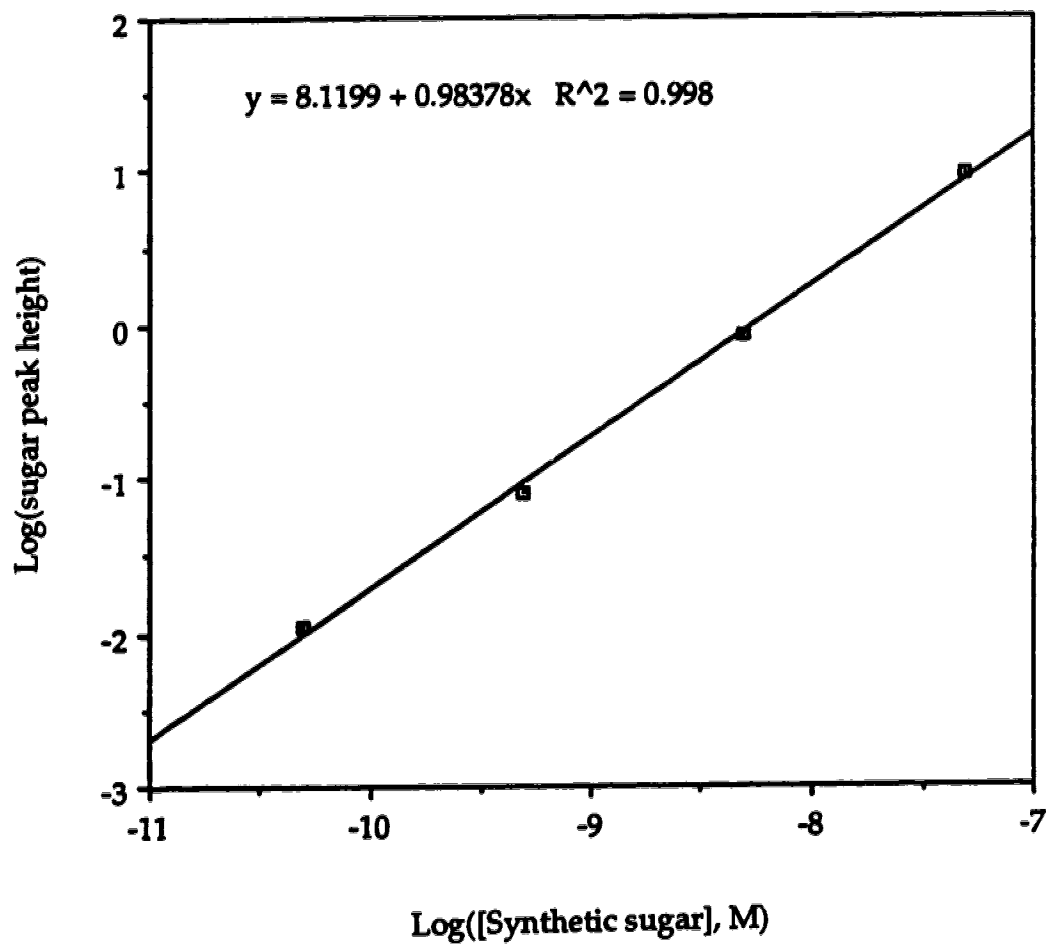


Figure 4.11 Log-log calibration curve for TRSE labeled synthetic sugar β -GlcNAc-O-(CH₂)₈-CO-NH-CH₂-CH₂-NH₂

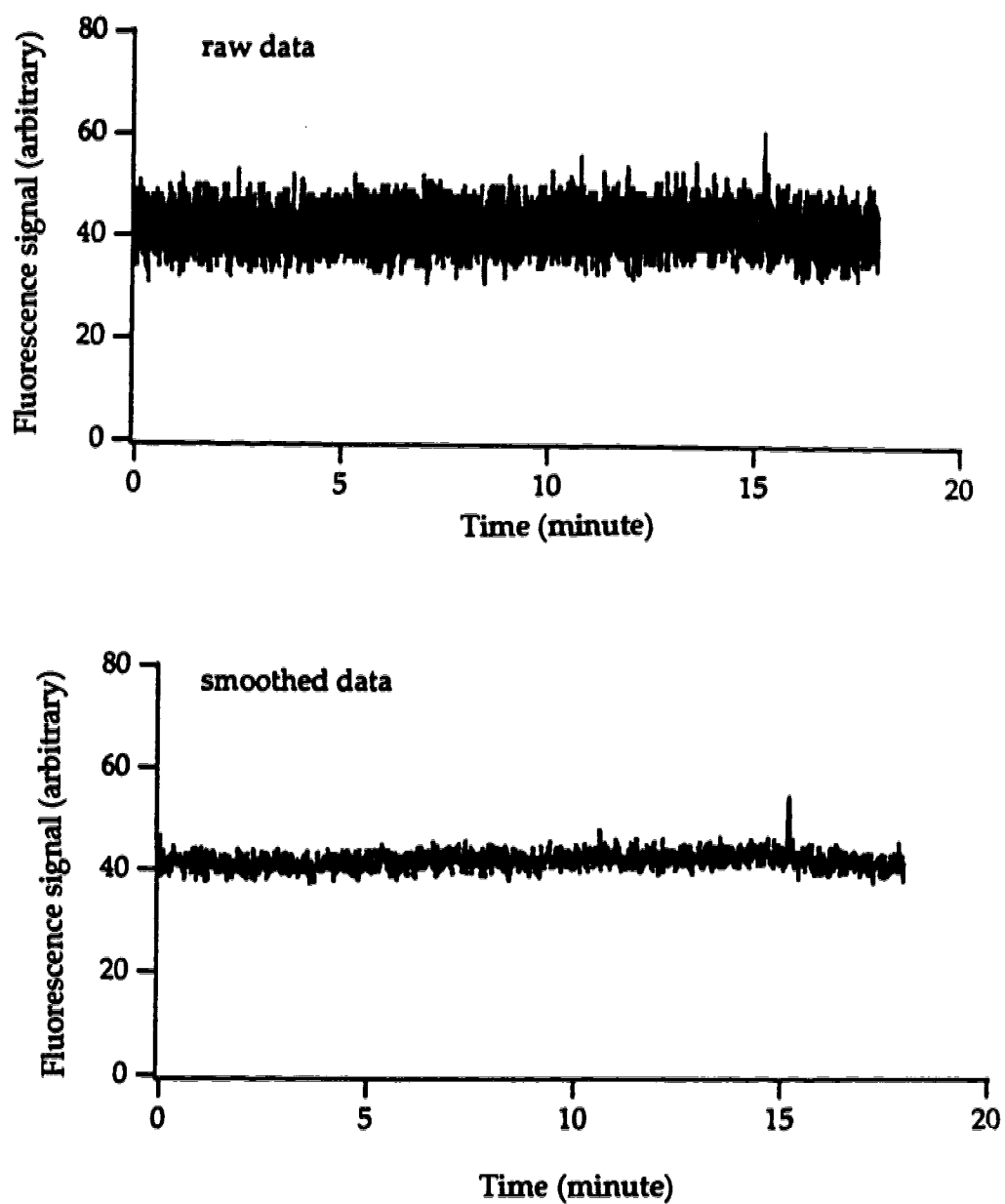


Figure 4.12 Electropherogram of 260 molecules of TRSE labeled synthetic sugar β -GlcNAc-O-(CH₂)₈-CO-NH-CH₂-CH₂-NH₂

4.3.3 The Labeling Reactions

Figure 4.13 presents the electropherogram of alanine labeled with TRSE. In this run, the total TRSE concentration was 3.7×10^{-9} M. Separation used a 50- μ m I.D. and 72.5-cm long capillary operated at 29 kV. The separation buffer was 10 mM borate with 10 mM SDS. The fluorescent label experiences fast hydrolysis in the reaction buffer containing 0.185 M NaHCO_3 (pH 8.3). After sitting in the reaction buffer for one hour, the TRSE showed no labeling product with alanine. Fortunately, the labeling reaction is faster compared to the hydrolysis of the fluorescent dye at room temperature. When alanine is in excess, the labeling reaction is almost complete. The TRSE labeled derivative (TRSE-Ala) is quite stable in pH 9.3 buffer.

Figure 4.14 shows the electropherogram of TRSE labeled Mannose- NH_2 . In this run, separation used a 10- μ m I.D. and 74.4-cm long capillary operated at 29 kV. The separation buffer was 20 mM Na_2HPO_4 , 20 mM phenylboronic acid, 10 mM borate, and 10 mM SDS. In addition to the hydrolysis products, there is only one peak corresponding to the TRSE labeled derivative. There are two competitive reactions taking place when the TRSE is mixed with an aminated sugar in a basic buffer: the labeling reaction between TRSE and the aminated sugar, and the hydrolysis of TRSE. The other five sugars also gave single labeling results and the same hydrolysis products of the dye.

4.3.4 Plate Counts

Electrophoresis peaks for the labeled sugars were always broader than the peaks for the dye or the hydrolysis products. **Table 4.3** lists the numbers of

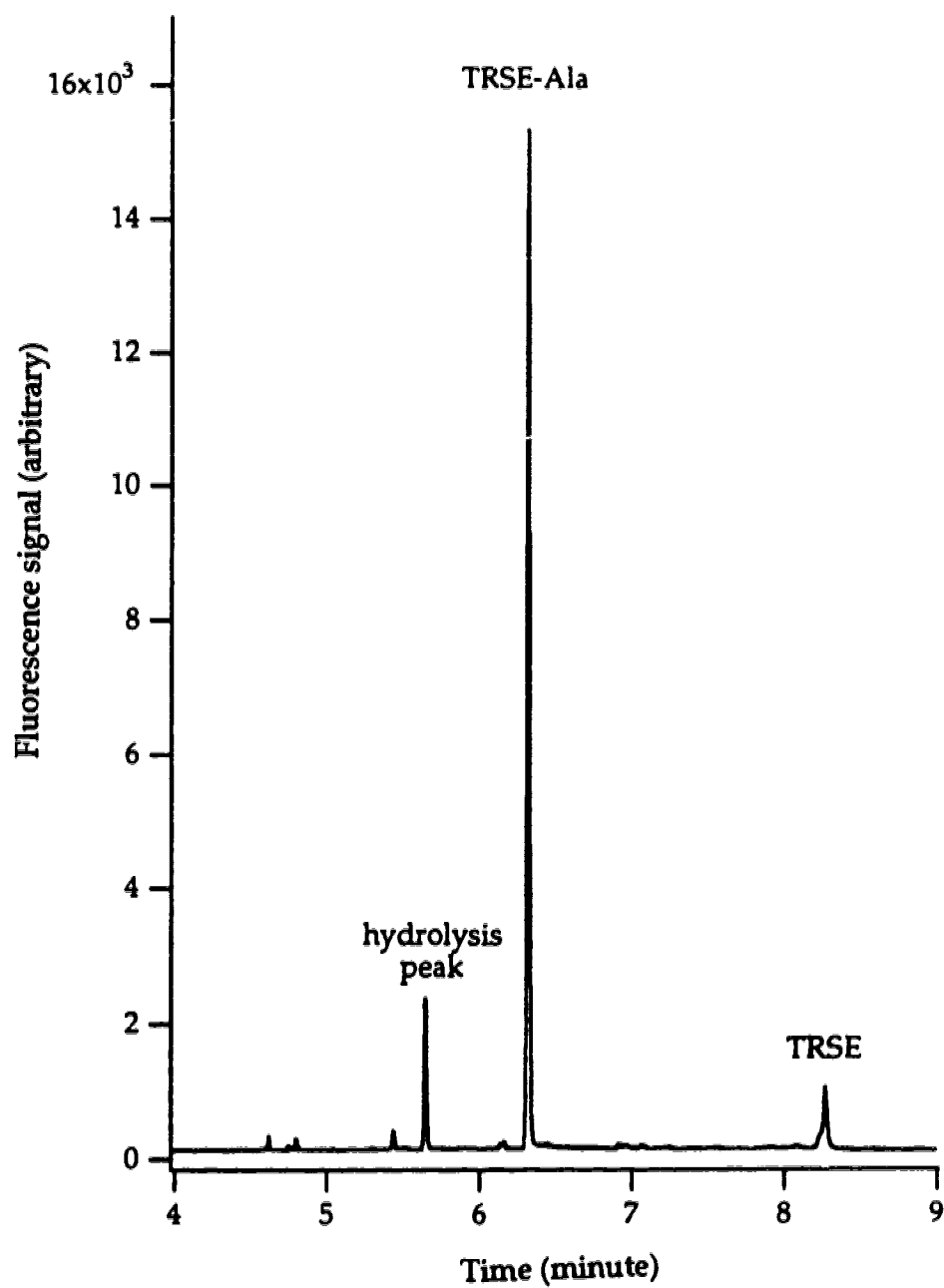


Figure 4.13 Electropherogram of TRSE labeled alanine

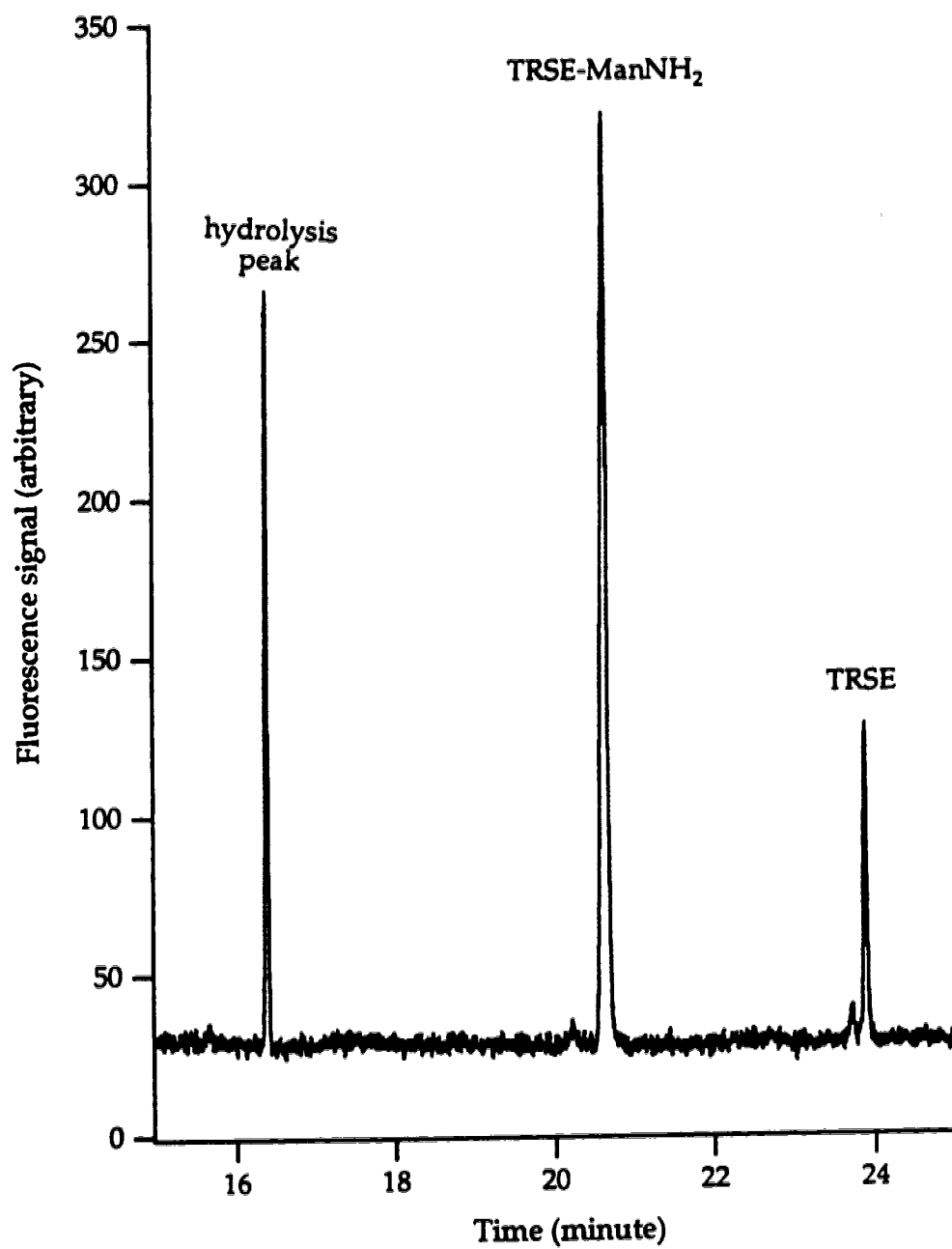


Figure 4.14 Electropherogram of TRSE labeled aminated mannose

theoretical plates for TRSE, its hydrolysis product, and the TRSE labeled sugars. The separation was performed in 20 mM phenyl boronic acid, 20 mM Na₂HPO₄, 10 mM borate with 10 mM SDS (pH 9.3). The 74.4-cm long capillary was operated at 29 kV.

Table 4.3 Numbers of theoretical plates for TRSE and TRSE labeled sugars

TRSE	1.5×10^6
hydrolysis product of TRSE	1.4×10^6
TRSE-GlcNH ₂	3.1×10^5
TRSE-2-GlcNH ₂	4.0×10^5
TRSE-2-GalNH ₂	2.4×10^5
TRSE-ManNH ₂	2.6×10^5
TRSE-GalNH ₂	3.1×10^5
TRSE-FucNH ₂	2.2×10^5

The number of theoretical plates of TRSE peak are about five times larger than that of the TRSE labeled sugar peak. This difference is surprising and may reflect different conformations generated by the sugars, leading to additional band-broadening. Further work is required to clarify the origin of this enhanced peak width.

4.3.5 Separation Buffer Effects

The six sugar standards have similar structures. Three of them are stereoisomers. After they were labeled with large TRSE, the differences between them were minor. Fortunately, the complexation between sugar hydroxyl

groups and borate can be used to enhance the mobility differences between the labeled monosaccharides. The first try was to use 10 mM borate buffer. But the separation of the six aminated monosaccharides was not complete. With 10 mM Na_2HPO_4 and 10 mM SDS added to the 10 mM borate buffer (PBS), the separation was not complete, either. However, addition of phenylboronic acid to the PBS buffer improved resolution markedly. Figure 4.15 presents the electropherogram of the complete base-line separation of the six sugar derivatives. The 10- μm I.D. capillary used was 74.4-cm long and electrophoresis was operated at 29 kV.

The separation results of using different buffer compositions revealed that borate and phenylboronic acid have opposite effects on the electrophoretic mobilities of two pairs of labeled monosaccharides: TRSE-GlcNH₂ and TRSE-2-GlcNH₂ or TRSE-ManNH₂ and TRSE-2-GalNH₂. Higher concentration of borate gives better separation between GlcNH-TRSE and 2-GalNH-TRSE, but more overlap between ManNH-TRSE and GalNH-TRSE. The best separation buffer composition, which was used for separation in Figure 4.15, is 18 mM phenyl boronic acid, 20 mM Na_2HPO_4 , 10 mM borate with 10 mM SDS (pH 9.3). This buffer can completely separate the six TRSE labeled aminated monosaccharides within 22 minutes, with no interference from the unreacted TRSE and its hydrolysis products.

4.4 CONCLUSIONS

5-carboxytetramethylrhodamine n-hydroxysuccinimidyl ester is a useful fluorescent label for aminated sugar monomers. The labeling reaction can be done at room temperature within one hour. The TRSE labeled sugars are very

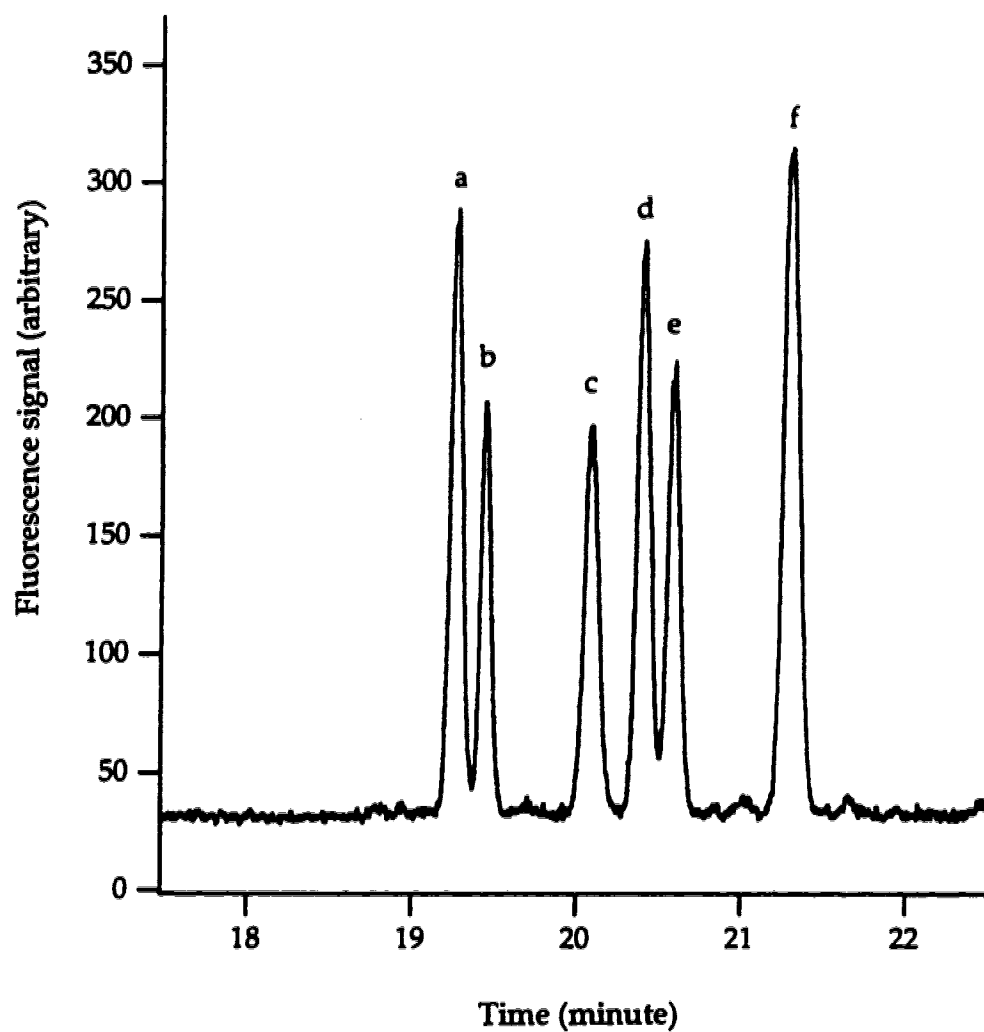


Figure 4.15 Separation electropherogram of TRSE labeled six monosaccharide standards. Peak identifications: a = TRSE-GlcNH₂, b = TRSE-2-GlcNH₂, c = TRSE-2-GalNH₂, d = TRSE-ManNH₂, e = TRSE-GalNH₂, and f = TRSE-FucNH₂.

stable at 4 °C in basic buffers. Unfortunately, the reaction requires high sugar concentration, 2×10^{-2} M, because the competition between the labeling reaction and the hydrolysis of the dye. Therefore, the analysis of real sugar samples would require to choose a more practical fluorescence dye, which either has better stability in basic buffer or generates much lower background signal.

The detection limit of the TRSE labeled monosaccharide is 60 molecules in this capillary electrophoresis system with post-column laser-induced fluorescence detection in a sheath flow cuvette. By carefully monitoring the separation buffer composition, one can use capillary electrophoresis with laser-induced fluorescence detection to analyze the monosaccharide fragments with ultrasensitivity. The next step in developing an oligosaccharide sequencing protocol is to develop a strategy for degrading the oligosaccharide chains.

REFERENCES

1. C. C. Sweeley, H. A. Nunez, *Ann. Rev. Biochem.* , **54**, 765-801 (1986).
2. S. Honda, S. Iwase, A. Makino, S. Fujwara, *Anal. Biochem.* , **176**, 72-77 (1989).
3. W. G. Kuhr, C. A. Monnig, *Anal. Chem.* , **64**, 389R-407R (1992).
4. E. M. Lees, H. Weigel, *J. Chromatogr.* , **16**, 360 (1964).
5. P. J. Garegg, B. Lindberg, *Acta Chem. Scand.*, **15**, 1913 (1961).
6. B. Lindberg, B. Swan, *Acta Chem. Scand.*, **14**, 1043 (1960).
7. M. Weigel, *Carbohydr. Chem.*, **18**, 61 (1963).
8. J. L. Frahn, J. A. Mills, *Aust. J. Chem.*, **12**, 65 (1959).
9. S. Hoffstetter-Kuhn, A. Paulus, E. Gassmann, H. M. Widmer, *Anal. Chem.* , **63**, 1541-1547 (1991).
10. J. Liu, O. Shirota, M. Novotny, *Anal. Chem.* , **63**, 413-417 (1991).
11. J. Liu, O. Shirota, M. Novotny, *J. Chromatogr.* , **559**, 223-235 (1991).
12. D. J. Bornhop, T. G. Nolan, N. J. Dovichi, *J. Chromatogr.*, **384**, 181-187 (1987).
13. T. W. Garner, E. S. Yeung, *J. Chromatogr.* , **515**, 639-644 (1990).
14. A. E. Vorndran, P. J. Oefner, H. Scherz, G. K. Bonn, *Chromatographia* , **33**, 163-168 (1992).
15. W. Nashabeh, Z. E. Rassi, *J. Chromatogr.* , **600**, 279-287 (1992).
16. R. F. Borch, M. D. Bernstein, H. D. Durst, *J. Am. Chem. Soc.*, **93**, 2897-2904 (1971).

17. J. Liu, O. Shirota, D. Wiesler, M. Novotny, *Proc. Natl. Acad. Sci.* , **88**, 2302-2306 (1991).
18. Y. F. Cheng, N. J. Dovichi, *Science* , **242**, 562-564 (1988).
19. J. Y. Zhao, D. Y. Chen, N. J. Dovichi, *J. Chromatogr.* , **608**, 117-120 (1992).
20. W. Wayne, H. Adkins, *J. Am. Chem. Soc.*, **62**, 3314 (1940).
21. F. W. Holly, E. W. Peel, R. Mozingo, K. Folkers, *J. Am. Chem. Soc.*, **72**, 5416 (1950).
22. F. Kagan, M. A. Rebenstorf, R. V. Heinzelman, *J. Am. Chem. Soc.*, **79**, 3541 (1957).
23. K. Bock, I. Christiansen-Brams, M. Meldal, *J. Carbohydr. Chem.*, **11**, 813 (1992).
24. J. E. Knoll, *J. Chrom. Sci.* , **23**, 422-425 (1985).

CHAPTER 5

DETECTION OF 100 MOLECULES OF ENZYME PRODUCT BY CAPILLARY ELECTROPHORESIS WITH LASER-INDUCED FLUORESCENCE DETECTION*

* A version of this chapter has been accepted for publication. *Glycobiology*, 4 (#2) (1994)

5.1 INTRODUCTION

Enzyme assays are becoming increasingly sensitive, with femtomole ($1 \text{ fmol} = 10^{-15} \text{ mol} = 6 \times 10^8 \text{ molecules}$) detection of products routine for many enzymes [1, 2]. While turnover numbers for enzymes range from 1 to 10^7 s^{-1} , the majority of enzymes have turnover numbers less than 1000 s^{-1} [3]. Thus, 100 to 100,000 molecules of enzyme are required for product detection in 2-hour reactions under ideal conditions. In practice, these numbers of enzyme molecules can be far from accessible in studies involving cellular differentiation, including embryonic development. Current technology is thus limited to studies of a few of the fastest enzymes, which are usually hydrolytic, and/or those enzymes present in very high abundance.

Glycosyltransferases are specific enzymes that play very important roles in biosynthesis of glycoconjugates. The carbohydrate chains of animal glycoproteins and glycolipids are biosynthesized by the sequential action of glycosyltransferases that transfer monosaccharide units from nucleotide-linked sugars to non-reducing ends of oligosaccharide chains, **Figure 5.1**. Specific inhibition of one of these selected enzymes could potentially result in a specific change in glycosylation on the surface of cells. The synthesis of complex cell surface carbohydrates requires the concerted action of a large number (>100) of different glycosyltransferases. The specificity of a glycosyltransferase will likely reside to a large extent in the recognition of the oligosaccharide acceptor and not in the nucleotide portion. Therefore, the ideal specific glycosyltransferase inhibitor should possess substantial structural features in common with the acceptor. For example, a series of specific glycosyltransferase inhibitors were

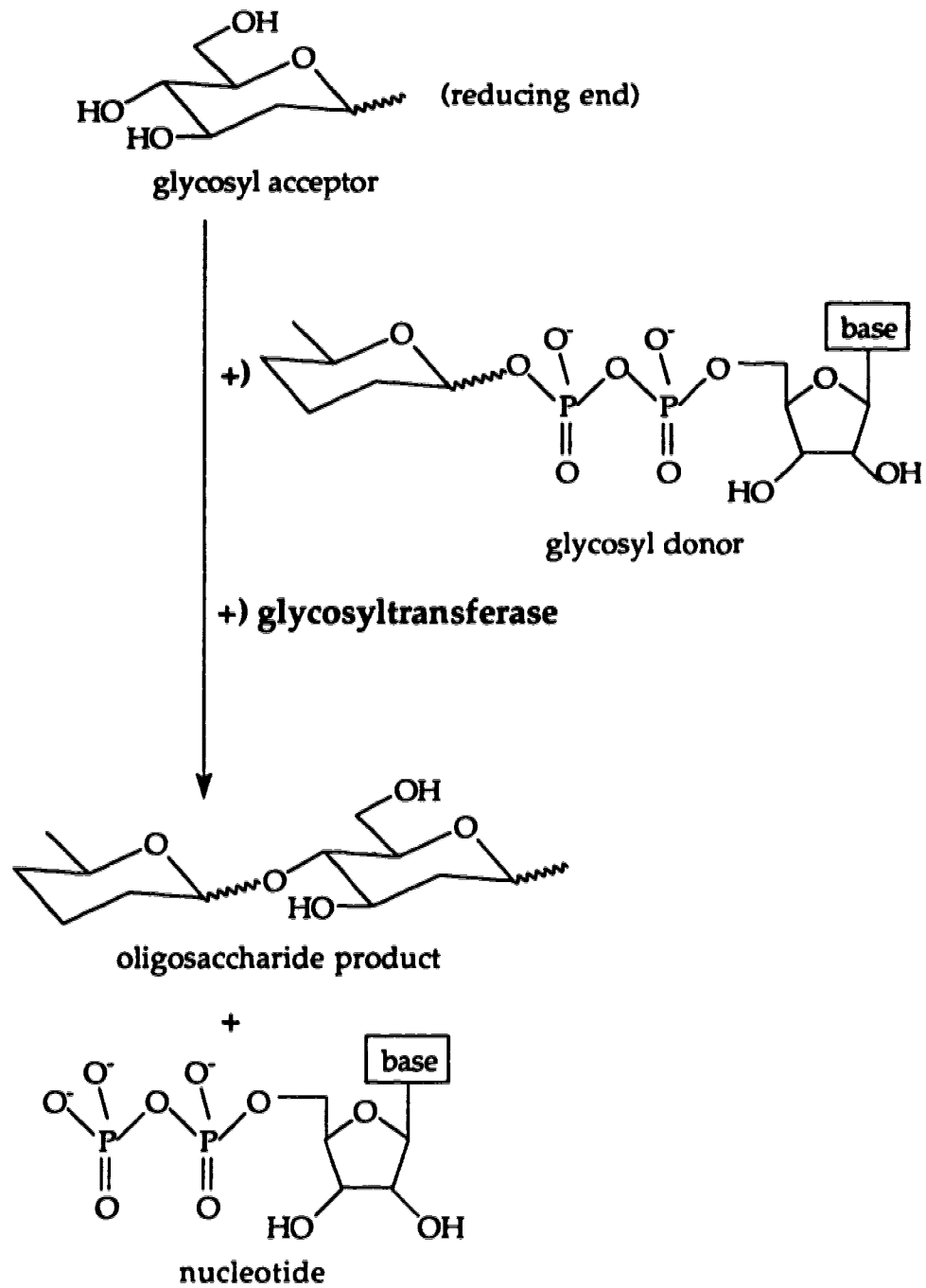


Figure 5.1 Biosynthesis of oligosaccharide catalyzed by glycosyltransferase

designed by chemically replacing the reactive hydroxyl group of a glycosyltransferase acceptor with hydrogen [4].

The changes in the completed oligosaccharide structures can result in several diseases [5-7], especially cancers. Some recent research results have revealed that the changes are related to the alternations in the enzyme expression [8-11]. Therefore, glycosyltransferase activities have been proposed as potential diagnostic markers of diseases [12, 13].

One unit of enzyme activity is the amount that catalyzes the formation of 1 micromole of product per minute using the acceptor (substrate). The estimation of glycosyltransferase activity may be done by quantitating one of the products of the enzymatic reaction, either the oligosaccharide or the nucleotide. Ideally, the oligosaccharide should also be structurally characterized. The methods commonly used for quantitation of an oligosaccharide include mass spectrometry, NMR, HPLC with spectroscopical measurements. Since glycosyltransferases are present intracellular in very low amounts, almost invariably radioactivity-based measurements are used. As a result, a single assay for the activity of a glycosyltransferase requires at least 10^5 cells to give an adequate signal to noise ratio. Ultimately, the challenge is to detect the products formed by the enzymes in a single cell so that the variation, if there is any, in the activity of a glycosyltransferase from cell to cell could be measured and the enzyme levels could be monitored during the cell division in early embryo-development, e.g. at the 8 to 16 cell stage of mouse embryo development.

The most sensitive direct (non-amplified) glycosyltransferase assay reported to date is one based on the detection of fluorescently labeled acceptor being converted to the corresponding product that is separated by capillary electrophoresis and detected by fluorescence with a detection limit as low as a

femtomole (10^{-15} mole) [14]. Since the problem in the enzyme assay is really the separation and quantitation of oligosaccharide product, much greater sensitivity could be achieved. Novotny's group reported a capillary electrophoresis system with laser-induced fluorescence detection that was used to separate and detect fluorescently labeled oligosaccharide derivatives of 3-(4-carboxybenzoyl)-2-quinolinecarboxaldehyde (CBQCA) with detection limits down to one attomole (10^{-18} mole) level [15], which demonstrates that 600,000 molecules could be seen.

Capillary electrophoresis is an emerging separation technique with high speed and high resolution. Laser-induced fluorescence detection in a sheath flow cuvette has proven to be the most sensitive detector for capillary electrophoresis [16, 17]. As demonstrated in chapter 4, a detection limit of 60 molecules has been achieved for a synthetic sugar labeled with a tetramethylrhodamine fluorophore using a low-cost helium-neon laser operating at 543.5 nm. It looks promising to apply this system to achieve ultra-sensitivity for glycosyltransferase assay.

There are a few problems associated with the traditional glycosyltransferase assays. First, almost all traditional glycosyltransferase assays measure the transfer rates of radioactively labeled sugars from the sugar-nucleotide donor to an appropriate oligosaccharide acceptor that must usually be isolated from biological sources [18]. It is necessary to separate the unreacted sugar-nucleotide (and its degradation products) from the enzyme product before quantitation by liquid scintillation counting. The time-consuming separation procedures generally include HPLC, gel-filtration chromatography, affinity chromatography, and/or high voltage paper electrophoresis. Second, because the natural oligosaccharide acceptors are frequently substrates for several enzymes, a further requirement is to separate and structurally verify the enzyme products in each assay. Instead of using radioactive labels, fluorescent labeling can provide a

more environmentally friendly way for glycosyltransferase assay. The great separation power of capillary electrophoresis can further simplify the separation procedure before quantitation. Synthetic analogs for natural oligosaccharide acceptors have been developed to solve the second problem mentioned above due to the fact that the synthetic acceptors can be made structurally "mono-specific" . An additional advantage of using synthetic acceptors is that they can be made available in large quantity [19].

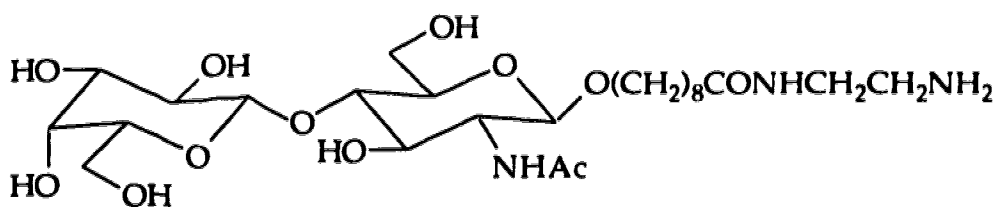
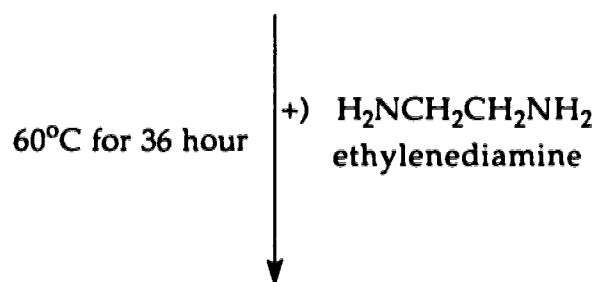
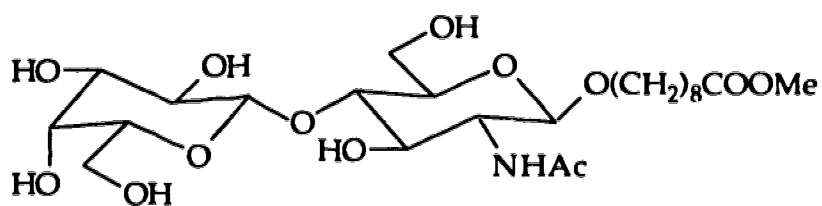
In this chapter, fluorescently labeled synthetic oligosaccharide substrates are used to demonstrate the separation and detection of enzyme products along with the unreacted substrates using micellar electrokinetic capillary electrophoresis (MECC) with laser-induced fluorescence detection in a sheath flow cuvette. 5-carboxytetramethylrhodamine N-hydroxysuccinimidyl ester (TRSE) was chosen to be the fluorescent labeling reagent.

5.2 EXPERIMENTAL

5.2.1 Synthesis of a Disaccharide

A synthetic disaccharide with a primary amine group available for fluorescent labeling was made by Dr. O. Hindsgaul (University of Alberta) from the known 8-methoxycarbonyl derivative [20] by reaction with ethylenediamine, **Figure 5.2**. The TRSE labeled synthetic disaccharide may be used as a substrate for glycosyltransferase assays.

8-methoxycarbonyloctyl 2-acetamido-2-deoxy-4-O-
(β -D-galactopyranosyl)- β -D-glucopyranoside

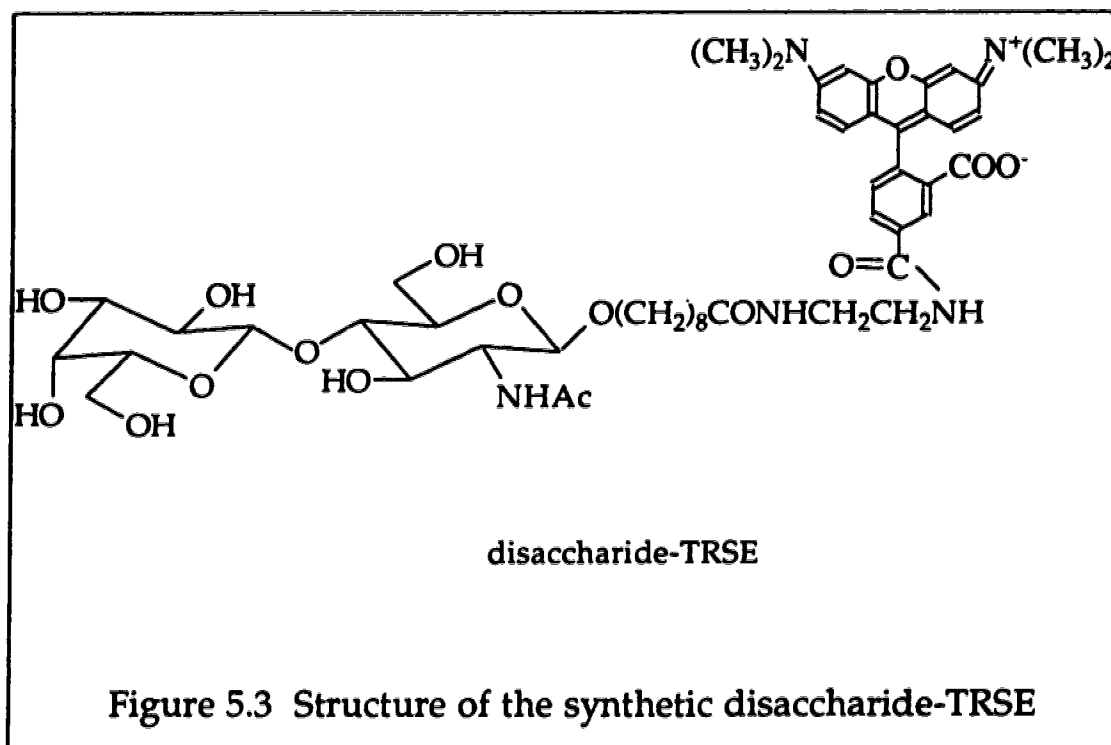


disaccharide

Figure 5.2 Synthesis of a disaccharide containing a primary amine

5.2.2 Labeling the Synthetic Disaccharide with TRSE

The synthetic disaccharide was dissolved in 0.185 M NaHCO₃ buffer (pH 8.3) and the concentration was 5×10^{-3} M. The concentration of TRSE stock solution was 2.4×10^{-3} M in dry dimethylformamide (DMF). The labeling reaction was carried out by mixing 30 μ L of the disaccharide stock solution with 5 μ L of the TRSE stock solution in a 1.5-ml dark brown polypropylene vial (Fisher Scientific, Pittsburgh, PA, USA) at room temperature in the dark for one hour. The reaction mixture was kept in a refrigerator (4°C) for future use. A blank solution was prepared by mixing 30 μ L 0.185 M NaHCO₃ buffer with 5 μ L TRSE stock. Figure 5.3 shows the structure of the fluorescently labeled disaccharide substrate.



5.2.3 Synthesis of the Substrate for Specific Glycosyltransferase assays (by Dr. O. Hindsgaul)

Reaction of 8-methoxycarbonyloctyl 2-acetamido-2-deoxy-4-O-(β -D-galactopyranosyl)- β -D-glucopyranoside with neat ethylene diamine at 60°C for 36 hours gave the ethylenediamine mono-amide obtained as a solid after solvent evaporation followed by lyophilization. Reaction of the residue with 2 equivalents of 5-carboxytetramethylrhodamine succinimidyl ester according to the manufacturer's (Molecular Probes) protocol then yielded disaccharide-TRSE that was purified by chromatography on a column of Iatrobeads (Iatron Laboratories, Japan) using dichloromethane-methanol-water 60:30:2 as solvent. Brilliant red disaccharide-TRSE had R_f 0.32 in silica gel TLC using 7:2:1 isopropanol:water:concentrated ammonium hydroxide as eluent. $^1\text{H-NMR}$ (D_2O): δ = 8.3-6.6 (9 H, aromatic), 4.44 (d, 1 H, $J_{1,2}$ = 8 Hz, Gal-H1), 4.39 (second-order m, $J_{1,2}$ = 8 Hz, 1 H, GlcNAc H-1), 3.19 (s, 12 H, NCH_3), 1.98 (s, 3H, NAc).

5.2.4 Enzymatic Reactions (by Dr. M. M. Palcic's Group)

Disaccharide-TRSE was found to be a good acceptor for a purified fucosyltransferase isolated from human milk [21]. Steady-state kinetics showed disaccharide-TRSE had a K_m of 250 μM and a k_{cat} (turnover number) 15% of that of the nonfluorescent precursor $\beta\text{Gal}(1,4)\beta\text{GlcNAc-O}(\text{CH}_2)_8\text{COOMe}$ (K_m 400 μM), although inhibition was observed at substrate concentration greater than 250 μM .

Figure 5.4 presents two enzymatic reactions for possible glycosyltransferase assays. For preparative fucosylation, 5 μg (5 nmol) of

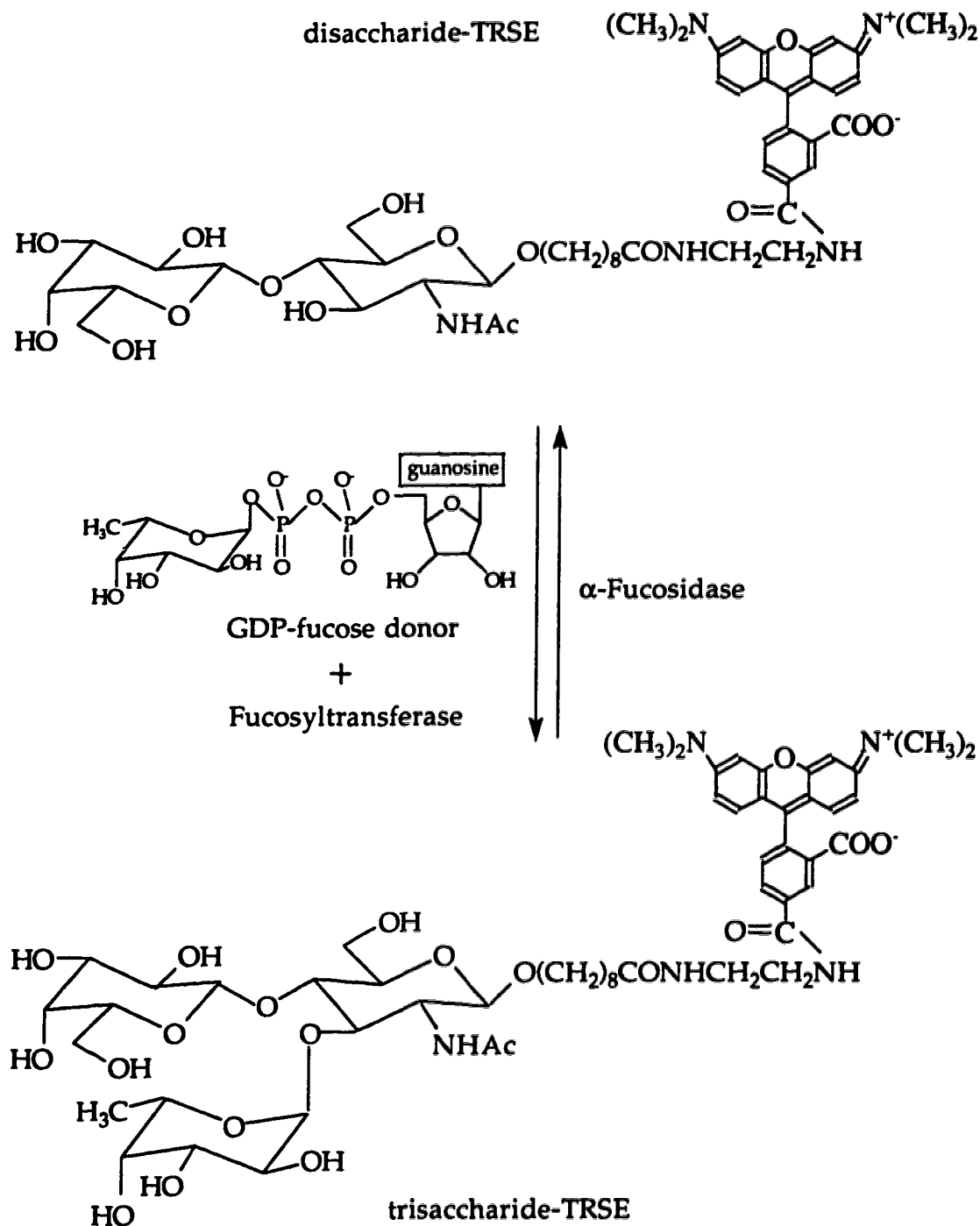


Figure 5.4 Fucosylation of disaccharide-TRSE to trisaccharide-TRSE by fucosyltransferase and de-fucosylation of trisaccharide-TRSE to disaccharide-TRSE by α -fucosidase.

disaccharide-TRSE was incubated for sixteen hours at 37°C with 2 nmol of GDP-fucose donor and 3.5 milliunits of purified human milk α 1-3/4 fucosyltransferase in 40 μ L of 20 mM HEPES buffer pH 7.0, containing 20 mM MnCl₂ and 0.2% bovine serum albumin. The reaction was carried out under conditions fixed for approximately 35% conversion to a trisaccharide-TRSE product. For preparative de-fucosylation, part of disaccharide-TRSE and trisaccharide-TRSE mixture was incubated with 10 μ units of almond meal fucosidase (Sigma Chemical Co., St. Louis, MO, USA) in 0.1 M citrate-0.2 M phosphate buffer (pH 5.5) at 37°C for 2.5 hours.

5.2.5 Instrument Setup

The capillary electrophoresis with laser-induced fluorescence detection system was set up in a similar way to the one described in chapter 2 of this thesis. Essentially, a modified flow cytometer is used to produce a very high sensitivity laser-induced fluorescent detector for the capillary electrophoresis system. The 148 μ m outer diameter capillary was placed within a 150 μ m square flow chamber, which was constructed from high optical quality quartz. A sheath stream, flowing at ~25 μ L/second, was used to draw the sample from the capillary in a narrow ~20 μ m diameter stream in the center of the flow chamber. A 0.75 mW helium neon laser (Melles Griot), operating in the green portion of the spectrum (λ = 543.5 nm), was focused with a 10x microscope objective into the cuvette about 50 μ m downstream from the capillary exit. A 50x high numerical aperture (0.60) microscope objective imaged fluorescence onto an iris. The iris was matched to the image of the illuminated sample stream and was used to spatially block scattered laser light. A 580DF40 bandpass spectral filter (Omega optical, Inc., Brattleboro, VT, USA) was used to attenuate further scattered laser light, and

a R1477 photomultiplier tube (Hamamatsu Corporation, San Jose, CA, USA) was operated at 1200 V at room temperature to detect the fluorescence. The photomultiplier tube current signal was converted into voltage through a $1\text{ M}\Omega$ resistor. The voltage signal was passed through a 0.1 second RC low-pass filter, Figure 5.5, and recorded with a Macintosh IIsi computer.

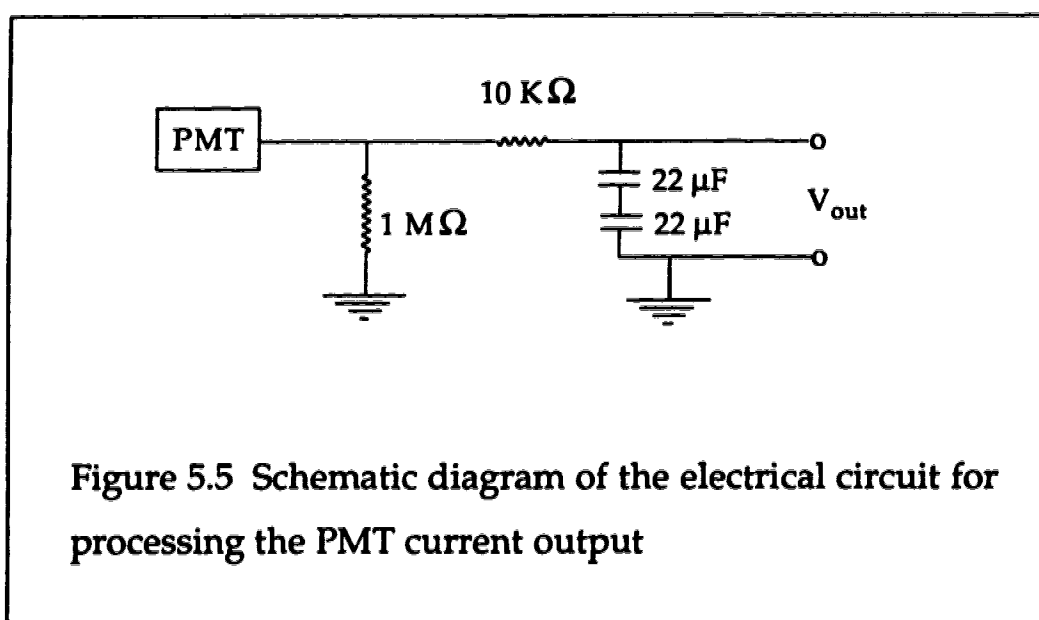


Figure 5.5 Schematic diagram of the electrical circuit for processing the PMT current output

5.2.6 Capillary Electrophoresis Conditions

Capillary electrophoresis separation buffer was 10 mM borate with 10 mM phosphate and 10 mM sodium dodecyl sulfate (pH 9.3). The uncoated fused silica capillaries used had 10 μm inner diameter (I.D.) and 150 μm outer diameter with different lengths (Polymicro Technologies, Phoenix, AZ, USA). Sample injections were performed electrokinetically at a certain voltage for 5 seconds.

Electrophoresis was driven at 29 kV with a high voltage power supply (Spellman CZE 1000R).

5.3 RESULTS AND DISCUSSION

5.3.1 Labeling Reaction Between Disaccharide and TRSE

The synthetic disaccharide with a free primary amine group reacted with the fluorescent dye, 5-carboxytetramethylrhodamine N-hydroxysuccinimidyl ester, and gave a single labeling peak at 6.37 minutes, as shown in Figure 5.6. Both of the mixtures of disaccharide with TRSE labeling reaction and the blank solutions were diluted to a total TRSE concentration of 6.9×10^{-9} M by the separation buffer containing 10 mM borate with 10 mM phosphate and 10 mM sodium dodecyl sulfate (pH 9.3). The dilute sample and blank solution were injected electrokinetically at 2000 V for 5 seconds into the 59.8 cm long and 10 μ m I.D. capillary.

5.3.2 Enzyme Reactions

Figure 5.7 shows the electropherograms of separation of disaccharide-TRSE and trisaccharide-TRSE. The raw data from the computer were treated with a Gaussian digital filter (0.6 second standard deviation) before presentation. The samples were run in a 70-cm long, 10- μ m I.D. fused silica capillary at an electrophoresis potential of 29 KV.

The electropherogram of a dilute solution, 2×10^{-9} M, of the pure disaccharide-TRSE standard is presented in Figure 5.7A. Sample injection was made by applying 2.5 KV high voltage for 5 seconds, which introduced 2.5

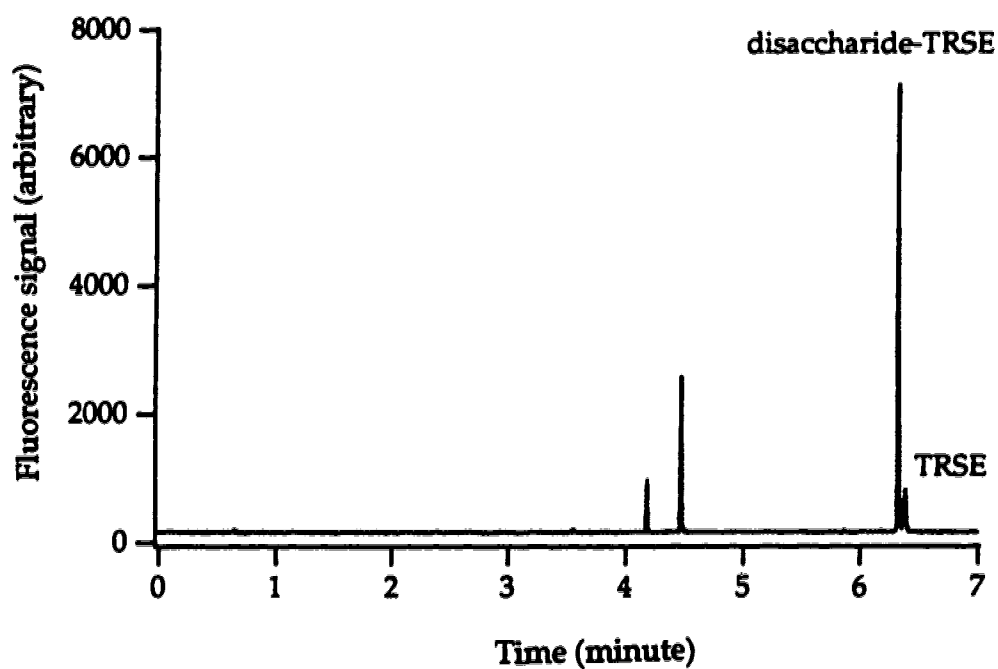
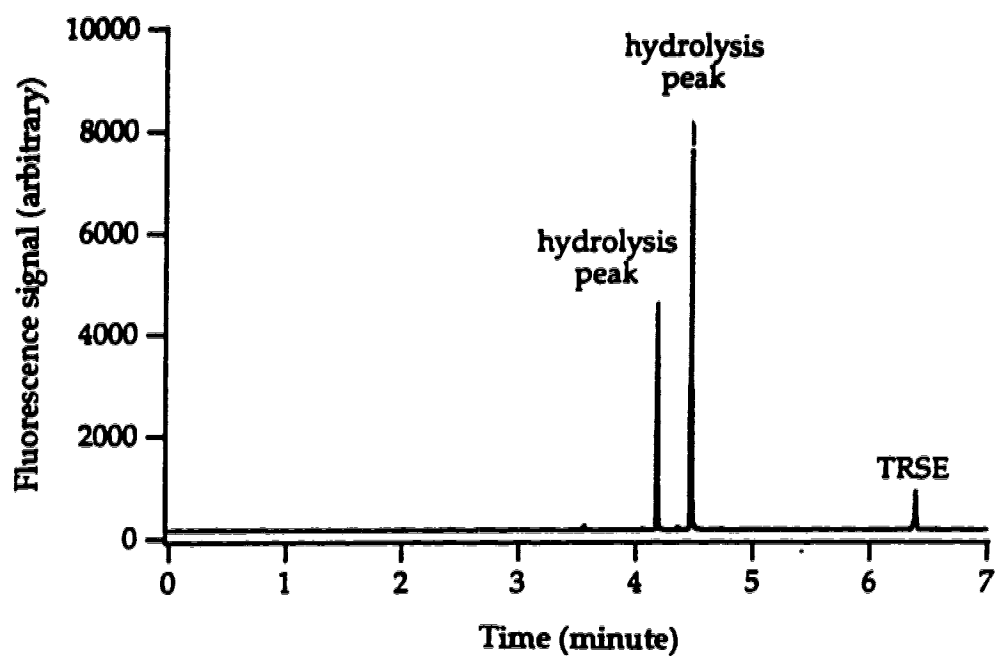


Figure 5.6 Electropherograms of labeling reaction blank and labeling mixture of disaccharide with TRSE

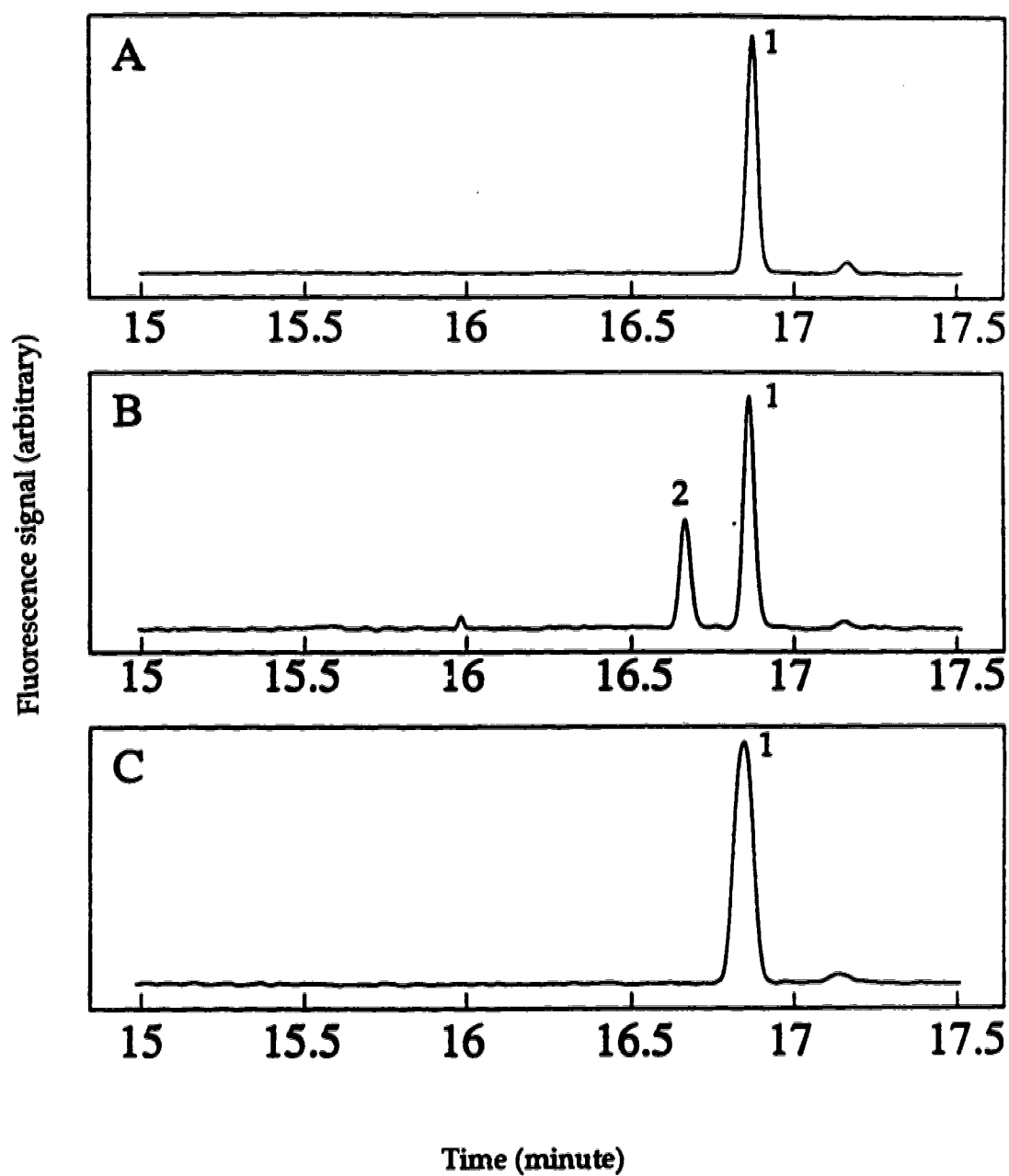


Figure 5.7 Separation electropherograms of TRSE labeled disaccharide (peak 1) and trisaccharide (peak 2)

picoliters of the sample. With the exception of a small peak due to hydrolyzed derivatizing reagent at 17.15-minute, the background was very low for this substrate. The electropherogram generated roughly 1 million theoretical plates for this separation, allowing efficient analysis of complex mixtures.

The electropherogram of the enzyme reaction mixture, **Figure 5.7B**, clearly indicates the formation of a new peak at 16.67-minute, which is consistent with the addition of a monosaccharide (fucose) to the disaccharide-TRSE substrate. Resolution of the disaccharide-TRSE and trisaccharide-TRSE is 4. High resolution is important because our enzyme assays will often require detection of minute amounts of product in the presence of a huge excess of substrate; the high resolution separation means that a small amount of product will not be swamped by the substrate. Inspection of the baseline for **Figure 5.7A** reveals that the electrophoresis system can detect conversion of as little as 0.01% of the substrate to the product.

As a second enzyme assay, part of the disaccharide-TRSE and trisaccharide-TRSE mixture was treated with commercially available α -fucosidase from almond meal. The electropherogram, **Figure 5.7C**, shows complete conversion of trisaccharide-TRSE back to disaccharide-TRSE after 2.5 hours at 37°C.

In **Figure 5.7B**, 25 picoliters of a 1.6×10^{-9} M solution of oligosaccharides was injected, which corresponds to 25,000 molecules of disaccharide-TRSE and 12,000 molecules of trisaccharide-TRSE. To demonstrate the sensitivity of this assay, the mixture of disaccharide-TRSE and trisaccharide-TRSE used for the electropherogram in **Figure 5.7B** was diluted by a factor of 10. **Figure 5.8** presents the electropherogram generated by injection of 550 molecules (900 ymol) of disaccharide-TRSE and 275 molecules (450 ymol) of trisaccharide-TRSE.

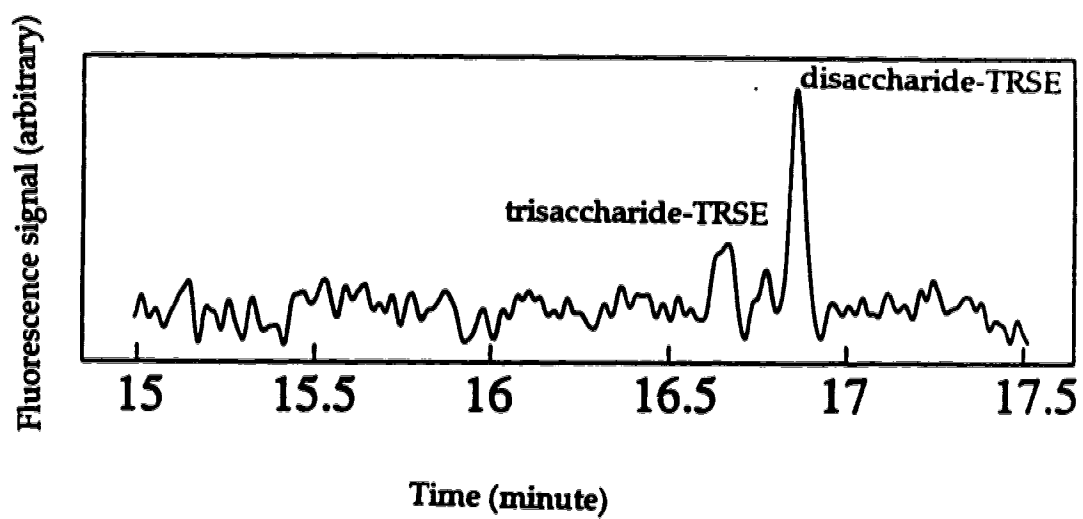


Figure 5.8 Electropherogram of a mixture of disaccharide-TRSE and trisaccharide-TRSE at concentrations close to detection limits

Detection limits (3σ) are 100 analyte molecules (125 ymol) injected onto the capillary. The assays are 6 orders of magnitude more sensitive than any reported for these two enzymes [14].

5.4 CONCLUSIONS

A relatively simple method for detection of 100 molecules (165 yoctomoles = 165 ymol = 165×10^{-24} mol) of enzyme substrate and product has been demonstrated in this chapter. In this method, a fluorescent synthetic substrate is enzymatically converted to a fluorescent product. The substrate and product are separated by capillary electrophoresis and detected by laser-induced fluorescence in a sheath flow cuvette.

The ultimate challenge in enzyme analysis is the determination of enzyme activity in single cells or organelles. There have been several reports [2, 22-24] on the detection of glycosidase activity in single cells using non-fluorescent substrates that are enzymatically hydrolyzed to yield the detectable fluorophores. The assays require 4000 molecules of hydrolase yielding roughly 1 femtomole of product, which is detected within the cell [2]. Some of these assays further require that lypophilic substrates pass through a cell membrane. As a result there is ambiguity in the assays because the fluorescent signal is related to both the uptake of the substrate by the cell and the enzyme activity within the cell.

On the other hand, the analysis that is presented here is independent of substrate take-up; the ratio of product to substrate is a direct measure of the enzyme activity and may be used, in principle, to assay any enzyme for which a fluorescent substrate may be synthesized. Conversion of a fluorescent substrate

to more than one product, for example by the action of either competing or sequential enzymes, could also be monitored. The limiting enzyme activity that can be measured is related to the efficiency with which the substrate and product can be separated, along with the purity of the fluorescent substrate. The data presented here indicate that 0.01% conversion of disaccharide-TRSE to trisaccharide-TRSE can be detected with a detection limit of 100 product molecules.

This assay is the most sensitive chemical analysis reported to date. While individual highly fluorescent molecules have been detected and counted in neat solutions [25, 26], this is the first report where yoctomole quantities of mixtures have been separated and identified. The combination of high sensitivity detection with high efficiency separation should have broad application in addition to the enzyme assay presented here to any enzyme for which a fluorescent substrate can be synthesized.

REFERENCES

1. J. Alam, J. L. Cook, *Anal. Biochem.* , **188**, 245 (1990).
2. V. K. Jain, I. T. Magrath, *Anal. Biochem.* , **199**, 119 (1991).
3. A. Fersht, *Enzyme Structure and Function* , W.H.Freeman and Co., second edition, Page 121 (1985).
4. O. Hindsgaul, K. J. Kaur, G. Srivastava, M. Blaszczyk-Thurin, S. C. Crawley, L.D. Heerze, M. M. Palcic, *J. Biol. Chem.* , **266**, 17858-17862 (1991).
5. L. Warren, C. A. Buck, P. Tuszynski, *Biochim. Biophys. Acta* , **516**, 97-127 (1978).
6. S. Hakomori, R. Kannagi, *J. Natl. Cancer Inst.* , **71**, 231-251 (1983).
7. S. Hakomori, *Annu. Rev. Immunol.* , **2**, 103-126 (1984).
8. E. H. Holmes, S. Hakomori, *J. Biol. Chem.* , **258**, 3706-3713 (1980).
9. K. Yamashita, Y. Tachibana, T. Ohkura, A. Kobata, *J. Biol. Chem.* , **260**, 3963-3969 (1985).
10. J. W. Dennis, S. Laferte, C. Waghorne, M. L. Breitman, R. S. Kerbel, *Science*, **236**, 582-585 (1987).
11. S. Narasimhan, H. Schachter, S. Rajalakshmi, *J. Biol. Chem.* , **263**, 1273-1281 (1988).
12. R. Madiyalakan, S. Yazawa, J. J. Barlow, K. L. Matta, *Cancer Lett.* , **30**, 201-205 (1986).
13. P. O. Skacel, W. M. Watkins, *Cancer Res.* , **43**, 3998-4001 (1988).
14. K. B. Lee, U. R. Desai, M. M. Palcic, O. Hindsgaul, R. J. Linhardt, *Anal. Biochem.* , **205**, 108-114 (1992).

15. J. Liu, O. Shirota, D. Wiesler, M. Novotny, *Proc. Natl. Acad. Sci.* , **88**, 2302-2306 (1991).
16. Y. F. Cheng, N. J. Dovichi, *Science* , **242**, 562-564 (1988).
17. J. Y. Zhao, D. Y. Chen, N. J. Dovichi, *J. Chromatogr.* , **608**, 117-120 (1992).
18. T. A. Beyer, J. E. Sadler, J. I. Rearick, J. C. Paulson, R. L. Hill, *Adv. Enzymol.* **52**, 23-175 (1981).
19. M. M. Palcic, *Carbohydrate Res.*, **196**, 133-140 (1990).
20. D. P. Khare, O. Hindsgaul, R. U. Lemieux, *Carbohydr. Res.* , **136**, 285 (1985).
21. M. M. Palcic, A. P. Venot, R. M. Ratcliffe, O. Hindsgaul, *Carbohydr. Res.* **190**, 1 (1989).
22. B. Rotman, *Proc. Natl. Acad. Sci.* , **47**, 1981 (1961).
23. J. Yashphe, H. O. Halvorson, *Science* , **191**, 1283 (1976).
24. G. P. M. Luyten, A. T. Hoogeveen, H. Galjaard, *J. Histochem. Cytochem.* , **33**, 965 (1985).
25. D. C. Nguyen, R. A. Keller, J. H. Jett, J. C. Martin, *Anal. Chem.* , **59**, 2158-2160 (1987).
26. K. Peck, L. Stryer, A. N. Glazer, R. A. Mathies, *Proc. Natl. Acad. Sci.* , **86**, 4087 (1989).

CHAPTER 6

THE USE OF A SHEATH FLOW CUVETTE FOR CHEMILUMINESCENCE DETECTION OF ISOLUMINOL THIOCARBAMYL-AMINO ACIDS SEPARATED BY MICELLAR CAPILLARY ELECTROPHORESIS*

* A version of this chapter has been published. *J. Microcol. Sep.*, 5, 331-339 (1993)

6.1 INTRODUCTION

Chemiluminescence has proven to be a rather sensitive detector in liquid chromatography, with detection limits of 10^{-12} M for diethylisoluminol [1]. Because both fluorescence and chemiluminescence are based on detection of an optical signal with a relatively low background, detection sensitivity is quite high. Unlike fluorescence, the chemiluminescence detection limit is usually determined by reagent purity rather than Raman scatter.

Chemiluminescence is an interesting detector for capillary electrophoresis. Because no external light source is required, the optical system is inherently simple. On the other hand, because chemiluminescence requires mixing of the analyte and a reagent stream, the flow system will be complicated. This complication can be severe because of the volumetric flow encountered in capillary electrophoresis. A mixing system must be designed with dead volume of a few nanoliters to minimize extra-column band broadening.

Zare's group reported the first chemiluminescence detection in capillary electrophoresis for separation of a two component mixture [2]. They introduced the separation capillary into a larger diameter reaction capillary. Catalyst was pumped into the reaction capillary and reagent was flowing continuously through the capillary. A small observation window was made by removing the polyimide coating outside of the reaction capillary. A parabolic mirror was used to collect the chemiluminescence signal and to deliver it to a photomultiplier tube. This system produced fair detection limits, 100 attomole, at the expense of poor separation efficiency; the number of theoretical plates, $N = 5,000$, for luminol. This poor separation efficiency is presumably due to turbulent mixing at the tip of the capillary.

Grayeski reported a detector for acridinium chemiluminescence [3]. A 50 μm I.D. separation capillary was inserted within a 400 μm I.D. reaction capillary with a T-fitting. Detection linearity of 2.5 orders of magnitude was reported with a detection limit of 650 attomoles. In this work, the effects of pH, post column flow rate, and peroxide concentration on sensitivity were reported. A four component mixture of acridiniums was presented. Separations produced roughly 4,000 theoretical plates.

Zare's and Grayeski's chemiluminescence detectors are similar to that reported by Rose and Jorgenson for post column reaction of amines with o-phthaldialdehyde [4]. They demonstrated the trade-off between flow rate and separation efficiency. The fluorescence detector produced detection limits of 100 attomole injected onto the capillary. Plate counts were 10,600 in the best case. A similar system was also reported by Tsuda [5]. In these systems, the internal capillary is not held at the center of the reaction capillary but instead tends to fall to the side of the reaction capillary. As a result, the hydrodynamic profile is not very reproducible in the reactor.

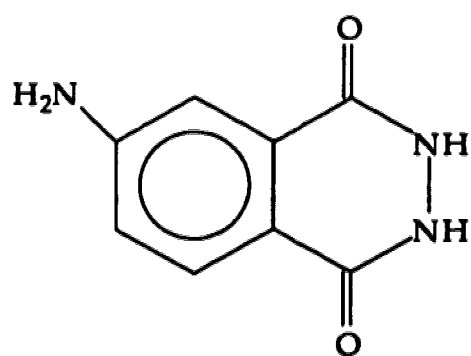
Care is required in the operation of the reactor. Ideally, there will be no turbulence and diffusion serves as the only mixing mechanism. The flow of the reagent and analyte must be carefully matched so that the reaction is complete in the detection chamber. If flow is too fast, analyte will be swept from the chamber before the reaction is complete. If flow is too slow, then band broadening will occur due to a long residence time in the detection chamber [4].

These post-column detectors are simple versions of the sheath flow cuvette used for fluorescence detection in both flow cytometry and capillary electrophoresis [6, 7, 8]. In the cuvette, the sample stream is introduced into the center of a square quartz cuvette. If the outer diameter of the tubing matches the

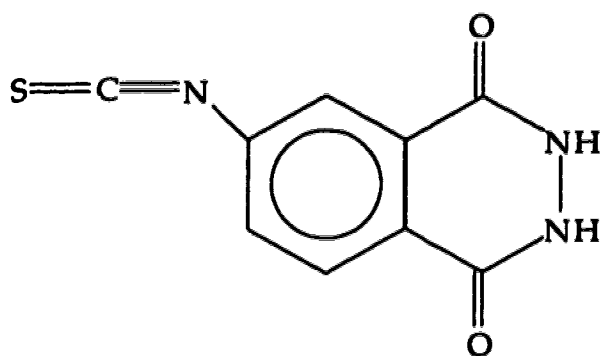
width of the square flow chamber, then the capillary is held in a reproducible position at the center of the stream. The hydrodynamics of the cuvette have been described in the absence [7] and presence [8] of diffusion. Turbulence is negligible with a well-designed sheath flow cuvette.

The chemiluminescence reaction of luminol with hydrogen peroxide and a catalyst in an alkaline solution has been extensively studied. Isoluminol (6-amino-2,3-dihydrophthalazine-1,4-dione) and its derivatives can also react with hydrogen peroxide and a variety of catalysts (non-enzymatic or enzymatic) to produce chemiluminescence light emission centered at 425 nm [9]. The isoluminol-hydrogen peroxide reaction is fast at room temperature. Schreoder and Volgelhut investigated a microperoxidase catalyzed detection system with isoluminol in a fast flow reactor. Millisecond reaction times were produced for picomolar analyte concentration [1]. It appears that efficient detection can be produced with sub-second response time; the capillary electrophoresis separation should not be degraded by the reaction response time.

Isoluminol isothiocyanate (ILITC), **Figure 6.1**, is a commercially available reagent possessing both the chemiluminescence isoluminol group and an isothiocyanate moiety for labeling amine groups [10]. Like other isothiocyanates, this reagent has potential application in protein sequencing as a modified Edman degradation reagent. The reagent was developed by M. Cooper of Clemson University, and has been used to form the thiocarbamyl derivatives of 17 amino acids (Ala, Arg, Asp, Gly, Glu, His, Hydroxyproline, Ile, Leu, Lys, Met, Phe, Pro, Ser, Thr, Tyr, Val) for separation by liquid chromatography and detection by chemiluminescence. Their post-column reaction detector mixed the eluted analyte with 0.3 M H_2O_2 and 0.01 M $\text{Fe}(\text{CN})_6^{3-}$ in 2.5 M NaOH to produce the chemiluminescence reaction.



isoluminol



isoluminol isothiocyanate

Figure 6.1 Structures of isoluminol and isoluminol isothiocyanate

The instrument produced detection limits of 10^{-14} mole in a 20 μL injection volume corresponding to a concentration of 5×10^{-10} M.

6.2 EXPERIMENTAL

6.2.1 Interface of a Chemiluminescence Detector with CE

Figure 6.2 shows the schematic diagram of the post-column chemiluminescence detector interface with capillary electrophoresis. Chemiluminescence detection was based on a modified sheath flow cuvette. A locally constructed sheath flow cuvette was used as a post-column reaction mixing chamber. The 200- μm square and 1.5-cm long flow chamber had 2-mm thick quartz windows and was held in a locally constructed stainless-steel body. Chemiluminescence or labeled analyte elutes from the capillary into the sheath flow cuvette. Diffusion occurs, intimately mixing the analyte with the chemiluminescence reagent.

Chemiluminescence was detected at right angles with two end-on photomultiplier tubes butted against the cuvette to collect about 50% of the emitted photons from the chemiluminescence reaction. Chemiluminescence emission from isoluminol-hydrogen peroxide reaction maximizes at 425 nm. A number of end-on multialkali photomultiplier tubes are available with quantum efficiency on the order of 25% at this wavelength. To keep the instrument compact, two 10-mm diameter end-on Hamamatsu R1635-02 tubes (Hamamatsu Photonics K.K., Japan) are used. The serial numbers of the two PMTs are WA4509 and WA 4566, some experimental results of single photon counting generated by the manufacture are presented in Table 6.1 and Figure 6.3 and 6.4.

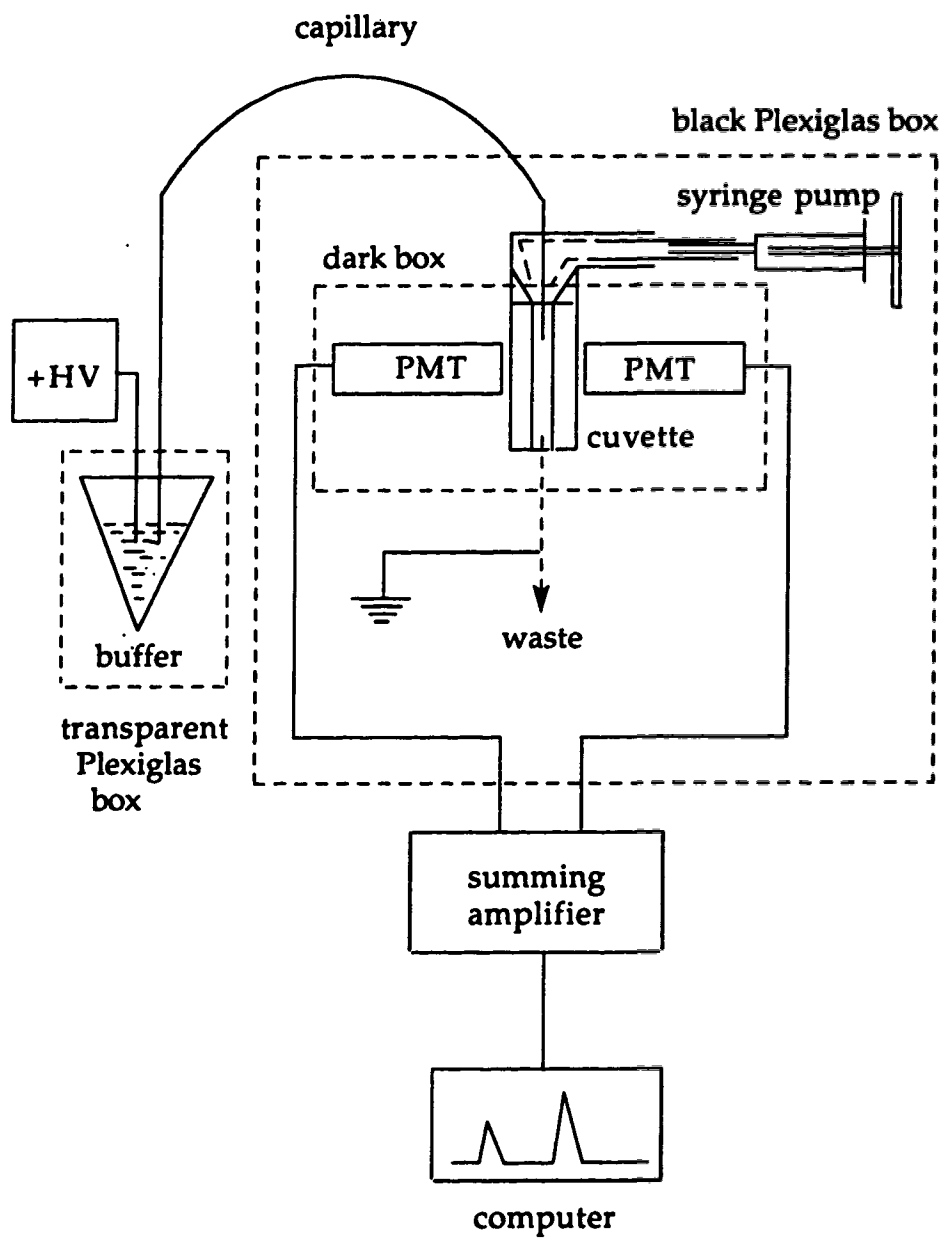


Figure 6.2 Schematic diagram of the capillary electrophoresis system with a post-column chemiluminescence detector

Table 6.1 Some parameters of the two R1635-02 PMTs

HAMAMATSU FINAL TEST SHEET
PHOTOMULTIPLIER TUBE TYPE : R1635-02

PAGE 001 OF 001

CUSTOMER : HC/UNIV OF ALBERTA(CA)

QUANTITY : 2 PCS

Serial Number	(1) Cathode Luminous Sens. $\mu A/lm$	(2) Anode Luminous Sens. A/lm	(3) Anode Dark Current nA	(4) Cathode Blue Sens. $\mu A/lm$ Blue			
WA4509	94.6	133.0	0.09	9.47			
WA4566	97.1	169.0	0.24	9.54			

NOTES

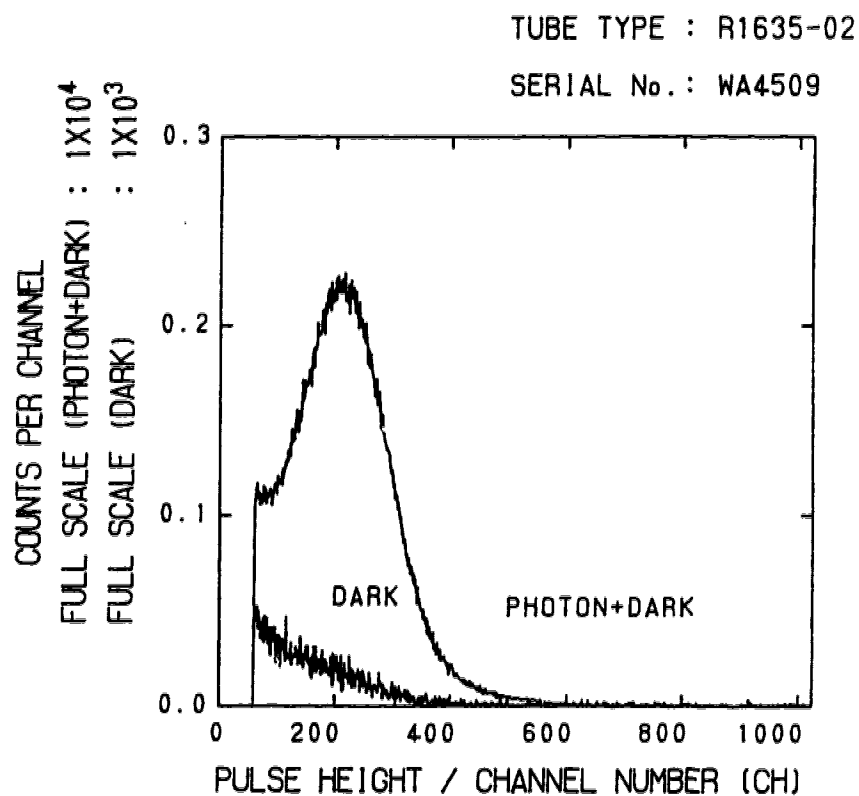
- (1)(2)(4) Light source : Tungsten filament lamp operated at 2856K.
 (2)(3) Overall supply voltage : 1250 [V]
 Voltage distribution : The standard voltage distribution ratio listed in the HAMAMATSU photomultiplier catalog.
 (3) The bulb of the tube is insulated from ground potential.
 (4) Measured with a Corning CS 5-58 blue filter (half stock thickness).

Date : JULY 9, 1992

Temperature : 25 °C

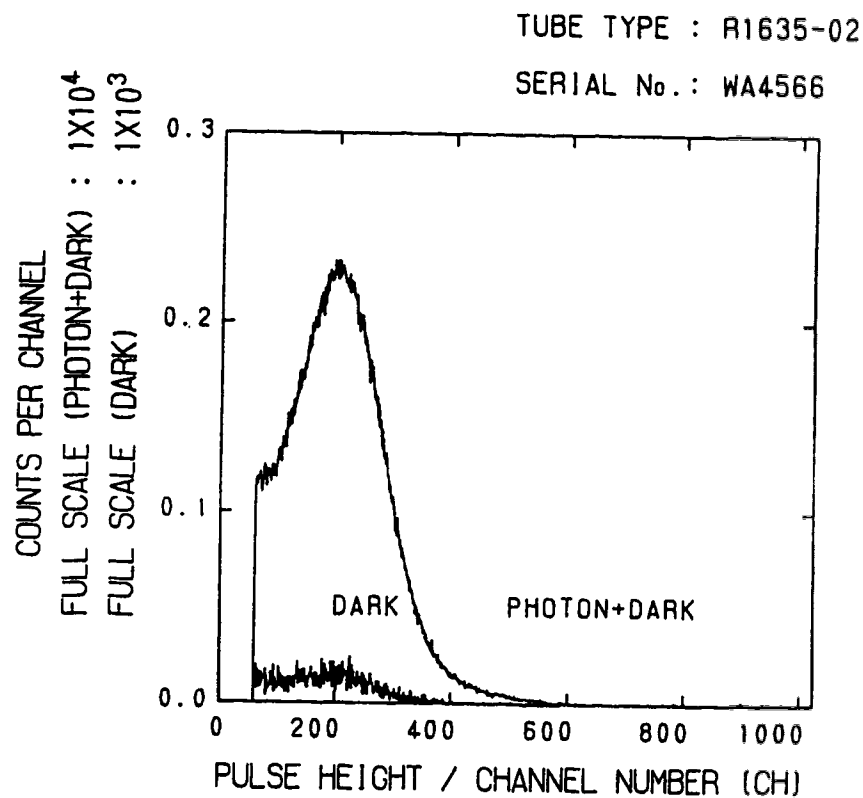
Approved by : *K. Nakamoto***HAMAMATSU**

Hamamatsu Photonics K.K., Electron Tube Division
 314-8, Shimokanzo, Toyooka-mura, Iwata-gun, Shizuoka-ken, 438-01 Japan, Telephone:0639/62/5248, Fax:0639/62/2206, Telex:4289-625



PHOTON+DARK COUNTS : 4613(cps)
 DARK COUNTS : 59(cps)
 WAVELENGTH OF INCIDENT LIGHT : 420(nm)
 SUPPLY VOLTAGE : -1250(V)
 LOWER LEVEL DISCRI. : 69(CH)
 UPPER LEVEL DISCRI. : 690(CH)
 LIVE TIME : 100(sec)
 P.H.A : NAIG-E / LINEAR AMP.: ORTEC 972
 PREAMP.: CANBERRA 2005
 COMMENT : 2- 6
 TEST DATE : APR.09.'92
 TEMPERATURE : 25 (°C)

Figure 6.3 Single photon counting results of a R1635-02 PMT (serial Number: WA4509) by the manufacturer (Hamamatsu)



PHOTON+DARK COUNTS : 4597(cps)
 DARK COUNTS : 31(cps)
 WAVELENGTH OF INCIDENT LIGHT : 420(nm)
 SUPPLY VOLTAGE : -1250(V)
 LOWER LEVEL DISCR. : 66(CH)
 UPPER LEVEL DISCR. : 669(CH)
 LIVE TIME : 100(sec)
 P.H.A : NAIC-E / LINEAR AMP. : ORTEC 972
 PREAMP. : CANBERRA 2005
 COMMENT : 2- 6
 TEST DATE : APR. 09. '92
 TEMPERATURE : 25 (°C)

Figure 6.4 Single photon counting results of a R1635-02 PMT (serial Number: WA4566) by the manufacturer (Hamamatsu)

The dark current counts of the two PMTs are very low, which predicts that low detection limits require both clean reagents and efficient reaction. The current from the photomultiplier tubes was summed with an operational amplifier and recorded with a Macintosh SE computer equipped with a National Instruments A/D board. Data were analyzed with software written in Matlab.

Stray light was an important concern in this instrument. A light-tight aluminum enclosure painted black was constructed to hold the two photomultiplier tubes and the cuvette holder, as shown in Figure 6.5. A fine adjustable screw was used to move the cuvette up and down. The cuvette-photomultiplier tube assembly and the syringe pump used for introducing the reagent were, in turn, held in a larger light-tight box constructed from black Plexiglas.

If hydrogen peroxide and microperoxidase were introduced as separate streams through two different inlets to the cuvette, the hydrogen peroxide was destroyed by the catalyst before reacting with the analyte coming out of the capillary and no chemiluminescent signal was observed. Zare's group added peroxide to the separation buffer and mixed catalyst in the detection chamber. The presence of relatively high concentration of peroxide (0.2 M) would perturb separations [3]. I found that it was difficult to degas hydrogen peroxide solutions and that bubble formation occurred in the separation capillary. These problems were eliminated by supplying the hydrogen peroxide through sheath flow and to add microperoxidase directly to the separation buffer; the catalyst and analyte are in intimate contact when mixed with the hydrogen peroxide in a post-column sheath flow cuvette, and large chemiluminescent signals are observed. Furthermore, the enzyme is present in micromolar concentration and does not influence the separation. The sheath stream was provided by a low-pressure

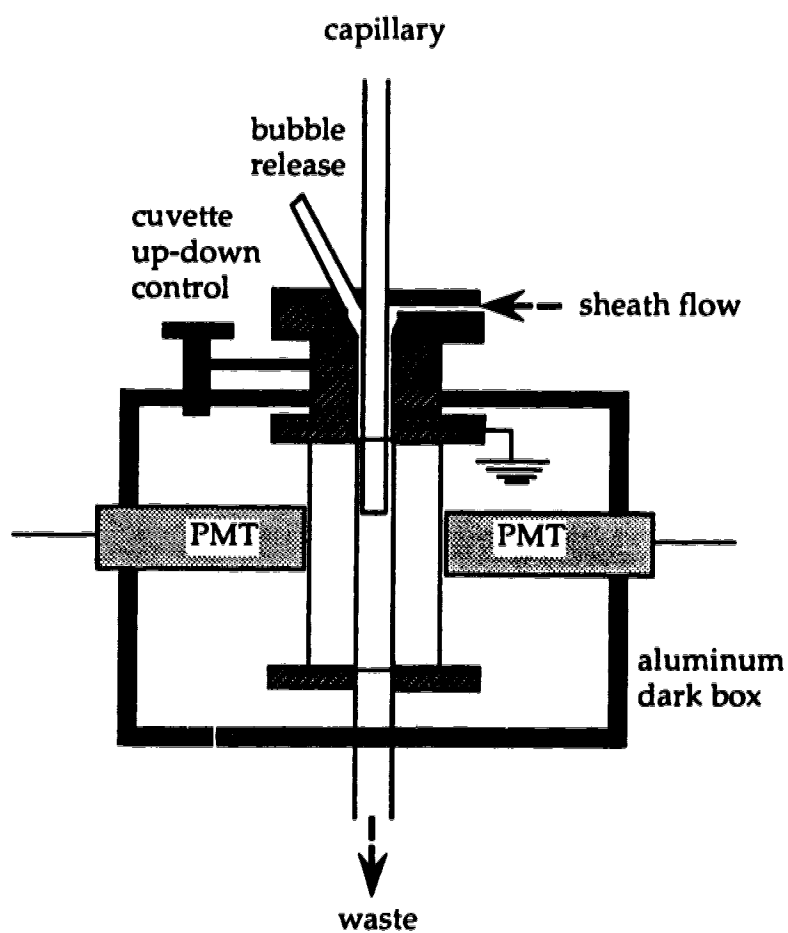


Figure 6.5 Cuvette and photomultiplier tube assembly in an aluminum box painted black

syringe pump (Harvard model 22) equipped with a 5 ml disposable syringe; the sheath solution was typically 2 mM hydrogen peroxide prepared in 10 mM borate buffer (pH 9.3).

6.3.2 Reagents

Isoluminol (Sigma) was dissolved in dimethylformamide (DMF); the solution was colorless and the molecular weight (M.Wt.) of isoluminol was 177.2 g/mole. Isoluminol isothiocyanate ((Molecular Probes, Inc.) was white powder and its stock solutions were made in DMF. The molecular weight of ILITC was 219.219 g/mole.

Microperoxidase (M6756, Sigma) is a heme-peptide [11], **Figure 6.6**, and has a molecular weight of 1881.4 g/mole. A 200 μ M stock solution was made in 10 mM Tris-HCl buffer (pH 7.4) and stored at 4°C. The 10 mM Tris-HCl buffer was prepared by mixing 20.7 ml 0.2 M Tris (hydroxymethyl) amino methane ($\text{C}_4\text{H}_{11}\text{NO}_3$, M.Wt. = 121.14 g/mole) with 25 ml 0.2 M HCl followed by dilution to a total volume of 100 ml, and then further dilution to 10 mM.

Hydrogen peroxide stock solution (29.0-32.0%, BDH Inc.) was diluted by 10 mM borate buffer to various concentrations. The concentration of the stock hydrogen peroxide was 10 M determined by titration with a KMnO_4 solution of known concentration. The KMnO_4 solution was prepared by dissolving 4.1040 g of KMnO_4 in distilled water in a glass beaker, and heated to boil for about 30 minutes, cooled to room temperature, and filtered with glass wool. A 25.00 ml 0.06368 M standard oxalic acid ($\text{H}_2\text{C}_2\text{O}_4 \cdot 2\text{H}_2\text{O}$, M.Wt. = 126.07 g/mole) mixed with 25 ml 2 M H_2SO_4 was titrated by the KMnO_4 solution; the calculated

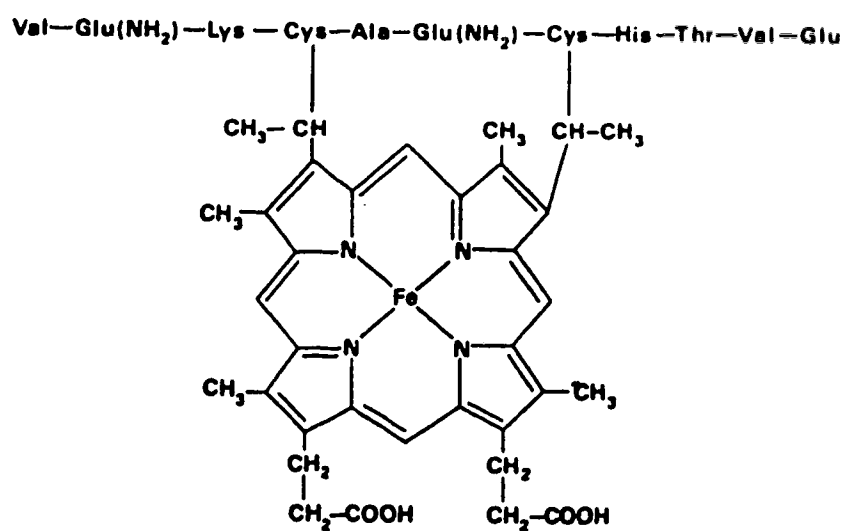


Figure 6.6 Structure of microperoxidase

concentration of KMnO_4 solution was 0.02651 M. The sheath flow solution of hydrogen peroxide was diluted daily fresh from this stock solution (10 M).

Deionized water from a Barnstead NANOpure system was used to prepare buffers. Both sheath flow solution and separation buffers were filtered with 0.22 mm pore-size membranes (Millipore).

6.2.3 Labeling Reactions

Isoluminol thiocarbamyl derivatives of amino acids were prepared by weighing accurately about 2 μmole isoluminol isothiocyanate and 40 μmol of each of the 20 common amino acids into a disposable centrifuge tube; amino acid was in excess. To each of these solid mixtures, 100 μl of 95% H_2O : 5% triethylamine (TEA) (V:V) (pH 11.7) coupling solvent was added. The mixtures were placed in an ultrasonic bath for one minute and briefly vortexed, and then allowed to react at room temperature in the dark for nine minutes. A blank was made by mixing ILITC with the coupling solvent for 10 minute. The reaction solutions were then evaporated to dryness using a vacuum centrifuge, SpeedVac SC110 (Savant Instruments, Inc., Farmingdale, NY, USA), over 2 to 4 hours. The dry isoluminol thiocarbamyl derivatives were refrigerated (4°C) until use.

6.2.4 Capillary Electrophoresis Conditions

The separation buffer used was typically 10 mM borate buffer with 10 mM SDS and 1.5-4.0 μM microperoxidase (pH 9.2). The dry isoluminol thiocarbamyl derivatives of amino acids were dissolved and diluted to the desired concentrations with the separation buffer. Separations were performed in a 50

μm I.D. and 190 μm O.D. fused silica capillaries (Polymicro Technologies, Phoenix, AZ, USA); capillaries were from 60 to 100 cm in length. A Spellman Model CZE 1000R high voltage power supply was used to drive the electrophoresis at 25 to 30 kV. Injections were performed by applying 2 kV voltage across the capillary for five seconds or otherwise described; injection volumes typically are 1 to 2 nanoliters.

6.3 RESULTS AND DISCUSSION

6.3.1 Catalyst: Microperoxidase

The chemiluminescence reaction between isoluminol and hydrogen peroxide requires a catalyst. A detailed study of the chemiluminescence yields and detection limits of some isoluminol derivatives in various oxidation systems was reported by Schroeder and Yeager in 1978 [9]. The popular ferricyanide-catalyzed system showed intermediate sensitivity, which requires high pH. The microperoxidase-catalyzed system produced the highest sensitivity with an additional advantage of being equally sensitive at pH from 8.6 to 13.0. I compared microperoxidase and potassium ferricyanide as catalysts using the chemiluminescence detector for capillary electrophoresis; better results were produced with microperoxidase.

6.3.2 Optimization of the Chemiluminescence Detection System

There are a number of parameters that can affect the sensitivity of the chemiluminescence detector. The chemiluminescence signal was optimized as functions of hydrogen peroxide concentration in the sheath flow,

microperoxidase concentration and SDS concentration in the separation buffer, the sheath flow rate that determines the residence time of the analyte within the view of the two photomultiplier tubes, and the distance from the capillary exit to the center of the cylindrical PMTs. Isoluminol was used in the optimization experiments.

6.3.2A As a Function of Hydrogen Peroxide Concentration

The effect of hydrogen peroxide concentration on the chemiluminescence signal generated by injection of isoluminol into the capillary was studied. Table 6.2 lists the experimental data and Figure 6.7 presents a log-log plot of signal against concentration of hydrogen peroxide. The isoluminol concentration used was 1.5×10^{-5} M. The photomultiplier tubes were operated at 1200 V, separation was at 26 kV in a 69 cm long capillary. The separation buffer contained 10 mM borate with 10 mM sodium dodecyl sulfate (pH 9.2) and 1.5 μ M microperoxidase. Hydrogen peroxide solutions at different concentrations were introduced at a sheath flow rate of 500 μ L/hour.

The maximum signal was observed with a concentration of peroxide in the range of 1 to 10 mM. Presumably, at low concentrations, the peroxide is not present in sufficient concentration to react quickly with all the analyte. At higher concentration, the peroxide may be in sufficient concentration to oxidize the catalytic enzyme. The optimal concentration of peroxide is roughly three orders of magnitude less than used in Zare's instrument [2]. However, a much larger volumetric flow of hydrogen peroxide was used in this instrument than in the previous report. A similar number of moles of hydrogen peroxide are added per second in both instruments.

Table 6.2 Experimental data of the effect of H₂O₂ concentration on CL signal

(H ₂ O ₂), M	log (H ₂ O ₂)	injection kV / sec	migration time, min	relative CL signal	log (rel.sig.)
0.3	-0.5228	26 / 5.06	335	3598	3.556
0.1	-1.0000	12 / 4.84	310	11459	4.059
0.03	-1.5228	12 / 5.02	296	12932	4.111
0.01	-2.0000	8 / 5.03	298	27000	4.431
0.003	-2.5228	5 / 5.04	284	31105	4.493
0.001	-3.0000	2 / 5.08	281	78670	4.890
0.0005	-3.3000	2 / 4.91	279	32590	4.513
0.00025	-3.6000	12 / 5.06	286	6629	3.820
0.0001	-4.0000	26 / 4.99	281	879	2.940

$$* \text{ relative CL signal} = \frac{(\text{CL signal}) \times (\text{migration time})}{(\text{injection voltage}) \times (\text{injection time})}$$

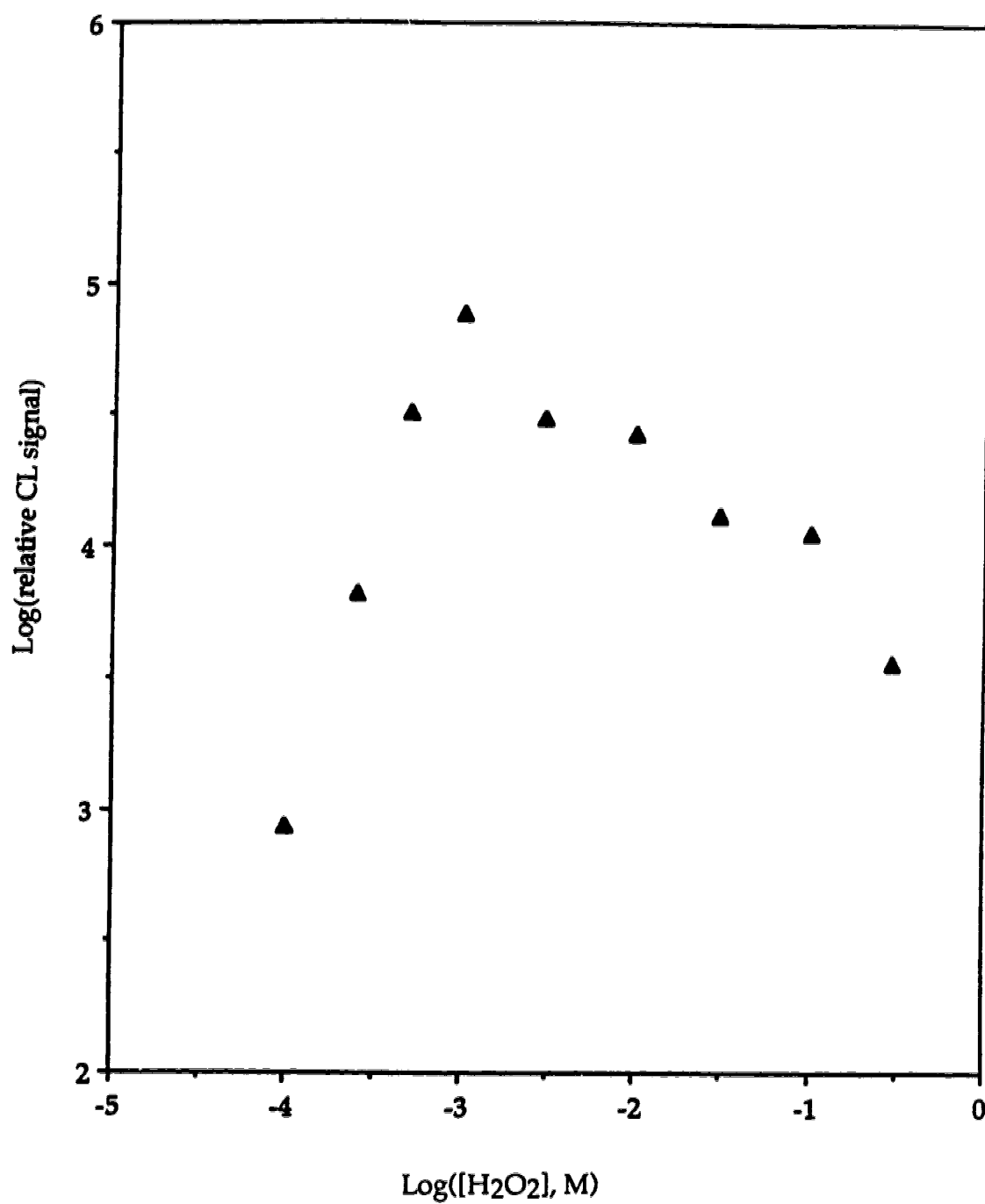


Figure 6.7 Chemiluminescence signal as a function of hydrogen peroxide concentration introduced into the sheath flow cuvette

6.3.2B As a Function of Microperoxidase Concentration

The concentration of microperoxidase is another factor affecting the chemiluminescence intensity in the flow reaction. Table 6.3 lists the experimental data and Figure 6.8 presents the plot of relative chemiluminescence signal versus microperoxidase concentration. The isoluminol concentration used was 1.5×10^{-5} M. The photomultiplier tubes were operated at 1200 V, separation was at 26 kV in a 69 cm long capillary. The separation buffer contained 10 mM borate with 10 mM sodium dodecyl sulfate (pH 9.2) and microperoxidase at various concentrations. Hydrogen peroxide solution (2 mM) was introduced at a sheath flow rate of 500 μ L/hour.

The decrease in chemiluminescence signal at higher concentrations of microperoxidase is presumably caused by complete consumption of hydrogen peroxide before the analyte reaches the detection region of the cuvette. Optimum microperoxidase concentration is from 0.5 to 5 μ M.

6.3.2C As a Function of the Residence Time

The residence time of analyte in the flow chamber will determine the extent of reaction. The residence time is determined by the flow rate of the hydrogen peroxide solution and the field-of-view of the photomultiplier tube (i.e. the diameter of the PMT); the latter parameter is fixed and roughly equal to the 8-mm diameter of the photocathode of the photomultiplier tube (R1635-02). The residence time can be effectively affected by the sheath flow rate of the hydrogen peroxide solution. Faster flow rate will apparently push the analyte out of the field-of-view of the PMTs before the chemiluminescence reaction is complete.

Table 6.3 Experimental data of the effect of microperoxidase concentration on chemiluminescence signal

microperoxidase concentration, μM	relative CL signal
0.236	7773
0.776	40500
1.508	84885
2.200	142419
3.174	15935
3.939	25973

$$* \text{ relative CL signal} = \frac{(\text{CL signal}) \times (\text{migration time})}{(\text{injection voltage}) \times (\text{injection time})}$$

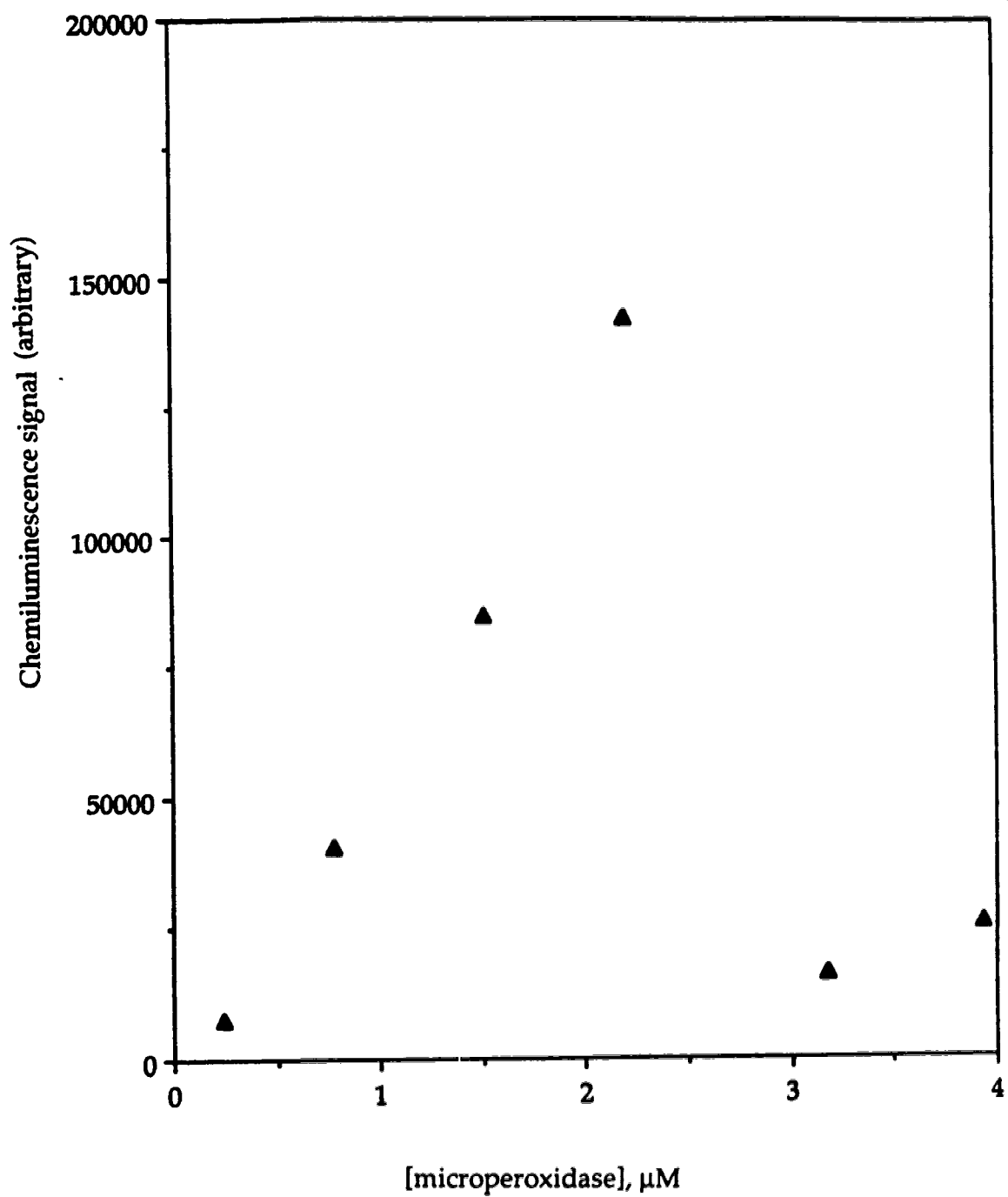


Figure 6.8 Chemiluminescence signal as a function of microperoxidase concentration in the separation buffer

Table 6.4 lists the experimental data. The isoluminol concentration used was 1.5×10^{-5} M. The PMTs were operated at 1200 V, separation was at 26 kV in a 69 cm long capillary. The separation buffer contained 10 mM borate with 10 mM sodium dodecyl sulfate (pH 9.2) and 1.5 μ M microperoxidase. Hydrogen peroxide solution (2 mM) was introduced at various sheath flow rates.

Figure 6.9 presents the plot of relative chemiluminescence signal versus residence time, along with a least-squares fit of an exponential function:

$$\text{CL signal} = 4.3 \times 10^4 \times (1 - e^{\text{residence time} \times 0.677 \text{ sec}^{-1}}) \quad (6.1)$$

The data are consistent with a pseudo-first order reaction with a rate constant of 0.677 sec^{-1} .

A long residence time could lead to excessive peak broadening. The longest residence time produced by my instrument is about 4.5 seconds. The observed peak width in the experiment was about eight seconds and was independent of residence time across the range studied.

6.3.2D As a Function of the Distance from the Exit of Capillary to the Center of the Cylindrical PMTs

Chemiluminescence intensity in a flow system will increase with distance downstream as analyte and chemiluminescence reagent diffuse together and react. However, further down stream, the analyte will be exhausted, and the chemiluminescence signal will drop to zero. In this chemiluminescence detector for capillary electrophoresis, the chemiluminescence signal changes with distance downstream from the exit of the separation capillary to the center of the field-of-view of the two PMTs.

Table 6.4 Experimental data of the effect of residence time of analyte within the field-of-view of the PMTs

pump dial	flow rate (ml/hour)	residence time (s)	relative CL signal
01	0.254	4.53	39772
02	0.508	2.26	36001
04	1.02	1.13	25265
06	1.63	0.70	18351
08	2.03	0.57	11703
10	2.54	0.45	6839

* residence time, $t_{\text{residence}}$ (s), is calculated by the following equations:

$$0.0200 \text{ (cm)} \times 0.0200 \text{ (cm)} \times v \text{ (cm/s)} = \text{flow rate (ml/hour)} \times 3600 \text{ s/hour}$$

$$t_{\text{residence}} = \frac{0.8 \text{ (cm)}}{v \text{ (cm/s)}}$$

$$t_{\text{residence}} = \frac{1.152 \text{ (s ml/hour)}}{\text{flow rate (ml/hour)}}$$

where v (cm/s) is the linear velocity of the sheath flow in the 200- μm square cuvette and 0.8 cm is the field-of-view of the PMTs.

$$\text{* relative CL signal} = \frac{(\text{CL signal}) \times (\text{migration time})}{(\text{injection voltage}) \times (\text{injection time})}$$

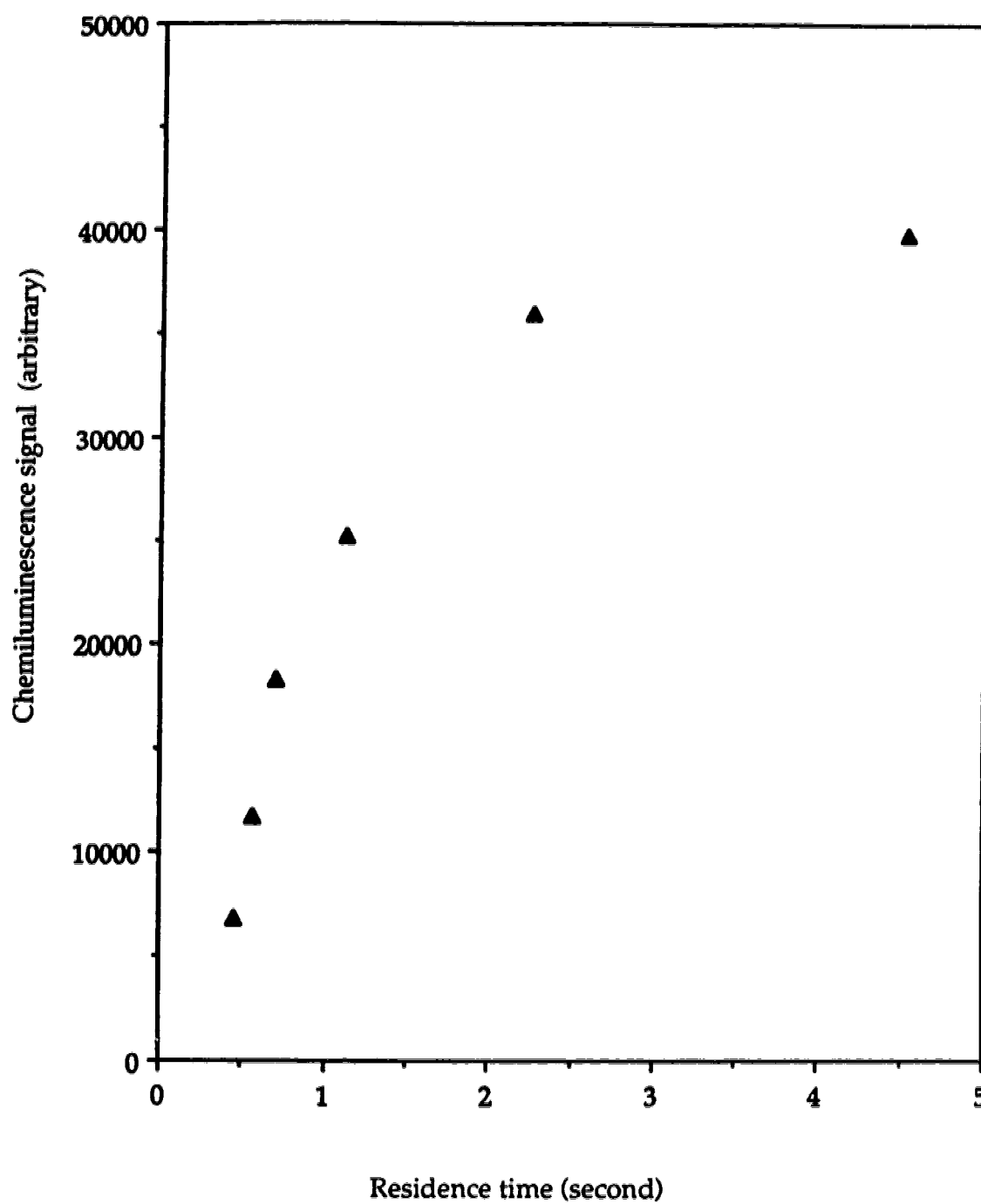


Figure 6.9 Chemiluminescence signal as a function of residence time of analyte within the field-of-view of the PMTs

Table 6.5 lists the experimental data of the effect of the distance downstream on the chemiluminescence signal. **Figure 6.10** presents the plot of relative chemiluminescence signal versus the distance. Since there was no accurate way to measure the initial distance (d_0), the distance from the exit of the capillary to the center of the PMTs was defined as $d_0 + X$.

The experiment was performed by running a 1.2×10^{-5} M isoluminol solution continuously through the capillary and the changing the distance by increments. The photomultiplier tubes were operated at 1200 V, separation was at 30 kV in a 84 cm long capillary. The separation buffer contained 10 mM borate with 10 mM sodium dodecyl sulfate (pH 9.2) and 1.5 μ M microperoxidase. Hydrogen peroxide solution (2 mM) was introduced at a flow rate of 500 μ L/hour.

The signal maximized a few millimeters below the exit of the capillary and decreased steadily downstream from the exit of the capillary. The signal was integrated over the 0.8 cm diameter of the photomultiplier tube. At the flow rate used in this experiment (500 μ L/hr), roughly 2.3 seconds were required for the analyte to pass through the field-of-view of the photomultiplier tubes. Given the rate constant of 0.677 sec^{-1} , the reaction should be ~80% complete during the transit time (2.3 s) across the detectors.

6.3.2E As a Function of the Concentration of Sodium Dodecyl Sulfate

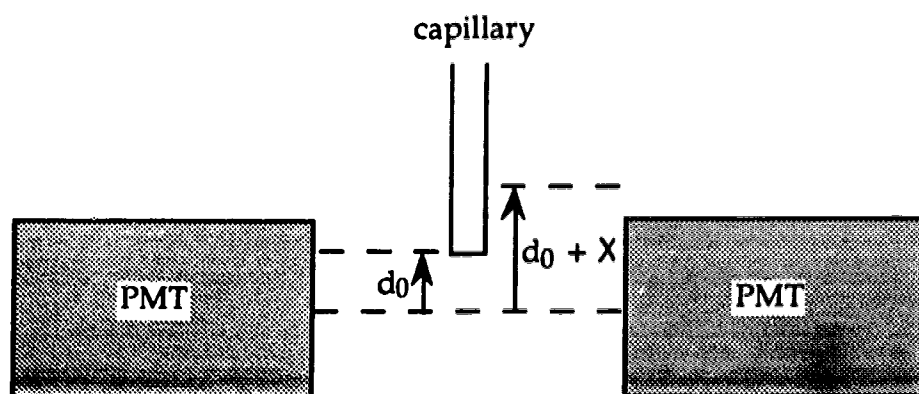
The separation of labeled amino acids is often improved by addition of the anionic surfactant sodium dodecyl sulfate (SDS) to the separation buffer. The effect of the SDS concentration on the chemiluminescence signal was studied. The isoluminol concentration used was 1.5×10^{-5} M. The photomultiplier tubes

Table 6.5 Experimental data of the effect of the distance downstream ($d_0 + X$) on the chemiluminescence signal

distance down stream (mm)	relative CL signal
d_0	2295
$d_0 + 2$	2458
$d_0 + 4$	2545
$d_0 + 6$	2451
$d_0 + 8$	2100
$d_0 + 10$	1913
$d_0 + 12$	1681
$d_0 + 13.8$	1417

*

Relative CL signal values were taken directly from the electropherograms.



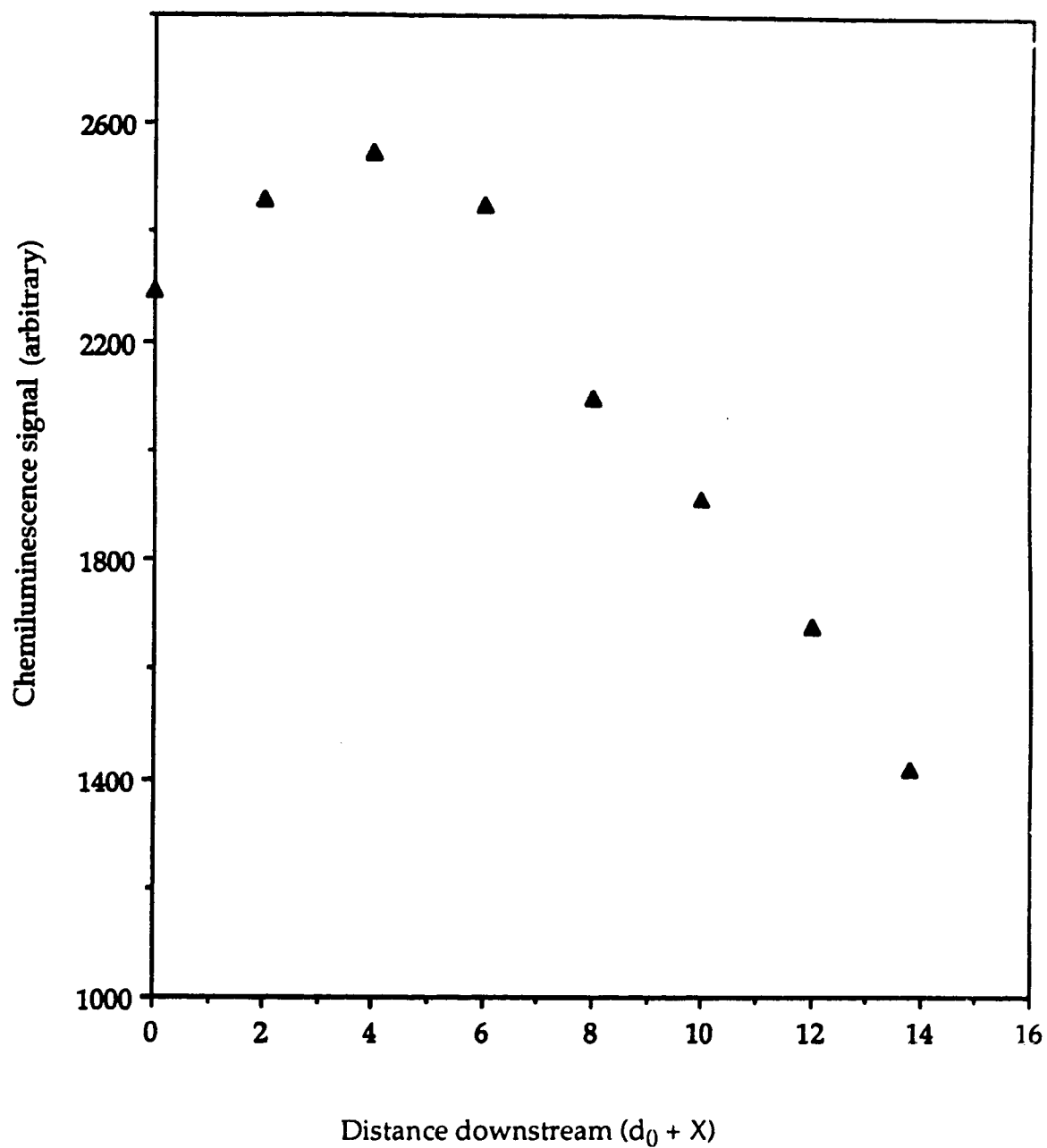


Figure 6.10 Chemiluminescence signal as a function of distance downstream from the exit of the capillary to the center of the PMTs

were operated at 1200 V, separation was at 26 kV in a 69-cm long capillary. The separation buffers contained 10 mM borate (pH 9.2) with SDS at various concentrations and 1.5 μ M microperoxidase. Hydrogen peroxide solution was introduced at a sheath flow rate of 500 μ L/hour.

Two sets of experimental data are listed in Table 6.6a and Table 6.6b that is plotted in Figure 6.11. Unfortunately, the presence of sodium dodecyl sulfate in the separation buffer degraded the chemiluminescence sensitivity. The surfactant may denature the microperoxidase, destroying the catalyst. Fortunately, a relatively low concentration (10 mM) SDS buffer produced the best separation of isoluminol thiocarbamyl derivatives of amino acids, with a small decrease of CL signal.

6.3.3 Background Signal Evaluation

The background signal appears to be chemical and not instrumental. Low noise photomultiplier tubes were used for the instrument, with typical dark counts less than 100 counts per second. The background signal observed was equivalent to 10^4 counts per second. The background was quite consistent from day to day. Furthermore, the dark count was not due to room lights; the background signal did not change as room lights were turned on or off. As an interesting source of background signal, the syringe pump used to add the hydrogen peroxide to the sheath flow cuvette had a red indicator lamp. The pump was placed within the dark Plexiglas box containing the sheath flow cuvette and photomultiplier tube assembly. The light on the pump proved to be the major source of background signal in the instrument; a piece of black electrician's tape placed over the light eliminated that source of background.

Table 6.6 Experimental data of the effect of the SDS concentration on the chemiluminescence signal

Table 6.6a

SDS concentration, mM	relative CL signal
0	3277
10	2666
20	2552

Table 6.6b

SDS concentration, mM	relative CL signal
20	2836
30	2594
40	1463
50	1390

* Table 6.6a and 6.6b were obtained on different days.

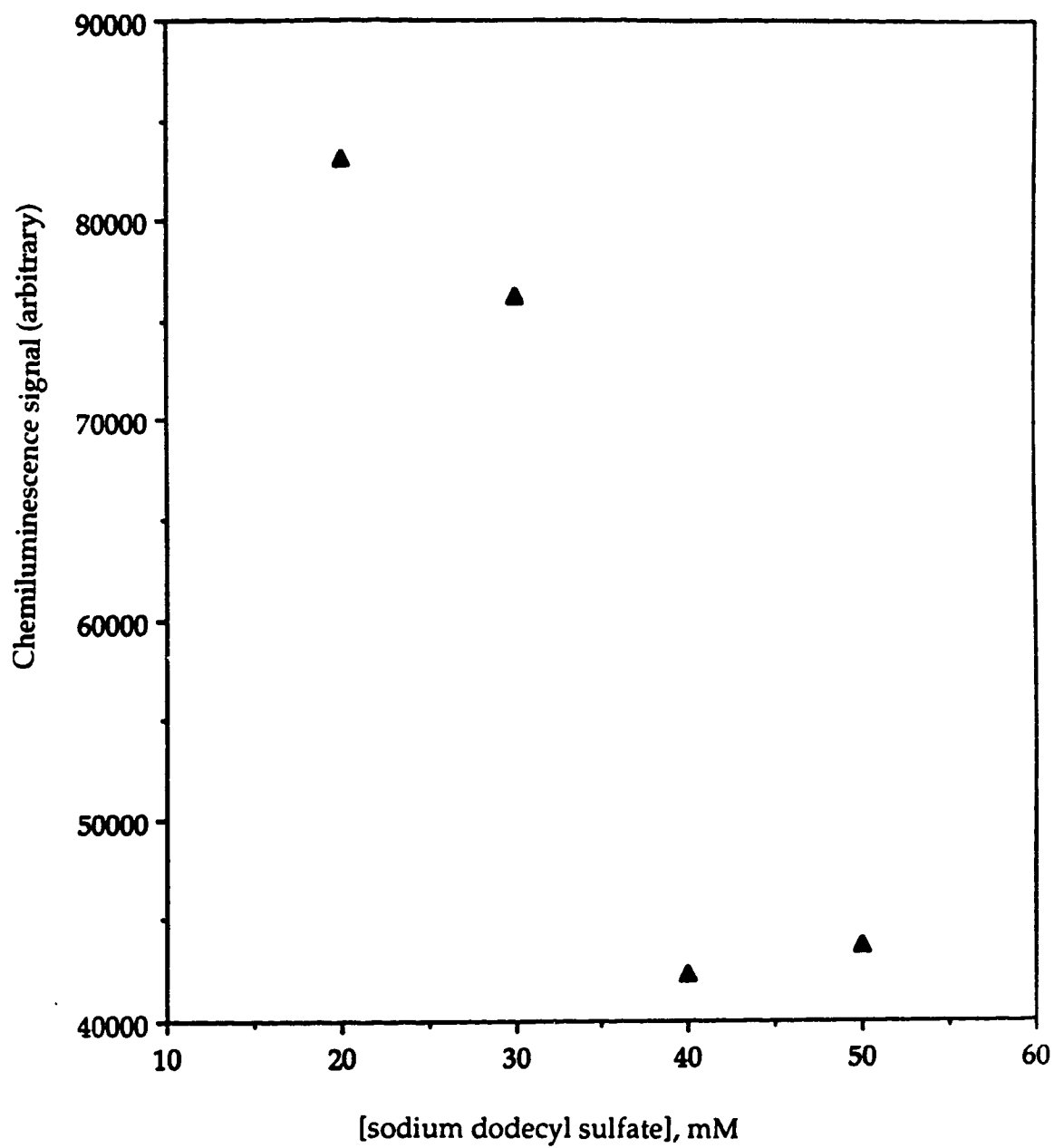


Figure 6.11 Chemiluminescence signal as a function of sodium dodecyl sulfate concentration in the separation buffer (according to Table 6.6b)

6.3.4 Calibration Curve and Detection Limit of Isoluminol

After the system was optimized with respect to surfactant concentration, microperoxidase concentration, hydrogen peroxide concentration, hydrogen peroxide addition rate, and the distance down stream, a calibration curve was constructed by injection of dilute isoluminol solutions. The photomultiplier tubes were operated at 1200 V, separation was at 26 kV in a 69 cm long capillary (50 μm I.D.). The separation buffers contained 10 mM borate (pH 9.2) with 10 mM SDS and 1.5 μM microperoxidase. Hydrogen peroxide solution (2 mM) was introduced at a sheath flow rate of 500 $\mu\text{L}/\text{hour}$. Figure 6.12 shows a typical electropherogram of isoluminol.

Table 6.7 lists the experimental data for constructing a calibration curve. The values of relative CL signal were the averages of four repeat runs at each concentration. Figure 6.13 presents the plot of log-log calibration curve. The linear ($r = 0.997$) range of the log-log curve covers at least a factor of 750, from 30 femtomoles injected to the detection limit of 40 attomoles or 2×10^{-8} M injected in a 2 nL volume.

6.3.5 Electropherograms of Isoluminol Isothiocyanate and ILITC Labeled Amino Acids

The electropherograms of isoluminol isothiocyanate, Figure 6.14, show two chemiluminescence peaks. Figure 6.14a was generated with a 7.0×10^{-5} M ILITC solution diluted from a fresh ILITC stock solution in dimethylformamide and Figure 6.14b was generated with a 7.0×10^{-5} M ILITC solution diluted from the ILITC stock solution which had been stored for three days. The separations were performed in an 84 cm long capillary (41 μm I.D.) operated at 30 kV. The

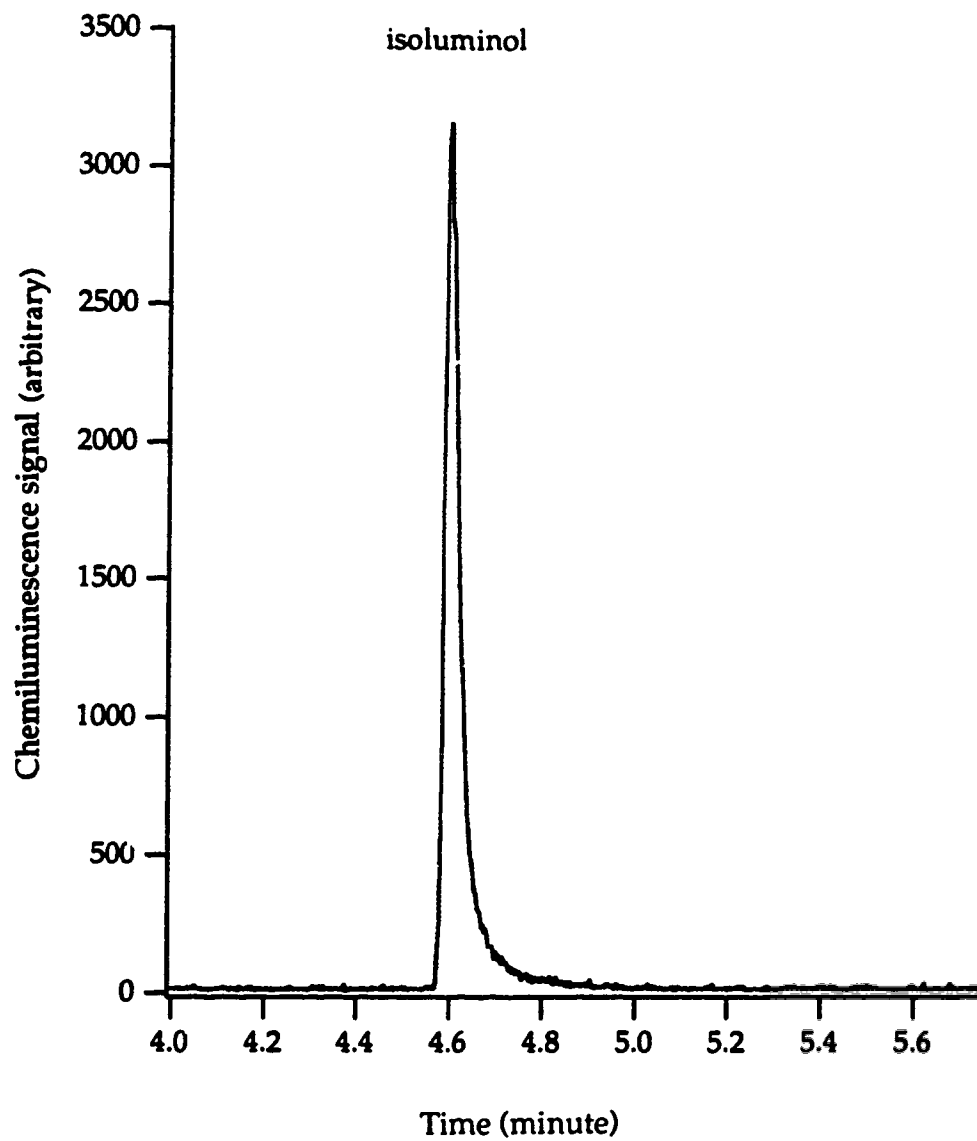


Figure 6.12 Electropherogram of isoluminol (1.5×10^{-5} M)

Table 6.7 Experimental data of a calibration curve for isoluminol

concentration, M	log(concentration)	average CL signal	log(ave.CL signal)
1.5×10^{-5}	-4.8	90834	4.95
1.5×10^{-6}	-5.8	13095	4.11
1.5×10^{-7}	-6.8	1224	3.08

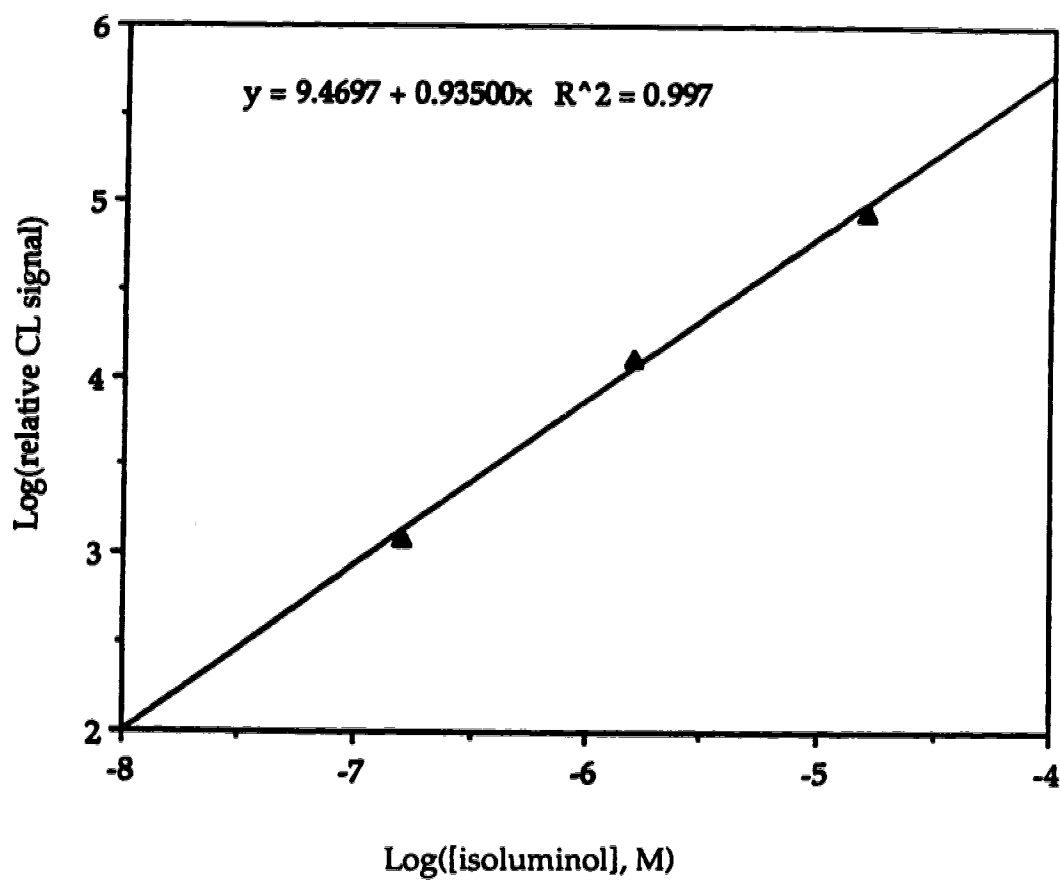


Figure 6.13 Log-log calibration curve for isoluminol

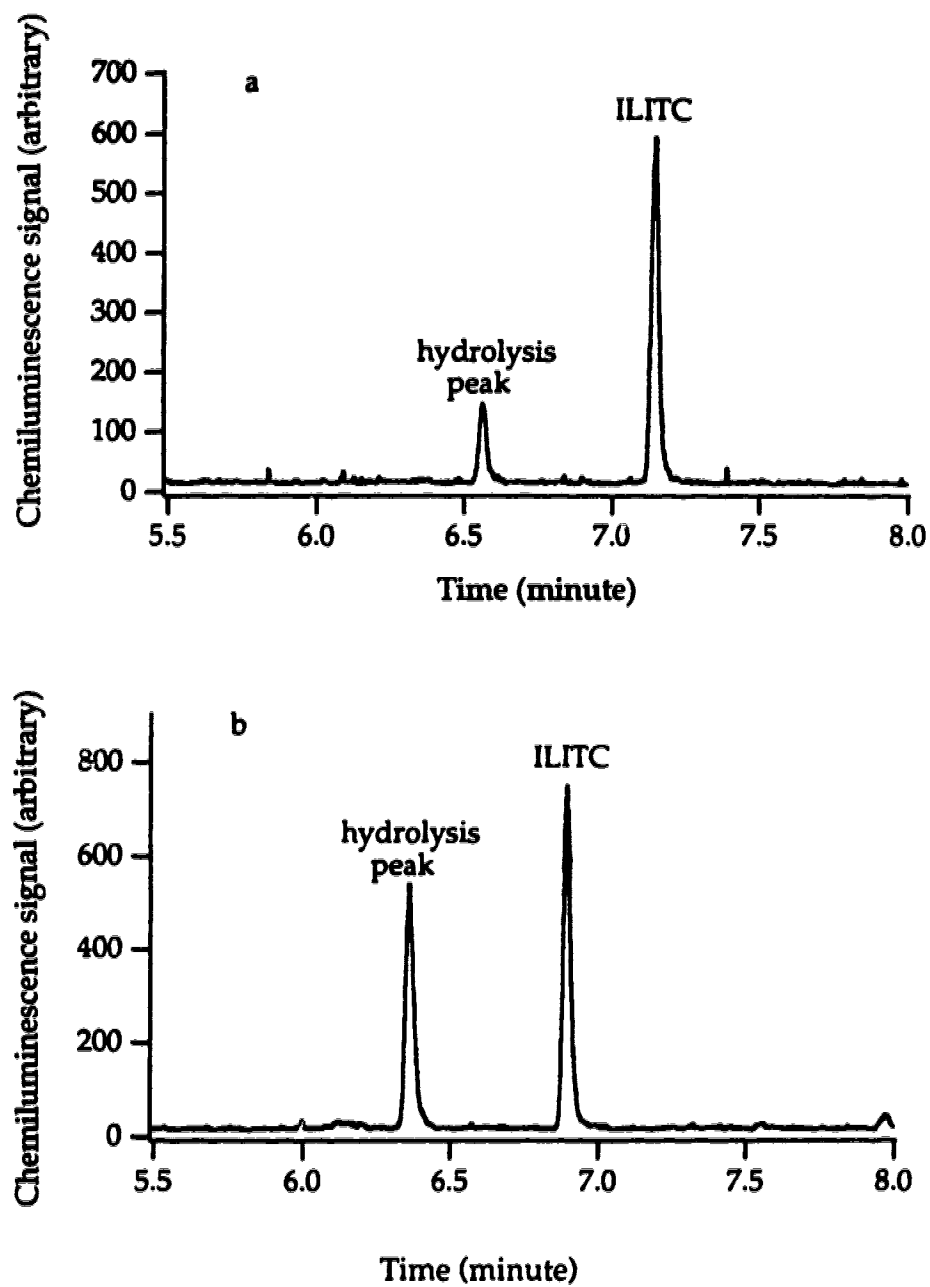


Figure 6.14 Electropherograms of ILITC (7.0×10^{-5} M)

separation buffer was 10 mM borate (pH 9.2) with 10 mM SDS and 1.6 μ M microperoxidase. Hydrogen peroxide solution (2 mM) was provided at a flow rate of 500 μ L/hour. Electrophoretic injections were employed at 5 kV for 5 seconds.

The major peak in Figure 6.14a co-elutes with isoluminol and appears to be the isoluminol isothiocyanate; the minor peak presumably corresponds to a hydrolysis product of ILITC in aqueous solution. The major peak almost disappeared, Figure 6.15, after performing a blank reaction of ILITC with the coupling solvent (95% H₂O : 5% triethylamine). The dry blank was dissolved in 10 mM borate buffer with 10 mM SDS and diluted to a concentration of 4.1×10^{-5} M by the separation buffer.

All twenty physiological amino acids (Ala, Asp, Asn, Arg, Cys, Gly, Gln, Glu, His, Ile, Leu, Lys, Met, Phe, Pro, Ser, Thr, Trp, Tyr, Val) were labeled with isoluminol isothiocyanate and detected with the chemiluminescence system. All amino acids give rise to a single labeled amino acid peak, except for lysine that gives rise to two peaks due to the side ϵ -amine group and cysteine that gives rise to two very small peaks. The labeling reaction always generates a peak with the same retention time as the hydrolysis product of isoluminol isothiocyanate.

The labeling reaction is complete in ten minutes at room temperature. Longer reaction time does not generate more derivative due to the competitive hydrolysis of isoluminol isothiocyanate. For most of the amino acids, the hydrolysis product peak is larger than that of the labeled amino acid, Figure 6.16a. However, proline generates a particularly large chemiluminescence signal, Figure 6.16b. It is not clear if this enhanced peak is due to efficient reaction or high chemiluminescence quantum yield for that derivative.

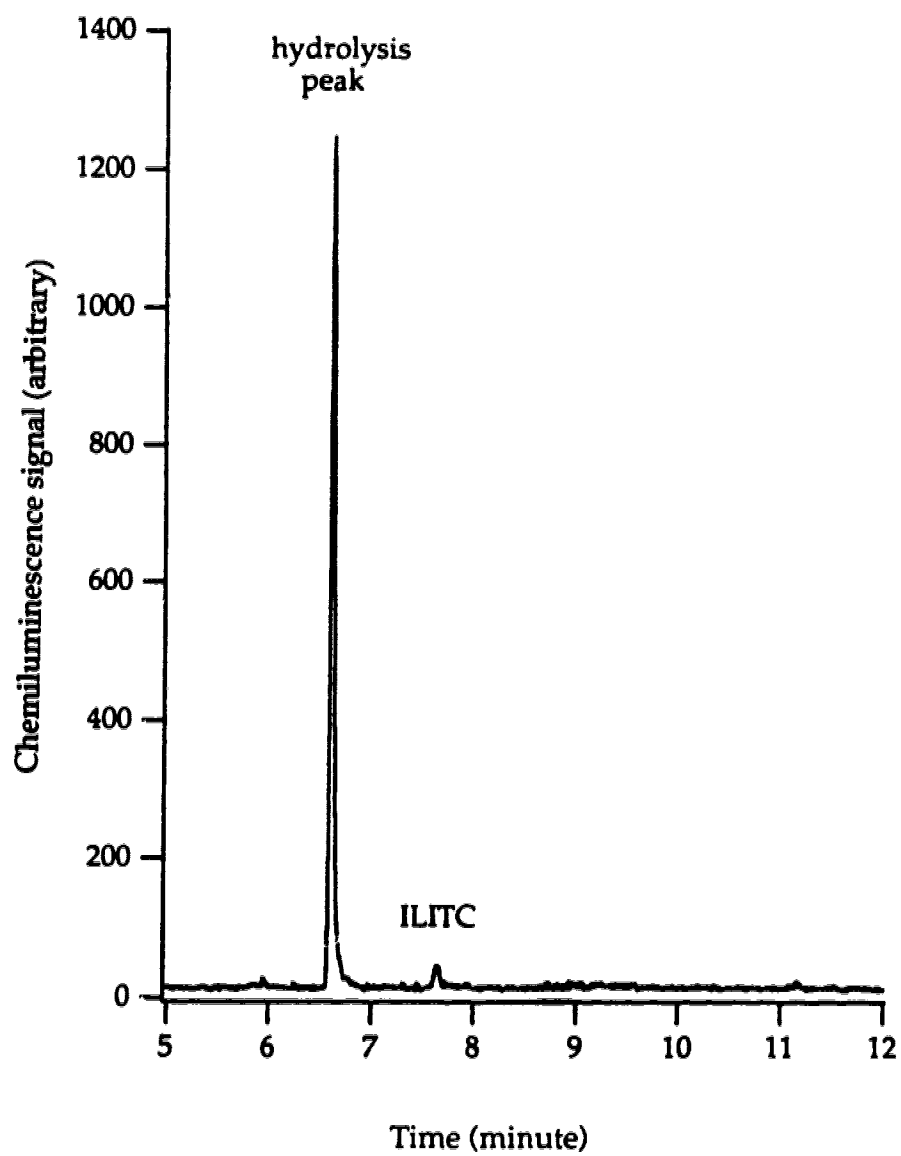


Figure 6.15 Electropherogram of ILITC blank (4.0×10^{-5} M)

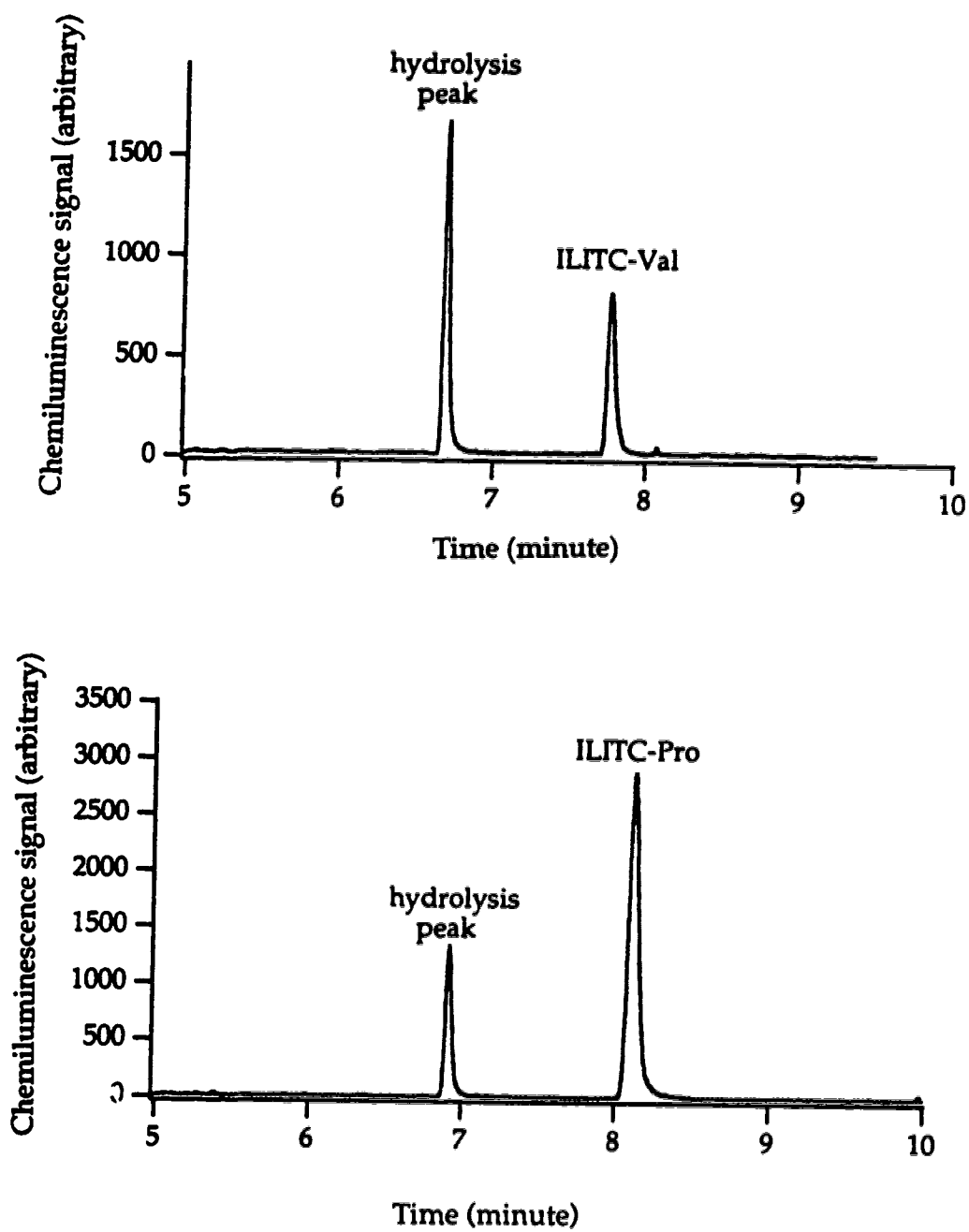


Figure 6.16 Electropherograms of ILITC labeled valine and proline

6.3.6 Calibration Curve, Theoretical Plate Counts and Detection Limit of ILITC Labeled Valine

The ratio of valine to ILITC in the labeling reaction was 17.8 to 1. The dry derivative was dissolved in 10 mM borate buffer with 10 mM SDS and diluted to a series of different concentrations by the separation buffer, which was made of 10 mM borate (pH 9.2) with 10 mM SDS and 3.8 μ M microperoxidase. The length of the capillary (41 μ m I.D.) was 84 cm operated at 30 kV. The photomultiplier tubes were operated at 1200 V. Hydrogen peroxide solution (2 mM) was introduced at a sheath flow rate of 500 μ L/hour. Injections were at 2-30 kV for about 5 seconds.

Table 6.8 lists the experimental data. The ILITC labeled valine concentrations were calculated based on the assumption that the limiting reagent ILITC was completely used to form thiocarbamyl derivative of valine. The amounts injected are from 440 to 6 femtomoles of isoluminol thiocarbamyl derivative of valine. A calibration curve was constructed, Figure 6.17, by $\log(\text{average CL signal})$ versus $\log([\text{ILITC-Val}], \text{M})$.

The number of theoretical plates were estimated by fitting a Gaussian function to the peak. Detection limit (3s) was estimated with the following procedure. The data was convoluted with a Gaussian function with variance equal to that of the peak. Next, the smoothed peak was fit with a Gaussian function to estimate the width of the smoothed peak. The maximum deviation in the baseline was determined from the smoothed data, typically over a few minute period at the end of the run. Plate counts in the capillary are good. The raw data produced 100,000 plates for valine-ILTC and 200,000 for isoluminol.

Table 6.8 Experimental data of a calibration curve for ILITC labeled valine

[ILITC-Val],M	log([ILITC-Val],M)	average CL signal	log(ave.CL signal)
4.56×10^{-4}	-3.34	1233.4	3.09
4.56×10^{-5}	-4.34	232.4	2.37
4.56×10^{-6}	-5.34	29.2	1.47
4.56×10^{-7}	-6.34	1.6	0.19

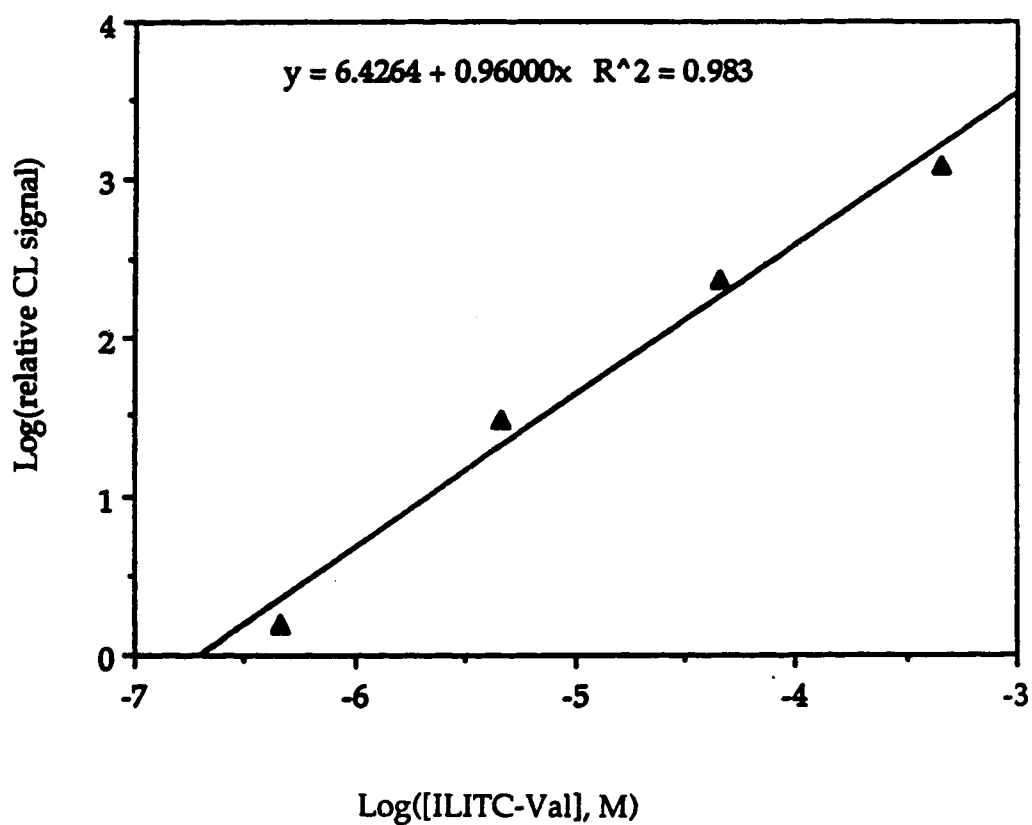


Figure 6.17 Log-log calibration curve for ILITC labeled valine

Then, Knoll's method was used to estimate the detection limit [12]. The appropriate peak width multiplier value of K_{Lod} was determined according to **Table 1.1**. The calculated detection limit was 500 attomoles of ILITC labeled valine. The detection limit produced by Knoll's method was consistently poorer by 15% than that produced by calculating the standard deviation in the baseline; typically the noise was measured over a period that is ten to twenty times the full-width at half-maximum of the smoothed peak. Knoll's method is more conservative than a simple calculation of standard deviation.

The calibration curve was linear over at least three orders of magnitude from 440 femtomoles injected to the detection limit of 500 attomoles. Detection limit assumes that the derivatization reaction went to completion. However, the peak area of the ILITC hydrolysis product peak was 1.4 ± 0.2 times larger than that of the ILITC labeled valine peak. If the ratio of peak areas is equal to the ratio of compound amounts, then the actual detection limit for this system is 250 attomoles of valine isoluminol thiocarbamyl injected onto the capillary.

The difference in detection limit between the labeled amino acid and isoluminol is due to two factors. First, the derivatizing reagent experiences hydrolysis that competes with the chemiluminescence labeling reaction, and the amount of derivatized product in the sample is certainly overestimated. Second, the chemiluminescence quantum yield is almost certainly higher for isoluminol than for the derivatized amino acid.

6.3.7 Separation of Isoluminol Thiocarbamyl Derivatives of 20 Amino Acids

Using 10 mM borate buffer (pH 9.2) with 10 mM SDS and micromolar microperoxidase, the labeled lysine and arginine peaks come out before the hydrolysis product peak, while the rest of the 20 ILITC labeled amino acid peaks come out after the hydrolysis peak. The separation of all 20 isoluminol thiocarbamyl derivatives of amino acids was performed in an 84-cm long capillary (41 μm I.D.) operated at 30 kV. Hydrogen peroxide (2 mM) was provided at a flow rate of 500 $\mu\text{L}/\text{hour}$. Unfortunately, complete separation of the 20 amino acid derivatives was not achieved. A typical separation electropherogram of nine amino acid derivatives is shown in Figure 6.18. Arginine and lysine are not well resolved, and histidine and valine show a minor overlap.

Other buffer systems tried include: (1) pure 10 mM borate; (2) 10 mM borate with 30 mM SDS; (3) 10 mM borate with 30 mM SDS and 4 M urea; (4) 10 mM borate with 30 mM SDS and 7 M urea; and (5) 10 mM borate with 50 mM SDS and 7 M urea. The separation was not improved by using high SDS concentration or buffer additive (urea), but high concentrations of SDS decreased the chemiluminescence signal, and high concentration of urea caused more noise in the baseline.

Alternative surfactants may be used in an attempt to improve the separation. However, the surfactant must be compatible with the chemiluminescence reaction. This constraint on separation buffer is a significant limitation in chemiluminescence detection.

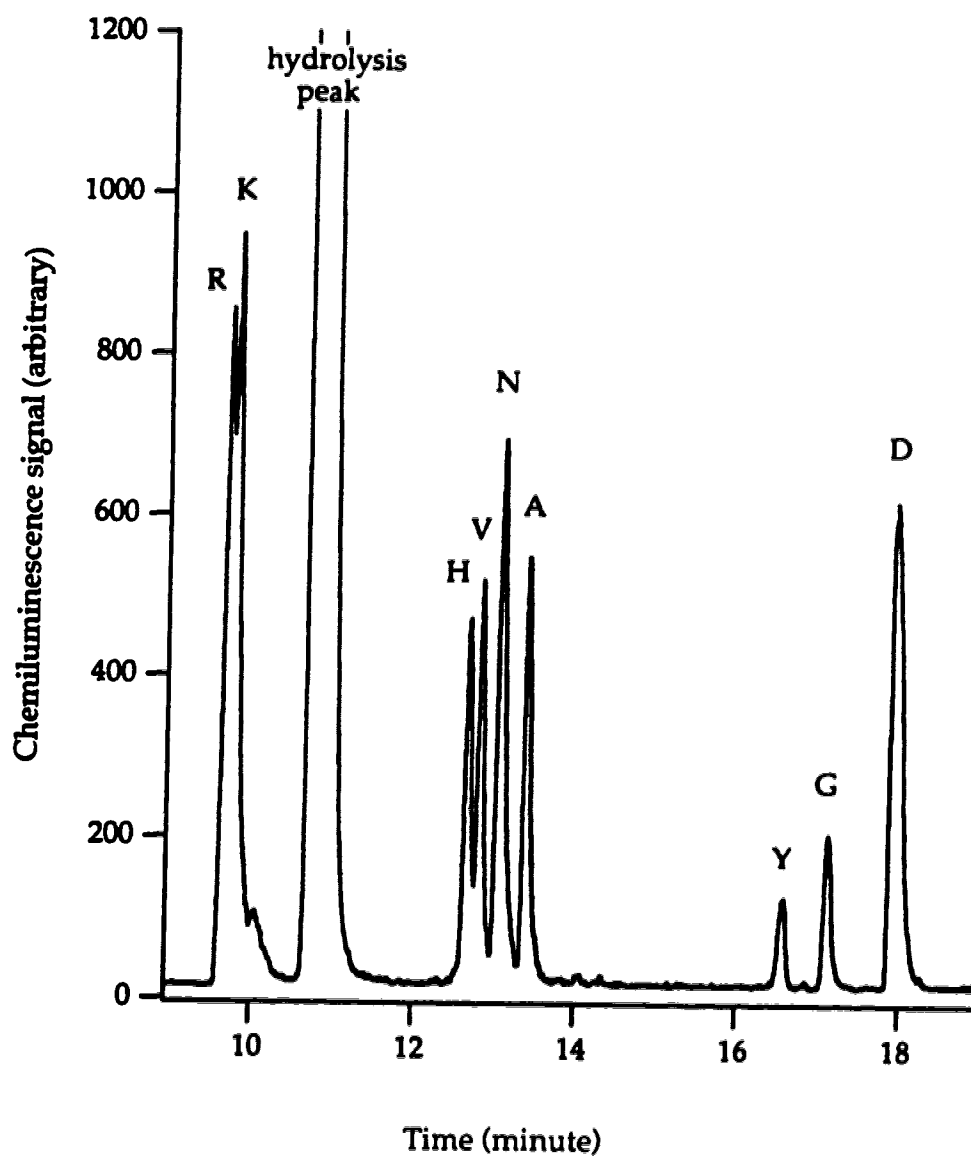


Figure 6.18 Electropherogram of ILITC labeled thiocarbamyl derivatives of nine amino acids

6.3.8 Possibility of Application in Protein Sequencing

If isoluminol isothiocyanate is to be used for protein sequencing, it is necessary to cyclize the thiocarbamyl derivative to a thiohydantoin under acidic conditions. Unfortunately, the conversion of thiocarbamyl into thiohydantoin was not successful. Presumably, the balance of electron donating and withdrawing characteristics of isoluminol isothiocyanate is weighted toward formation of the thiocarbamyl. It appears that the reagent must be modified to be useful for protein sequencing by the Edman degradation reaction.

6.4 CONCLUSIONS

Chemiluminescence detection in capillary electrophoresis provides sub-femtomole detection limits and good dynamic range. While much lower detection limits appear to be possible if the background signal can be reduced, cleaner chemistry will remain difficult because of the complex buffers typically used in capillary electrophoresis.

It is important to note that these detection limits are for the isoluminol thiocarbamyl derivative of the amino acid; that is, the detection limit is for the chemiluminescence instrument. The detection limit for the derivatization scheme is much poorer; the reaction chemistry has not been optimized to label amino acids at very low concentrations.

Labeling of low concentration amino acids is difficult. First, hydrolysis of the derivatizing reagent liberates isoluminol; this hydrolysis product overlaps analyte peaks in the electropherogram. As a result, the reaction conditions must be manipulated so that the reaction with analyte is faster than the hydrolysis of

the reagent. However, to produce rapid kinetics, the labeling reagent must be present in much higher concentration than analyte. Therefore, unreacted labeling compound will be present in excess; the unreacted reagent will interfere with analyte peaks in the electropherogram.

There are several strategies to label dilute solutions of analyte without generation of large signal from the blank reaction. First, a labeling reagent can be used that rapidly reacts with analyte and is stable against hydrolysis; in this case, it is not necessary to use a large excess of derivatizing reagent. Second, a labeling reagent can be used that is not luminescent but does form a luminescent product with the analyte; excess reagent does not lead to interference in the separation. Third, a solid-phase reaction scheme can be used wherein the analyte is bound to a support. The analyte is allowed to react with label, excess label is flushed away, and the labeled analyte is cleaved from the support into a clean buffer for separation. This procedure is used in protein sequencing with phenyl isothiocyanate and may be used with other reagents.

The raw data routinely produces 100,000 theoretical plates for labeled amino acids, which is an order of magnitude superior to that produced by competitive reactors. The high efficiency is produced both by careful design of the flow chamber to eliminate turbulent mixing and by use of a sufficiently short residence time of the reaction mixture in the detection chamber.

The limited success in separating all 20 isoluminol thiocarbamyl amino acids shows that the sensitivity of the chemiluminescence signal is affected by the buffer composition and buffer additives. Given the limited range of separation buffers, the isoluminol reaction will be useful only for relatively simple samples.

References

1. H. R. Schroeder, P. O. Volgelhut, *Anal. Chem.* , **51**, 1583-1585 (1979).
2. R. Dadoo, L. A. Colon, R. N. Zare, *J. High Resolut. Chromatogr.* , **15**, 133-135 (1992).
3. M. A. Ruberto, M. L. Grayeski, *Anal. Chem.* , **64**, 2758-2762 (1992).
4. D. J. Rose, J. W. Jorgenson, *J. Chromatogr.* , **447**, 117-131 (1988).
5. T. Tsuda, Y. Kobayashi, A. Hori, T. Matsumoto, O. Suzuki, *J. Chromatogr.* , **456**, 375-381 (1988).
6. J. A. Steinkamp, *Res. Sci. Instrum.* , **55**, 1375-1400 (1984).
7. F. Zarrin, N. J. Dovichi, *Anal. Chem.* , **57**, 2690-2692 (1985).
8. Y. F. Cheng, S. Wu, D. Y. Chen, N. J. Dovichi, *Anal. Chem.* , **62**, 496-503 (1990).
9. H. R. Schroeder, F. M. Yeager, *Anal. Chem.* , **50**, 1114-1120 (1978).
10. S. R. Spurlin, M. M. Cooper, *Anal. Lett.* , **19**, 2277-2283 (1986).
11. N. Feder, *J. Histochem. Cytochem.* , **18**, 911-913 (1970).
12. J. E. Knoll, *J. Chrom. Sci.* , **23**, 422-425 (1985).